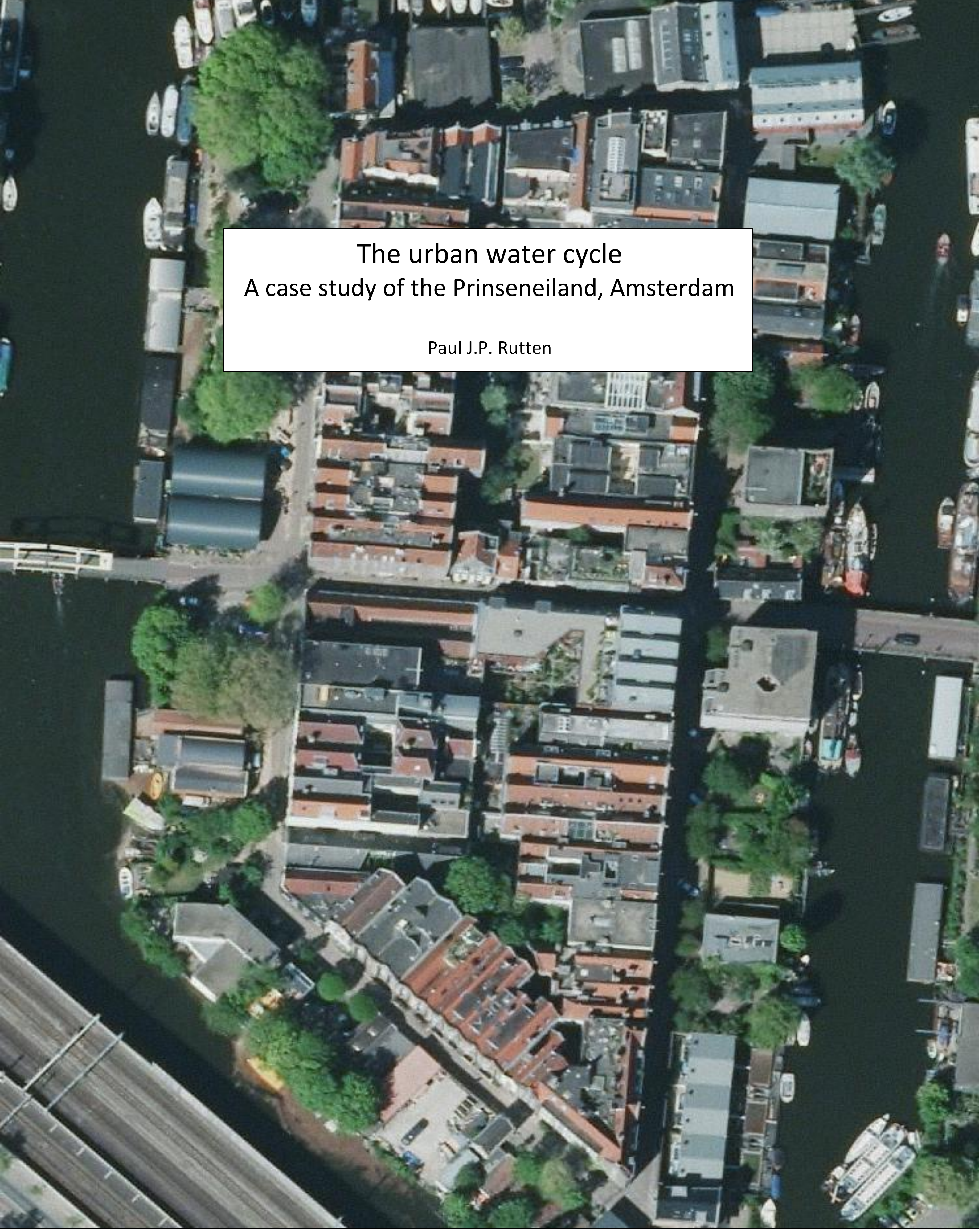

The urban water cycle
A case study of the Prinseneiland, Amsterdam

Paul J.P. Rutten

TU Delft Delft University of Technology

Challenge the future

Deltares Enabling Delta Life

The urban water cycle:
A case study of the Prinseneiland, Amsterdam

Master of Science Thesis

For the degree of Master of Science in Water management
at the Delft University of Technology

Paul J.P. Rutten

August 21, 2013

Graduation Committee:

Prof.dr.ir. N.C. van de Giesen	TU Delft, Water Resources Management
Dr.ir. F.H.M. van de Ven	TU Delft, Water Resources Management/ Deltares
Drs. M.C. Hoogvliet	Deltares
Dr.ir. J.A.E. ten Veldhuis	TU Delft, Sanitary Engineering
Dr.ir. A.M.J. Coenders	TU Delft, Hydrology

Preface

In this report the study on the urban water cycle performed for obtaining the degree of Master of Science at the Delft University of Technology is described. The study is a part of the Deltares project 'Naar een bestendige stedelijke waterbalans', which was carried out for the second Delta Programme[1]. The project is part of on-going research into how the Netherlands can remain an 'attracting location for living, working, investing and recreating for generations to come'.

For achieving this water managers need to know what the effects of droughts and climate change are on the urban water cycle. Knowledge on the possible effects can be used for reducing the effects and keeping the urban areas attracting locations for the urban population.

Readers interested in the general effects of drought and climate change on the urban water cycle may find their answers in the conclusions and discussion. More detailed results can be found in sections 6.3 (effects of land use), 6.4 (effects of drought), 6.5 and 13 (effects of climate change in combination with drought). The model that was used for the study is described in section 5.

[1] Delta Programme website: http://www.deltacommissaris.nl/english/

Acknowledgements

Here I would like to thank some people that directly or indirectly helped me doing this study (not in order of importance!).

First of all, I would like to thank the members of the graduation committee for sharing their ideas on the topic and giving advice on possibilities for improvement. I am especially grateful to Frans van de Ven for keeping an eye on the progress of the study and pushing me towards more general applicable conclusions.

Secondly, I would like to thank the people at Deltares I have had the pleasure of meeting during the course of the Deltares project/lunch/coffee/etc. It has been interesting to learn from them about their experiences on managing/working on projects, the encountered problems and their solutions. Special thanks to the members of the project group, who have taught me a lot on project practices and on how to present results to and write a report for readers without a technical background.

The third group of people I would like to thank are my fellow-graduators from room 4.93. They helped me a lot improving my work by having short talks/discussions, which gave me new ideas and other perspectives. Furthermore, helping them out with their theses and having talks on other subjects provided me with renewed energy to work on my thesis.

Lastly, I would like to thank my family for their support and encouragements throughout my study.

Paul Rutten,
August 21, 2013

Summary

Background information
The field of urban water management focusses on managing the (temporary) storages and flows of drinking, waste-, ground- , surface and storm water in urban environments. Adequate water management forms a prerequisite for pleasant living conditions .

A difficulty urban water managers face is the limited or complete lack of control over some of the processes in urban areas, such as precipitation, evaporation, etc. Furthermore, the characteristics of an area in which the water needs to be managed forms a semi-fixed condition for the fluxes, as they cannot be manipulated to suit short term water management needs.

Structural measures that can be taken in an area to improve the are relatively expensive and are therefore only possible once every (few) decade(s). This means that proposed changes to an area should result in similar or -preferably- improved living conditions for a long period of time.

Next to the limited control, two other potential challenges to satisfactory management of water in urban areas are droughts and climate change. In order to be able to predict the merit of proposed measures during current and changed climatic conditions and droughts, more information is required on the possible consequences for the water cycle.

Goals
The goal of this research is therefore to investigate the relations between processes in the water cycle and their interdependencies. This thesis is also aimed at finding an indication of the possible effects of droughts and climate change on the urban water cycle.

Approach
For this study the water cycle of the Prinseneiland was used as a case study. The characteristics of the area were determined during a field survey. Further measurements on groundwater levels and sewer discharges were performed. Data on precipitation and potential evaporation were obtained from nearby measuring locations.

A lumped, conceptual model was made for simulating the water cycle of the area. The model results were validated on the measured groundwater levels and sewer discharges. The model was used to simulate the effects of drought and climate change scenarios on the water cycle of the Prinseneiland.

Conclusions
Due to less precipitation in a dry year the interception evaporation, infiltration and surface runoff fluxes also decrease. Transpiration increases slightly due to higher potential evaporation. Groundwater recharge is decreases due to less infiltration and more transpiration. This causes the groundwater levels to drop more relative to normal situations. These effects are more or less proportional to the severity of the drought. Transpiration, however, is restricted by available soil moisture, which causes transpiration to remain relatively constant compared to the other fluxes.

The effects of climate change mainly depend on whether the prevailing wind patterns change or not. In the latter case precipitation and potential evaporation increase, resulting in larger fluxes compared to the normal situation. When the wind patterns do change (as in the KNMI'06 'W+' scenario) precipitation is concentrated in winter. During the summer months precipitation decreases and potential evaporation increases compared to the current situation. The interception evaporation, infiltration and surface runoff fluxes decrease. Transpiration increases due to higher potential evaporation. Groundwater levels are higher during winter due to higher winter precipitation and thus infiltration. In the summer groundwater levels decrease further compared to the normal situation.

Table of Contents

List of figures

List of tables

1 Introduction

1.1 Background information

The field of urban water management focusses on managing the (temporary) storages and flows of drinking, waste-, ground- , surface and storm water in urban environments. All these storages and fluxes need to be managed as a condition for pleasant living conditions in urban areas. If one of these storages or flows is not managed properly the living conditions may deteriorate to unacceptable levels.

A difficulty urban water managers face is the limited or complete lack of control over some of the processes in urban areas. It is for instance impossible to control the amount of precipitation falling on an area. Next to that evaporation, transpiration, infiltration and surface runoff fluxes mostly depend on water availability (precipitation/soil moisture) and the characteristics of an area. These characteristics are e.g. land use or features being connected to a sewer or not, etc.

The characteristics of an area form a semi-fixed condition for the fluxes, as they cannot be manipulated to suit short term water management needs. They can only be changed by replacing (some of) the existing features with other new features with other characteristics. For instance, replacing an asphalt road with a brick street will probably result in more infiltration and less sewer inflow. It is also possible to replace some paved surfaces with vegetation, which will change the amount of infiltration and thus groundwater recharge.

Measures like converting paved surfaces to unpaved ones and other possible changes to an area are relatively expensive and are therefore only possible once every (few) decade(s). This means that proposed changes to an area should result in similar or -preferably- improved living conditions for a long period of time. In order to select the best suited changes to an area, the possible effects of the potential changes on the storages and fluxes of water in an urban area should be identified.

Next to the limited control, two other potential challenges to satisfactory management of water in urban areas are droughts and climate change. Droughts form a challenge as the precipitation in an urban area is reduced for a prolonged period of time, possibly resulting in water quality and quantity problems. In order to reduce these problems, artificial inlet of water may be required. At times when artificial inlet is not possible or sufficient the affected area may suffer damages via (several) damage mechanism(s) as described in e.g. Deltares (November 2012).

Climate change forms a challenge to urban water management as the yearly precipitation sums and the amount of potential evaporation may change. Climate change may also result in differences in general wind patterns, which will probably cause a change in the precipitation patterns over the year. In an advantageous scenario a change in general wind pattern may result in a shift in precipitation towards the dryer months. In a disadvantageous scenario the opposite may happen, which probably results in a larger likeliness of problems occurring.

In order to be able to take on these challenges more information is required on the possible consequences for the urban water cycle. It is for instance important to know how much less precipitation an area receives during a dry period and what the consequences are for e.g. the groundwater levels. It is also important to have predictions on the potential effects of climate change on urban areas. With such information it would be possible to prevent or lessen these consequences and maintain pleasant living conditions in the urban areas.

The required information may (partly) be acquired by modelling the urban water cycle in a case study area. With a model the relations between processes in the urban water cycle may be quantified and their interdependencies revealed. Knowledge on the relations and interdependencies can be used to predict the effects of droughts and climate change. Models on the urban water cycle also enable the determination of the effectiveness of potential measures opted for reducing the effects of drought or climate change.

1.2 The research

1.2.1 Goal of the research

The goal of this research is to investigate the relations between processes in the urban water cycle and their interdependencies. This thesis is also aimed at finding an indication of the possible effects of droughts and climate change on the urban water cycle.

1.2.2 Research questions

1 *What are the relative contributions of the processes in the urban hydrological cycle to the urban water cycle?*

2 *What are the effects of drought on the urban water cycle?*

3 *What are the effects of climate change on the urban water cycle?*

1.2.3 Sub questions

1.1 *What are the dominant processes in the urban water cycle?*
1.2 *How much does paved area reduce groundwater recharge compared to unpaved area?*
1.3 *How much does an urban environment reduce groundwater recharge compared to a hypothetical 'natural' state (unpaved) of the same area?*

2.1 *How much less precipitation is there in a dry or extremely dry year compared to a normal year?*
2.2 *How much further does the groundwater table drop due to drought compared to an normal year?*

3.1 *On which parts of the urban hydrological cycle does a changing climate have the most impact?*

1.2.4 Approach

To gain more insight into the urban water cycle a case study of the Prinseneiland in Amsterdam has been done. During this case study measuring equipment was placed in the area and a survey of the area was done. With the information that was generated about the area a simple urban water balance model was built with the aim of simulating the water balance of the island.

In this model both the urban water system and the urban hydrological cycle are simulated. The characteristics of the study area are fed into the model by categorization of the features of the island. The model is calibrated on and validated with measurements that were carried out during the study period.

In order to determine the effects of drought and climate change, scenarios were run with the aforementioned model. The scenarios consist of meteorological time series of three years with varying dry spells. These time series were adapted to account for the climate change described in climate scenarios. The results of the scenarios are compared with the results from runs with the original time series to be able to determine the effects of the simulated climate change.

1.3 Outline of the report

In the second chapter of the report the urban water cycle is discussed. First the definitions on the sub-cycles of the urban water cycle used in this report are described. After that the processes in the urban water cycle and the sub-cycles that are discerned in this thesis are described.

In the third chapter the area on which the case study was done is described. After the introduction of the area the reasons for choosing this area for the study of the urban water cycle are discussed. At the end of the chapter more detailed information on the land use, the fate of precipitation on the area and the structure of the subsurface of the area is given.

The data and measurements used in the study are described In the fourth chapter. Further some additional information on the data (sources) is given.

In the fifth chapter the model that was made for the study is described. The description entails an overview of the model structure, the processes that were modelled and how they are implemented in the model. The chapter ends with the parameter values that were chosen or calibrated for the model runs.

In the sixth chapter the results of the model runs are presented and discussed. The chapter consists of the results for the validation run, the land use, drought and climate scenarios runs. The answers to the sub-research questions can also be found in this chapter.
The conclusions that were drawn from the research can be found in chapter seven.

The discussion on the study can be found in chapter eight.

2 The urban water cycle

In this section of the report the sub-cycles/systems of the urban water cycle are described. In the second part of the section the processes and storages discerned in the urban water cycle are described.

2.1 Definitions used in this thesis:

Hydrological cycle: The storage and circulation of water between the biosphere, atmosphere, lithosphere, and the hydrosphere.
Urban hydrological cycle (UHC): The hydrological cycle in an urbanized area.

Small urban water cycle (SUWC): Drinking water supply and wastewater collection (and treatment) systems. The term 'small' in this definition does not carry any meaning on the importance of this flux on the urban water cycle.
Urban water system (UWS): Combination of the small urban water cycle, urban surface and groundwater bodies, storm water drainage and infiltration systems, water retention and irrigation systems and the subsurface drainage system.

Urban water cycle (UWC): The combination of the urban hydrological cycle and the urban water system of an area.

In Figure 2.1 the urban water cycle (red box) is shown with the mayor processes that occur in an urban area. Next to that the urban hydrological cycle (green box), the small urban water cycle (dark grey box) and the urban water system (blue box) are shown. The widths of the arrows are based on the model results for the urban water cycle of the Prinseneiland over the years 2010 and 2011. The mayor processes in the urban water cycle are described in the following section.

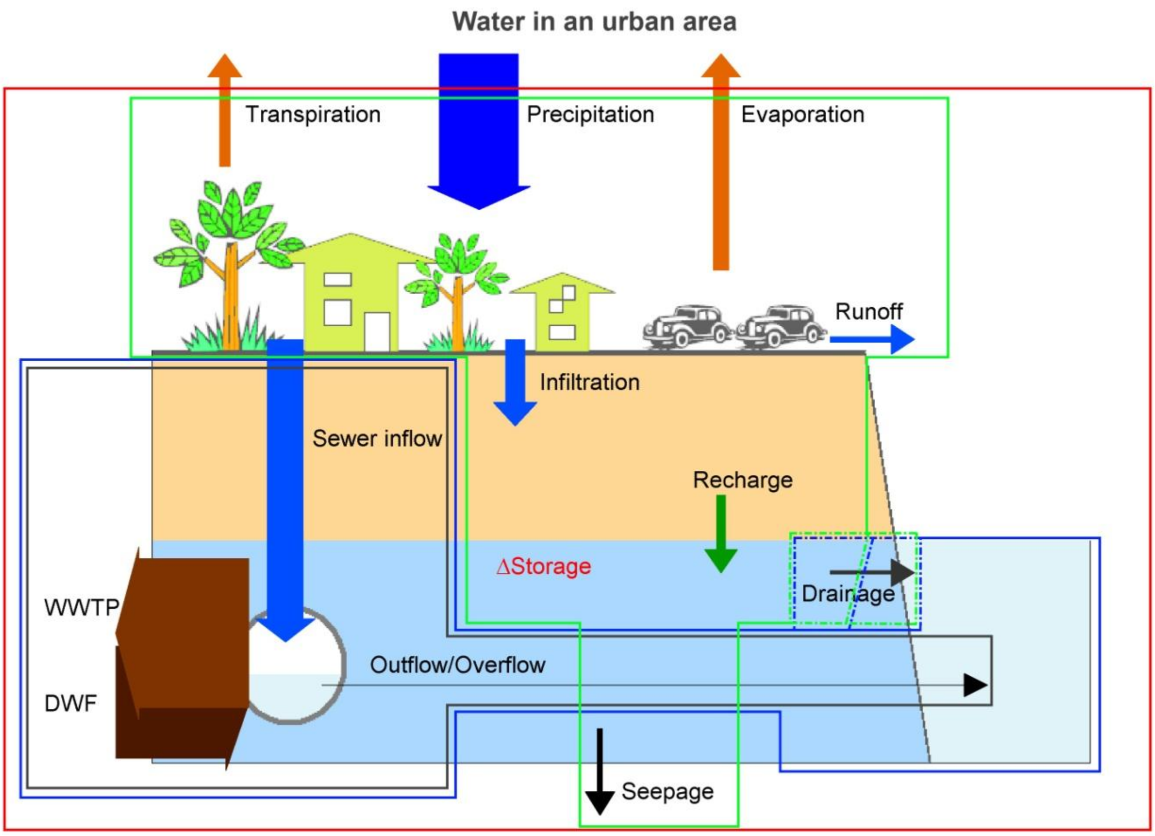

Figure 2.1. Schematisation of the urban water cycle (red box). The urban water cycle consists of the urban hydrological cycle (green box) and the urban water system (blue box). The small urban water cycle is shown in the dark grey box.

2.2 The urban water cycle

In this section all mayor processes that can take place in an urbanized area are described. The processes are grouped in natural (UHC) and manmade (UWS) processes. If a different name was used in Figure 2.1 for a (group of) process(es), that name is shown between apostrophes. Processes that are described, but not shown in Figure 2.1 are indicated with an asterisk (*). The descriptions also contain references to earlier research to provide more background information.

2.2.1 Urban hydrological cycle

Fluxes:

- Precipitation:
  Rain, snow, sleet, or hail that falls to or condenses on the ground (definition from the Oxford dictionary)

- Evaporation
  The evaporation flux in Figure 2.1 is a summation of the interception process, evaporation of precipitation stored in depressions in the surface, evaporation of water moisturizing the surface and open water evaporation.

- Transpiration of water from the root zone by vegetation.

- Overland flow
  The overland flow consists mainly of precipitation on paved areas and roofs that is discharged to a sewer or a nearby surface water. The first is called 'Sewer inflow' in Figure 2.1, the latter 'Runoff'. It is also possible to have overland flow to unpaved (permeable) areas. This flux mostly stems from paved areas that are not connected to a sewer or occurs in high intensity precipitation events when not all water can be discharged via the normal pathways. The contributing area to the first term can easily be estimated from a land use

map and knowledge of water flows in an area. The second term is harder to estimate and is (usually) negligible when looking at longer periods.

In high intensity precipitation events it is also possible to have infiltration excess overland flow from unpaved areas. In such conditions the precipitation rate exceeds the infiltration rate, which results in ponding of water on the surface and possibly flow to a nearby paved area connected to a sewer.

- Infiltration, (infiltration systems)
  Infiltration of water into the unsaturated zone from permeable surfaces and through localized infiltration in semi-permeable surfaces. This process includes precipitation that is collected from roofs and/or paved areas and is led into an infiltration system for infiltration into the subsoil.

- Percolation - capillary rise, 'Recharge' or 'Depletion'
  Exchange of water between the unsaturated and the saturated zone. Percolation is the downward flow of water from the unsaturated zone that could not be held by capillary forces against gravity. Capillary rise is the reverse of percolation and takes place when the capillary forces are larger than the gravitational pull on the water in the soil. Both processes may take place alternatingly over a year. A net downward flux is called recharge and a net upward flux depletion.

- Seepage (upward /downward)
  Flow between the phreatic groundwater body and a deeper groundwater body. The magnitude of the flow depends on the difference in head between the groundwater bodies and the resistance to flow of the soil in between the groundwater bodies.

- Drainage
  Flow from the urban groundwater to a nearby surface water. The magnitude of the flow depends on the difference in head between the ground- and surface water bodies, the hydraulic conductivity of the soil and the distance the water has to travel. To determine the amount of drainage from an area one needs to know the areal averages of the head difference, hydraulic conductivity and the travel distance.

Storages:

- On the surface*
  Temporary storage of precipitation on surfaces above the terrain surface by interception
  Temporary storage of precipitation in depressions in the surface
  Temporary storage of precipitation by moisturizing of the surface

- In vegetation*
  (Temporary) storage of water in the stems and leaves of vegetation.

- In the unsaturated/vadose zone
  Storage of water in the unsaturated zone that is held against gravity and water that is percolating to the saturated zone, but that did not leave the unsaturated zone yet.

- In the saturated zone/groundwater
  Storage of water in the phreatic groundwater body of an area. This water consists of water that slowly flows through the pores in the soil and water that flows more rapid through macro-pores in the soil.

2.2.2 Urban water system

Fluxes

- Storm water drainage, 'Sewer inflow'
  Overland flow of precipitation on (semi-)impervious surfaces to gully pots, collection of precipitation on roofs though gutters and drain pipes and subsequent discharge to the sewer.

- Drinking water supply, 'DWF'

Drinking water supplied to the households, offices and businesses in an urban area. Forms (most of) the base flow of the sewer discharge.

- Wastewater collection*
  The collection of used drinking water and excrements from houses, offices and businesses in the sewer.

- Sewer outflow/overflow
  The intentional outflow of (clean,) collected storm water out of a rainwater conduit of a separated sewer system into a nearby surface water body.
  Overflow of a combined sewer due to an overloading of the system.

- Sewer system discharge, 'WWTP'
  The discharge of wastewater from the sewer system to the wastewater treatment plant.

- Artificial drainage by subsurface drains/drainage ditches, 'Drainage'
  Flow via a subsurface drain from the urban groundwater to a nearby ditch dug for the drainage of an area or a natural surface water.

- Groundwater abstractions*
  The abstraction of groundwater by means of a (pumped) well in the city either for groundwater control considerations or for establishing a reliable (drinking) water source.

- Irrigation/garden watering*
  A supply of water to an urban area for vegetation watering, groundwater level control and/or mitigation of the urban heat island.

Storages:

- Surface water
  (Temporary) storage of water in surface water bodies of any kind. E.g. ponds, canals.
- Sewer system
  Temporary storage of waste- and storm water prior to discharge to a wastewater treatment plant or a surface water body.
- Drinking water supply system*
  Storage of water in drinking water mains and storage tanks.
- Water retention systems*
  Storage of water in systems that are designed to keep water in an urban area for a longer period of time for future use.

3 The study area

In this section more information about the area on which this study focusses is presented. Firstly the Prinseneiland in Amsterdam is introduced. After that the reasons for choosing this location for a case study are discussed. Lastly, more information on the area is given in the study site description.

3.1 Introducing the Prinseneiland

The case-study in this research is about the Prinseneiland in Amsterdam, the Netherlands. The Prinseneiland is located in the northwest of the old city-centre of Amsterdam (see Figure 3.1, pp. 10) and is a member of the 'Westelijke Eilanden' (Western Islands). These islands were created between 1611 and 1615 by pinning down sections of peat that floated around in that part of the IJ estuary[2]. The surface level was then raised by an integral fill with the material that became available when the nearby canals were dug. This provided the islands with the necessary freeboard and soil bearing capacity, which allowed for the employment of the area.

In that time the centre of the Prinseneiland was mainly build up with warehouses for storing wood and tar. The verges of the island were occupied by shipping wharves. While all but one of the shipping wharves disappeared over time, most of these original warehouses still stand tall on the island. They are no longer used for storing goods, but have been transformed into apartment buildings or are in use by small companies. The limits of the island are now build up with houses, offices and small storage buildings or are made into gardens or parking spaces. An aerial photograph of the island is shown in Figure 3.1.

The island is connected with the rest of the city of Amsterdam by three bridges. These are located to the west, north and east of the island. The bridges to the east and west are linked by the 'Galgenstraat', which is on the centre of the island. The other road going round the island is called the 'Prinseneiland'.

3.2 Suitability of the area for the study

The main reason for choosing this area to study the urban water balance is its relative isolation from the rest of Amsterdam, its simple sewer system and its small size.

A clear boundary
The area is bounded by canals, whose bottom cuts into a clay layer underneath the area, blocking influences from the surrounding areas. The canals have a controlled water level that varies[3] slightly around a median level of 0.40 metres below N.A.P.[4]. This gives the area a known boundary condition that is relatively constant over time and which is roughly the same for the entire perimeter of the island.

A simple sewer system
The sewer system on the island is a combined system. This means that both the wastewater from the households and businesses on the island and precipitation runoff from paved and roof surfaces connected to the sewer are collected in the same system. The sewage water is pumped out of the area by a pumping station in the west of the island, which only discharges water stemming from the Prinseneiland.

---

[2] During the Roman times the IJ was an estuary of the North Sea. This connection later closed naturally and the IJ became an estuary of the newly formed Southern Sea. In the middle of the nineteenth century the estuary was closed off with a dam, effectively converting the IJ estuary into a lake.

[3] The variation in the level is caused by a pseudo-tide in lake 'IJ', which lies to the north of the city and into which the city is drained. The pseudo-tide is caused by the sluice and pumping station at Ijmuiden, which discharges most of the excess water in lake IJ by gravity during low sea water levels to the north sea. At high tide water is stored in lake IJ, which causes the water levels in lake IJ and connected water bodies (including the canals around the Prinseneiland) to rise. The sluice and pumping station at Ijmuiden is operated to keep water levels around the target level of 40 centimetres below N.A.P. Deviations that occur are between 50 and 35 centimetres below N.A.P..

[4] N.A.P. is an abbreviation for 'Normaal Amsterdams Peil', which is the standardized datum for the Netherlands. N.A.P. roughly corresponds to the mean sea level, but is not defined as such.

The system consists of six stretches of pipe with a total length of less than 700 metres. The system has one emergency overflow structure in the north of the island, which by design is activated only in the most extreme circumstances.

A small size

The small size of the area (about 125 x 275 metres, 3.4 hectares) is also a pro for the Prinseneiland as a research area, as it is easier to do a thorough survey of a small study area. Next to that a small area does not have the disadvantage of averaging out of the extremes and will thus give more informative results.

Due to the limited size of the island, the natural drainage of the groundwater is sufficient to keep the groundwater levels from becoming too high. Because of the natural drainage being enough to prevent groundwater nuisance, no subsurface drainage system has been installed by the authorities on the island, which reduces complexity.

Discussion of the (dis)advantages of having a subsurface drainage system in a study area.

This higher complexity of areas with a subsurface drainage system is caused by the clogging and subsequent cleaning of the drains. The processes governing the clogging and the self-cleaning capacity of the drainage systems are not yet clear. This makes modelling the processes in a subsurface drainage system quite difficult and the resulting groundwater drainage discharges uncertain.

A disadvantage of not having a drainage system is not having a direct means of measuring the groundwater drainage. Measurements on an artificial drainage system that drains only a part of a research area will not give one the magnitude of the entire flux. They will, however, show the dynamics in the flux and therefore allow for validation of simulated drainage fluxes.

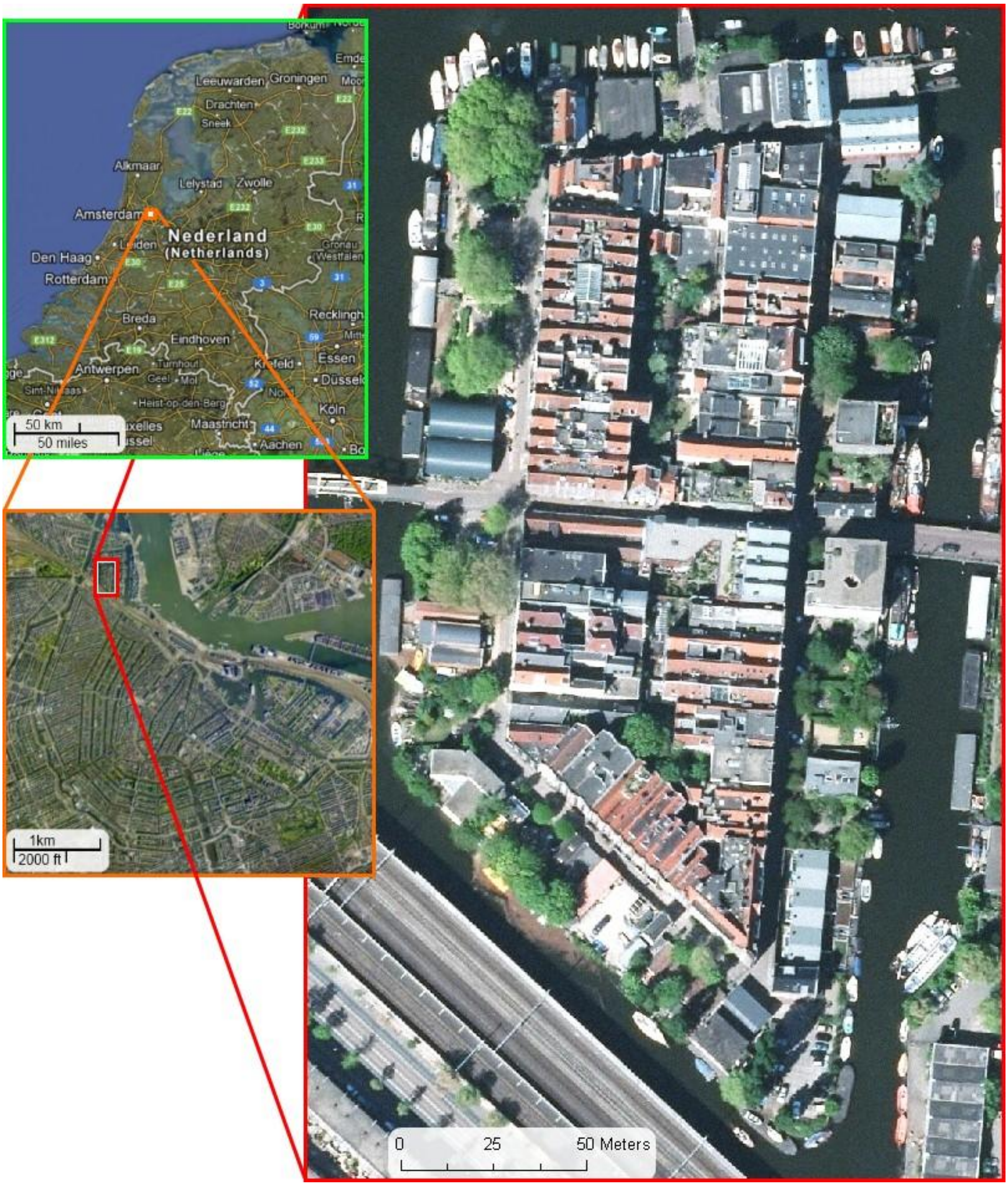

Figure 3.1. Location of Amsterdam in the Netherlands (green box). The city centre of Amsterdam (orange box) with the Prinseneiland in the North-west (both from Google maps). On the right (red box) an aerial photograph of the Prinseneiland taken in 2011 is shown (Courtesy of Waternet).

3.3 Study site description

In this section the characteristics of the Prinseneiland are discussed. Firstly the land use on the Prinseneiland is dealt with. After that the two step (crude + refining) framework used for classifying the features on the island by where most of the precipitation on the feature ends up is discussed. In the end the overall structure of the subsoil of the Prinseneiland is deliberated upon.

3.3.1 Land use types

Classification principle
For this study the features of the Prinseneiland have been classified into four land use types. These land use types are *paved*, *unpaved*, *build* and *water*.

- The land use type *paved* consists of streets, sidewalks, garden paths and other features that have a paved surface.
- The type *unpaved* is made up of gardens, lawns, hedges and other features that have a non-covered surface.
- The land use type *build* contains all buildings on the island ranging from the large warehouses to sheds.
- The land use type *water* consists of ponds, swimming pools and other features that have surface water. This land use type is not present at the island, but was added to the classification to arrive at a framework that can be used in other areas that do have surface water.

Classification of the Prinseneiland
From Figure 3.1 it can be seen that a large part of the Prinseneiland is build up, that there is quite some paved area and that a relatively large part of the area remains hidden because of overhanging tree canopies. When the fractions of the land use types with respect to the total area of the island are calculated, it turns out that 49% of the area is built up, 31% is paved (of which 18% is road/parking lot and 13% is sidewalk/garden path). The remaining 20% consists of unpaved area. The fractions are shown in Table 3.1 and Figure 3.2 to provide a clearer overview of the numbers.

Classification of individual features
With the help of a detailed land use map Figure 3.3 was made. In this figure the land use of the features on the Prinseneiland is shown in five classes. The buildings are shown in red, the paved area is shown in the two shades of grey. The lighter one of these depicts the paved areas that consist of sidewalks and garden paths. The darker shade represents the roads and paved parking spaces. In green unpaved areas consisting of gardens and other non-covered surfaces are depicted.

As can be seen from Figure 3.3, the buildings are mostly concentrated into two blocks of buildings on the middle of the island. Due to the scarcity of the land, the buildings are built almost build back to back leaving very little space as a backyard. Most of the unpaved area is therefore located to the edges of the island.

> The land use type build has not been divided into inclined and flat roofs. This distinction has not been made, because most roofs on the Prinseneiland (91%) are inclined and only a small fraction (9%) is flat. When the fractions inclined and flat roof are closer together, the distinction between the two types should be incorporated into the classification of the area.

Overhanging tree canopies
From Figure 3.1 it can be seen that there are quite some trees scattered across the Prinseneiland. A survey of their canopies using the aerial photograph and a GIS system showed that about 8.5% of the Prinseneiland is overhung by tree canopy. The resulting numbers in Table 3.1 show that most of the canopy is above paved and unpaved surface and that only a small fraction is above a building.

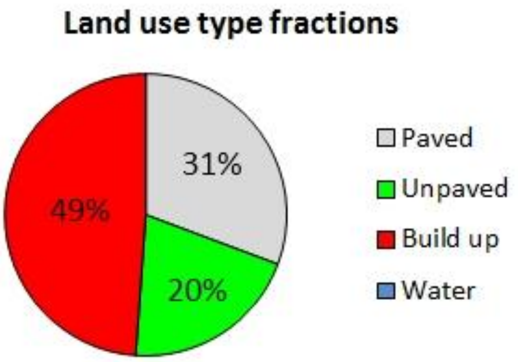

Figure 3.2. Land use type fractions

Table 3.1 Land use type fractions

Land use class	Fraction [%]	Fraction trees [%]
Paved	49	4.4
Unpaved	20	3.7
Build	31	0.4
Water	0	0
Total	100	8.5

Figure 3.3. Land use types assigned to the features on the map of the island.

Figure 3.4. Assumed fraction of the precipitation on features not being discharged to a sewer.

3.3.2 Precipitation discharge modes

Classification principle

For this study features of the Prinseneiland have been classified into four 'precipitation discharge modes'. These 'modes' are defined as the **assumed main destination of precipitation on a feature** and form a crude classification of the features on where most of the precipitation on the feature ends up. The four modes that are discerned are '*combined*', '*separated*', '*not connected*' and '*external*'.

- The *combined* precipitation discharge mode means that it is <u>assumed</u> that <u>most of the precipitation</u> on a feature classified as *combined* <u>flows to</u> the **combined sewer**.
- *Separated* denotes that it is assumed that most of the precipitation on a *separated* feature flows to the **separated sewer**.
- The mode *Not connected* stands for the feature to be assumed to discharge most of the received precipitation to the subsoil via **infiltration**.
- The *external* mode means that it is assumed that most of the precipitation is discharged directly **outside** the **study area boundaries**.

In the definition of the precipitation discharge modes the word *main* is used to denote that not all precipitation on a feature has to have the same destination. A brick street may for instance discharge most of the precipitation to a sewer. A fraction of the precipitation, however, might infiltrate into the underground. Following the definition of the modes, the brick street is classified as combined (or separated depending on the type of sewer it is connected to). The division of the precipitation over the sewer inflow and infiltration flux is described in section 3.3.3 on the routing of the precipitation.

The word *assumed* is incorporated into the definition to stress that the classification depends on a subjective view on the precipitation routing in the area. The subjectivity of the classification can be reduced by collecting as much information on the area as possible and by performing a field survey. The survey should focus on determining the (most likely) destination of precipitation on a building/section of a street. It is not always possible to ascertain the destination, but it may be possible to deduce the most likely option by linking the location of a drainpipe with that of a sewer.

Classification of the Prinseneiland

The features of the Prinseneiland were classified by combining information on the land use type shown in Figure 3.3 and information from a field survey of the area shown in section 10 in the appendix. The combination of the information resulted in a classification of the features of the Prinseneiland. The (sums of) the areas of combinations of land use type and precipitation discharge mode are shown in

Table 3.2. The fractions of these areas with respect to the area of the island are shown in Table 3.3.

From these tables it can be seen that about 60% of the area discharges most of the precipitation on the combined sewer. Two thirds of the connected area consist of buildings and the remaining part of paved areas.
Further it can be seen that all of the unpaved area is assumed to be not connected. The unpaved area makes up two thirds of the area not connected. The other not connected part is made up of paved areas like garden paths that are not connected to a sewer. Of the build-up area about 80% is connected to a sewer and about 20% discharges its water outside the area boundaries into a canal.

The not connected buildings consist of shelters that do not have a drainpipe. The external paved areas entail terraces or paths adjacent to the canals.

Table 3.2. Overview of the (sums of) areas (m^2) belonging to combinations of land use type and precipitation discharge modes

Areas [m^2]		Precipitation discharge mode					
		Combined	Separated	Not connected	External	Total	Trees
Land use type	Paved	6792	0	3467	181	10439	1490
	Unpaved	0	0	6948	0	6948	1252
	Build	13438	0	127	3047	16613	150
	Water	0	0	0	0	0	0

	Total	20230	0	10542	3228	34000	2892

Table 3.3. Overview of the (sums of) fractions of the entire area (34.000 m^2) belonging to combinations of land use type and precipitation discharge modes. The numbers marked green are used in the above description.

Fractions [-]		Precipitation discharge mode					
		Combined	Separated	Not connected	External	Total	Trees
Land use type	Paved	0.20	0.00	0.10	0.01	0.31	0.044
	Unpaved	0.00	0.00	0.20	0.00	0.20	0.037
	Build	0.40	0.00	0.00	0.09	0.49	0.004
	Water	0.00	0.00	0.00	0.00	0.00	0.000
	Total	0.60	0.00	0.31	0.09	1.00	0.09

Classification of individual features

In Figure 3.4 the assumed fractions of a feature not connected to a sewer are shown. The dark grey colour indicates features that are not connected to any sewer. The light grey colour means that half of the features area is assumed to discharge most precipitation to a sewer. A white coloured feature is assumed to discharge most precipitation from its entire area to a sewer.

In Figure 10.1 in the appendix the fraction of a feature that discharges most precipitation directly outside the boundaries of the area are shown. A light grey colour indicates that most precipitation on half of the features area is discharged externally.

3.3.3 Precipitation routing

After the classification of the features of the Prinseneiland into the specified land use types in section 3.3.1 and precipitation discharge modes in section 3.3.2 the division of the precipitation over the four pathways is still not completely clear. This is mainly caused by the fact that the precipitation discharge modes specify the *main* pathways. Some of the precipitation on a brick street connected to a sewer will probably infiltrate into the subsoil.

Therefore, for each combination of land use type and precipitation discharge mode the division of precipitation over the four identified destinations is further specified. In Table 3.4 the division of precipitation on the land use types of the Prinseneiland connected to a combined sewer is shown. Following the numbers specified in the table, 63% of the precipitation on paved area (streets) connected to a sewer flows to the combined sewer. The rest (37%) of the precipitation infiltrates into the soil.

Table 3.4. Fractions of the precipitation on land use types connected to a combined sewer following a specific pathway. The numbers marked green are used in the above description.

Precipitation discharge mode		Combined				
Fractions [-]		Combined	Separated	Infiltration	External	
Land use type	Paved	0,63	0	0,37	0	
	Unpaved	0	0	1	0	
	Build	1	0	0	0	
	Water	-	-	-	-	

From Table 3.4 it can also be seen that the pathways do not receive water from all land use types. Furthermore, the pathway to the separated sewer obviously receives no water from features classified with the 'combined' precipitation discharge mode. The high number of parameters that are not informative makes the used framework look a bit inefficient. In future research a more direct framework might prove more efficient.

3.3.4 Structure of the subsoil

The structure of the subsoil of the Prinseneiland is mostly a result of the rise and fall of sea water levels and the resulting processes. As complicating factors the structure of the subsoil of the Prinseneiland has been changed by human intervention and by the shifting of the bed of the IJ estuary throughout the ages. The substrate may thus exhibit large differences in structure over the area. Due to the high degree of heterogeneity (especially in the fill layer), the following description is a reflection of the overall structure of the subsurface. Local deviations in structure are not described here to keep the general picture clear. In Figure 3.5 and Table 3.5 the overall substructure is visualised and summarized.

Fill material:
The top layer of the subsurface of the Prinseneiland is formed by the fill material. This material consists mainly of peat and clay, which was available after the excavation of the surrounding canals. Under the roads (part of) this layer is removed and replaced with sand with debris. Locally, the fill layer also contains wood residues resulting from habitation in earlier ages.

First clay layer, 'Jonge zeeklei':
The layer beneath the fill material consists of marine clay ('Jonge zeeklei') . This clay layer is locally mixed with some peat, or contains thin peat layers. The top of this layer resides between 2 and 3.5 metres below N.A.P.

First peat layer, 'Hollandveen':
Underneath the first clay layer a layer of peat ('Hollandveen') can be found. Locally, the layer contains some clay. The top of the layer lies at a depth of 3 to 4 metres below N.A.P.

Second clay layer, 'Oude zeeklei':
Below the first peat layer lies another layer of marine clay ('Oude zeeklei'). This layer locally contains some sand and/or peat. Also remains of shells can be found in this layer. Because of the twisting and winding of the channel of the IJ estuary throughout the ages, in parts of the area this layer has been (partially) replaced with one or more sand layers (Estuarine deposits). This process mainly took place in the eastern parts of the area. The top of this clay layer resides between 4.5 and 5 metres below N.A.P.. The estuarine deposits start at a depth of 5.5 to 6.5 metres below N.A.P..

Second peat layer, 'Basisveen':
Below the second clay layer lies a thin layer of peat ('Basisveen'). This layer is relatively thin (max. 30 cm.) compared to other locations in the Netherlands. This is caused by intrusions of the sea and/or moving of the IJ estuary scouring most of the sediments away. In the east of the island this layer is moderately to strongly mixed with (estuarine) sand. The top of this layer lies at a depth of 12.5 metres below N.A.P..

Pleistocene sand:
Below the second peat layer lies the Pleistocene sand. This layer starts at a depth of 12.5 to 13.5 metres below N.A.P.

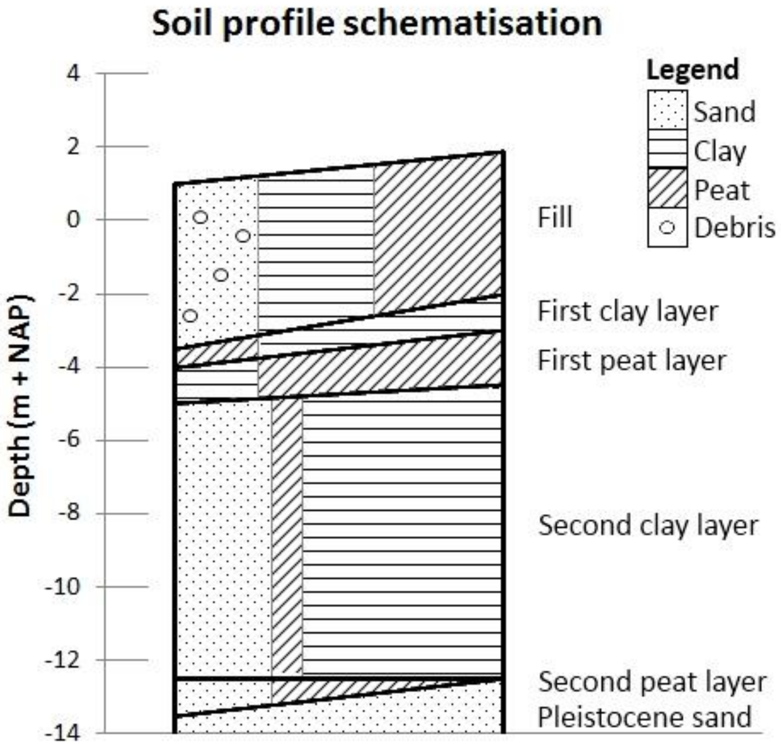

Figure 3.5. Schematisation of the soil profile of the Prinseneiland. The lines between the soil layers indicate differences in depth of the layer boundaries over the island. The shown ratios of soil material in a layer give a crude indication of the extent to which the material is generally present over the area. Even over short distances between locations the rations can differ significantly from each other and the ratios in this figure.

Table 3.5. General soil profile of the Prinseneiland.

Soil layer	Soil type	Depth top of layer
Fill material	Clay and peat, locally garden mould, sand with debris and wooden remains.	Surface
First clay layer, 'Jonge zeeklei'	Clay, locally containing some peat or this peat layers	2 - 3.5m below N.A.P.
First peat layer, 'Hollandveen'	Peat, locally containing some clay	3 - 4 m below N.A.P.
Second clay layer, 'Oude zeeklei'	Clay, locally containing some sand, peat and/or seashells. Replaced locally with estuarine deposits (sand)	4.5 - 5 below N.A.P.
Second peat layer, 'Basisveen'	Peat	12.5 m below N.A.P.
Pleistocene sand	Sand	12.5 - 13.5 m below N.A.P.

4 Available data and information

In this section the measurements that were used/looked at during the study are shown and discussed. In the second part of this section other available information about the Prinseneiland is presented.

4.1 Data from measurements

4.1.1 Precipitation

Available measuring stations
During the research a tipping bucket was used to measure the precipitation in the research area. The tipping bucket was put on top of a roof of a low building (± 3 metres above the surface level) in the north of the Prinseneiland. This location does not meet the standards of the World Meteorological Organisation (WMO[5]) for measuring precipitation, but was chosen because of its secure location and the lack of better, nearby alternatives.

Next to the tipping bucket in the research area data from a KNMI precipitation measurement station in Amsterdam is available. The station is located in the north-eastern edge of the city centre some three kilometres east-southeast of the research area (top right Figure 4.1). In this station precipitation sums are measured by reading a measurement cup at 08:00 UTC[6] each day. This means that a measurement at a particular day consists of precipitation that has fallen between 08:00 hours on the previous day until 08:00 hours on the measuring day. The obtained measurement is validated by the KNMI to ensure a good quality of the data.

The KNMI station at Amsterdam Airport Schiphol[7] is also a potential candidate to retrieve data from for the study. In this station the precipitation sums along with other meteorological variables are measured on an hourly basis. The station is located about ten kilometres to the southwest of the Prinseneiland (bottom left Figure 4.1). Due to this relatively large distance the timing of the measured precipitation may not be representative for the precipitation that fell on the Prinseneiland. Therefore, the hourly precipitation measurements are not used for this study. The daily totals of the measurements over the years 2010 till 2012 are shown in the bottom of Figure 4.2.

Correlation between the time series
Due to the aforementioned problems with and the limited period of the precipitation measurements at the Prinseneiland the representativeness of the measurements at the KNMI stations were investigated to determine whether they can replace the in-situ measurements. The representativeness of the other datasets were determined with the bivariate linear correlation coefficient (see Eq. 4.1.)

$$r = \frac{\sum_{i=1}^{n}\left(x_i - \bar{x}\right)\times\left(y_i - \bar{y}\right)}{\sqrt{\sum_{i=1}^{n}\left(x_i - \bar{x}\right)^2}\times\sqrt{\sum_{i=1}^{n}\left(y_i - \bar{y}\right)^2}} \qquad \text{Eq. 4.1}$$

In which:

r	is the bivariate linear correlation coefficient
x_i	is observation i of variable x
$\bar{x}$	is the average of the observations of variable x
y_i	is observation i of variable y
$\bar{y}$	is the average of the observations of variable y
n	is the number of observations

[5] The WMO website can be found at: http://www.wmo.int/pages/index_en.html
[6] UTC is an abbreviation for Coordinated Universal Time which is the primary time standard by which the world regulates clocks and time. Source: Wikipedia. http://en.wikipedia.org/wiki/UTC
[7] For simplicity Amsterdam Airport Schiphol is abbreviated to Schiphol in the rest of the report

The calculated correlation between daily (08:00 – 08:00) precipitation totals from the tipping bucket at the Prinseneiland and the selected KNMI stations are quite good. The correlation between the measurements from the Prinseneiland and the KNMI stations is 0.88 for both stations. The correlation between the daily totals from the KNMI stations (distance 10.75 km) is also quite good. The bivariate linear correlation coefficient for the daily totals over the period 20010-2012 is 0.86.

Representativeness of the KNMI stations for the Prinseneiland
These numbers show that precipitation measurements at various locations in and near Amsterdam have a quite good correlation. It is therefore assumed that both time series would give a good estimate of the precipitation at the Prinseneiland.

The figures in appendix 11.1, however, show that although the correlation between the measuring stations is quite good there are still differences in precipitation patterns between the locations. The station in Amsterdam measured 22% more precipitation over the period 2010-2012 than the station at Schiphol (over the period 1971-2011 the difference was 10%). It is important to note that this difference in yearly precipitation totals is not caused by an all year higher precipitation rate in Amsterdam. The measurements shows that there is more precipitation in Amsterdam than at Schiphol between September/October and May/June and less during the rest of the year. This may be caused by the effects of urbanisation and/or by the influence of lake IJ on precipitation patterns. Because of these considerations the data from Amsterdam is used for the rest of the study.

Figure 4.1. Locations of the KNMI stations and the Prinseneiland. The location of the Prinseneiland is indicated with the red dot in the top right corner. The locations of the KNMI stations are indicated with the white stars. (Source: Google Maps)

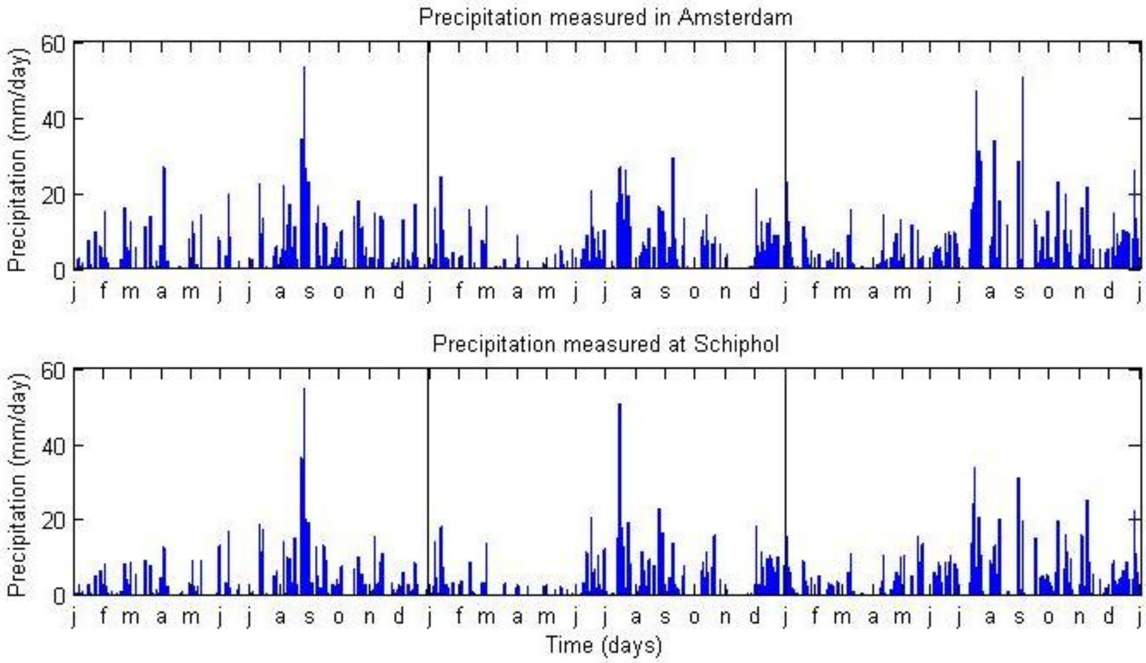

Figure 4.2. Daily (08:00 - 08:00) precipitation sums measured in Amsterdam (top) and at Schiphol (bottom) over the years 2010 till 2012.

4.1.2 Sewer discharges

The sewer discharge from the pumping station on the island are measured with an electromagnetic flow meter. The discharge is measured every minute, but the data that was made available for the study was integrated over a five minute period. This data was then integrated over an entire model day (08:00 - 08:00) to allow the data to be used for validation of the model results. In Figure 4.3 the daily sums of the sewer discharges are shown as a layer of water over the entire study area. This layer of water was arrived at by dividing the daily totals with the surface area of the study area (34.000 m^2).

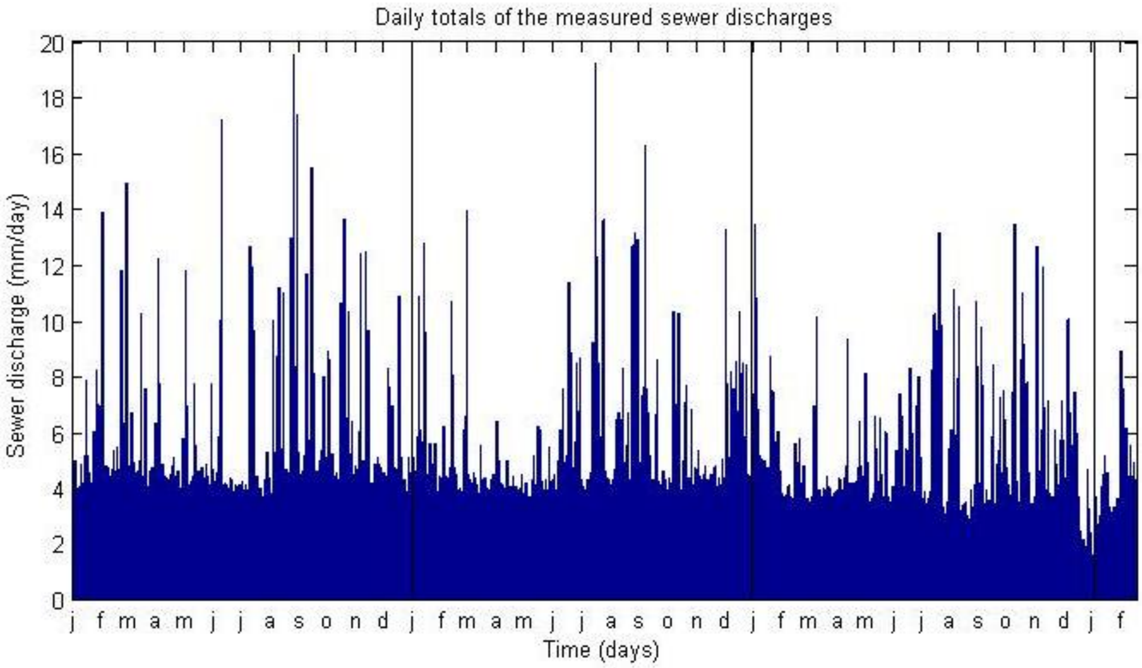

Figure 4.3. The daily totals of the measured sewer discharges of the Prinseneiland over the period Jan. 2010 - Feb. 2013. The labels on the x-axis indicate the first day of the month.

From Figure 4.3 the peak discharges resulting from precipitation events are clearly visible. The more extreme precipitation events not only generate high discharge peaks, but also combined sewer overflow events. These events are not represented in the data.

From the figure it can be seen that there is a seasonal pattern in the base flow of the sewer discharges. This can be caused by seasonal differences in dry weather flow or by water leaking into or out of the sewer. In the results sections of the report the cause for the seasonal pattern is dealt with in more detail. Furthermore, it seems from the graph that the base flow of the sewer discharges is declining over the years. This could be caused by less wastewater being discharged, less groundwater infiltrating into the sewer, more water leaking out of the sewer or a slowly increasing discrepancy between the converted measured signal and the actual discharge.

The data contains an anomaly between the thirteenth of December 2012 and the beginning of January 2013. In that period the base flow and the peak flows are lower than before and after this period. The cause of the anomaly is unknown, but has no influence on the results of the study.

4.1.3 Groundwater levels

Phreatic groundwater levels
The groundwater levels on the Prinseneiland are measured by Waternet at seven locations. The measuring point in the Galgenstraat (centre of the island) was installed in 1994 and is measured by hand between four and ten times per year. A diver was installed in this piezometer at the second of November 2012, which measures every half an hour with a precision of half a centimetre.

In the piezometers on the ‘corners’ of the island and in piezometers ‘C05268’ and ‘C05270’ divers were installed at the start of the study. The diver measures the groundwater level each half an hour. The data that was made available by Waternet covers the period from the nineteenth of September 2012 till the fifteenth of February 2013. The time series from the diver at the Galgenstraat also ends at the fifteenth of February. In Table 4.2 more specifics on the groundwater measuring locations are given.

Figure 4.4. Locations of the piezometers, tipping bucket and sewer discharge measurements. The circles indicate the locations of the piezometers. The 'C0' numbers are the codes for the piezometers. The star specifies the location of the tipping bucket. The square indicates the location of the sewer pump on the island.

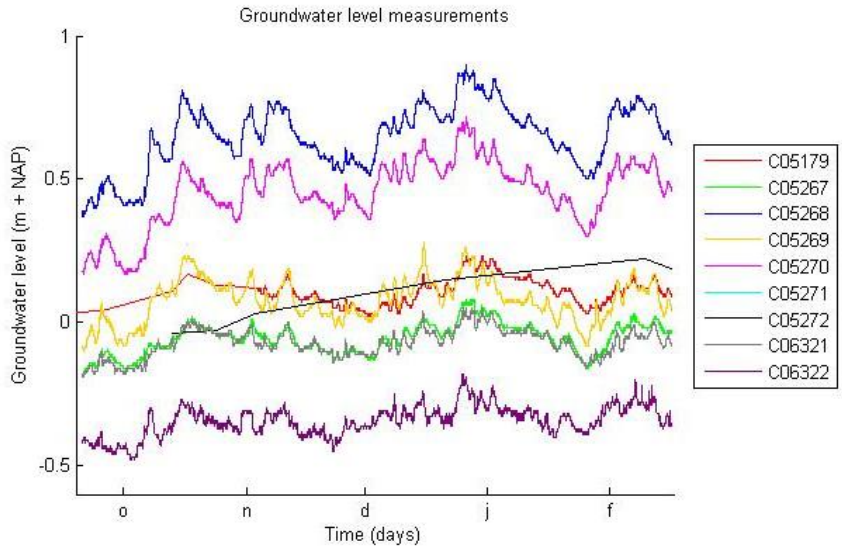

Figure 4.5. Groundwater level measurements over the period from nineteenth of September 2012 till the fifteenth of February 2013. The ticks on the x-axis indicate the beginning of the months. The water level in the nearby canals is at -0.4 metres.

Table 4.1. Names and locations of groundwater level measuring points.

Name	Location
C05179	Galgenstraat
C05267	North West
C05268	Backyard North
C05269	South West
C05270	Backyard South
C05271	Centre North
C05272	West
C06321	North East
C06322	South East

Discussion of the measurements

As can be seen from Figure 4.5, the measured groundwater levels fluctuate at roughly the same moment in time as a result of precipitation events. The magnitude of the variation differs between measuring locations. This is partly due to differences in the fractions of precipitation that infiltrate into the ground. Some differences may be contributed to influences of nearby objects, which cause higher and lower precipitation amounts over the area. Next to those influences there are also loss and delay processes taking place on the surface and in the unsaturated zone. All these influences make predicting groundwater levels a complicated business.

Next to the similarities in timing of the fluctuations in the measured groundwater levels the great range in water levels over such a small island is striking. The two lines at the top are the groundwater level measurements in the backyards of the two blocks of buildings. Their higher mean level can be attributed to a higher fraction of precipitation infiltrating. As a result, the groundwater levels in the backyards are about one third of to half a meter higher than measured elsewhere on the island.

The measured groundwater levels in the south east (C06322) are just above or around the water level of the nearby canals. This can be caused by a high connectivity between the canal and the subsurface and/or a higher flux to deeper groundwater. A higher connectivity with the canal could be caused by an unknown subsurface drain. A higher flux to the deeper groundwater can be caused by a thinner resistance (clay/peat) layer and/or punctures in the resistance layer due to removed pile foundations of replaced buildings.

The groundwater levels measured in the south west of the island (C05269) show a fluctuation that is most likely caused by the higher infiltration in the gardens in the vicinity of the measuring point. The higher mean groundwater levels could be caused by a sheet pile wall stretching the southern perimeter of the island hampering the drainage to the canals and thereby causing a higher groundwater level.

Deeper groundwater levels

In Figure 4.6 the groundwater levels in the Pleistocene sand layer over the years 2010 and 2011 measured near Planciusstraat 50 in Amsterdam (180 metres to the west of the Prinseneiland) are shown. In the same figure the phreatic groundwater levels measured at the Galgenstraat are shown for comparison. As can be seen from the figure, the groundwater level in the Pleistocene sand layer varies around 1.5 metres below N.A.P.. Because of the likely connection between the Pleistocene sand layer at both locations, it is assumed that the groundwater level in the Pleistocene sand layer at the Prinseneiland is the same as in the Planciusstraat.

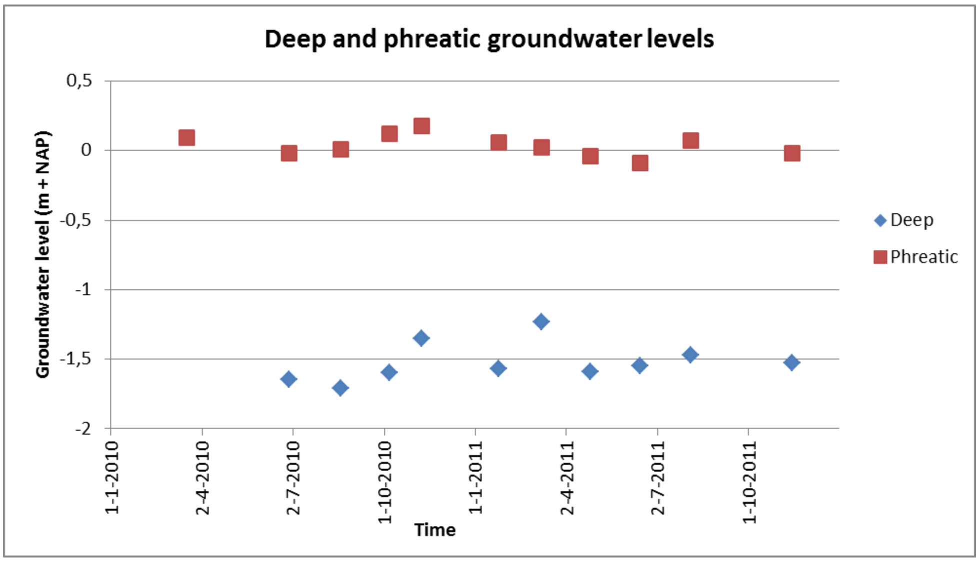

Figure 4.6. Groundwater levels over the years 2010 and 2011 in the Pleistocene sand layer (Deep) and the phreatic groundwater measured at the Galgenstraat.

Table 4.2. Details on the groundwater measuring locations.

Code	Location	R.D. X (m)	R.D. Y (m)	Surface (m + NAP)	Ref. point (m + NAP)	Top filter (m + NAP)	Bottom filter (m + NAP)	Distance to canal (m)
C05179	Galgenstraat 14	120949	488755	1,41	1,38	-1,1	-2,1	52
C05267	Prinseneiland 18	120923	488852	1,06	0,96	-1,54	-2,54	21
C05268	Prinseneiland 73	120950	488789	1,27	1,27	-0,26	-1,26	50
C05269	Prinseneiland 24A	120912	488693	1,43	1,31	-1,19	-2,19	20
C05270	Prinseneiland 269	120957	488686	1,85	1,68	-0,82	-1,82	45
C05271	Prinseneiland 45	120955	488834	1,14	1,11	-0,82	-1,82	40
C05272	Prinseneiland 19	120919	488734	1,9	1,83	-0,55	-1,55	25
C06321	Prinseneiland 33	120988	488859	1,12	1,05	-0,88	-1,88	21
C06322	Prinseneiland 345	120986	488653	1,47	1,42	-1,03	-2,03	25
C05177	Planciusstraat 50	120786	488833	1,48	1,62	-12,9	-13,9	-

4.1.4 Potential (crop) evaporation data

The best estimate for the potential evaporation at the Prinseneiland can be obtained from the KNMI measuring station at Schiphol. The KNMI publishes the meteorological measurements from all its major measuring stations on its website[8]. The data includes hourly or daily averages of the wind speed, temperature, relative humidity and incoming radiation and precipitation sums. Next to these data the reference crop evaporation calculated with the Makkink formula (Eq. 4.2) is given.

The reference crop evaporation is an indication for plant transpiration and is defined as the amount of transpiration from a well-watered and well-fertilized field covered with grass. In order to derive actual transpiration the reference evaporation has to be multiplied with a crop factor to correct for the crop type and a water stress function to correct for water shortages.

The open water evaporation was calculated with the Penman formula (Eq. 4.3) using the meteorological data from the KNMI station at Schiphol.

[8] Website: http://www.knmi.nl/index_en.html or http://www.knmi.nl/ (in Dutch)
http://www.knmi.nl/klimatologie/uurgegevens/ For hourly data from the main weather stations.
http://www.knmi.nl/klimatologie/daggegevens/download.html for daily data from the main weather stations.
http://www.knmi.nl/klimatologie/monv/reeksen/ for daily data from the precipitation measuring stations.

$$\lambda \times E_{ref} = 0.65 \times \frac{s}{s+\gamma} \times K_{in}$$ Eq. 4.2

$$E_O = \frac{\frac{s \times R_N}{\rho \times \lambda} + \frac{c_p \times \rho_a}{\rho \times \lambda} \times \frac{e_s - e_a}{r_a}}{s+\gamma}$$ Eq. 4.3

In which,

λ	latent heat of vaporization (2.45 MJ/kg)
E_{ref}	reference crop evaporation (kg/m^2.s)
s	slope of the saturation vapour pressure-temperature curve (kPa/°K)
γ	psychometric constant (0.066 kPa/°K)
K_{in}	incoming shortwave radiation (W/m^2)
E_O	open water evaporation (m/d)
R_N	net radiation on the earth's surface (J/d.m^2)
ρ	density of water (kg/m^3)
c_p	specific heat of air at constant pressure (1004 J/kg. °K)
ρ_a	density of air (1.205 kg/m^3)
e_s	saturation vapour pressure for the air at two metres height (kPa)
e_a	actual vapour pressure in the air at two metres height (kPa)
r_a	aerodynamic resistance (d/m)

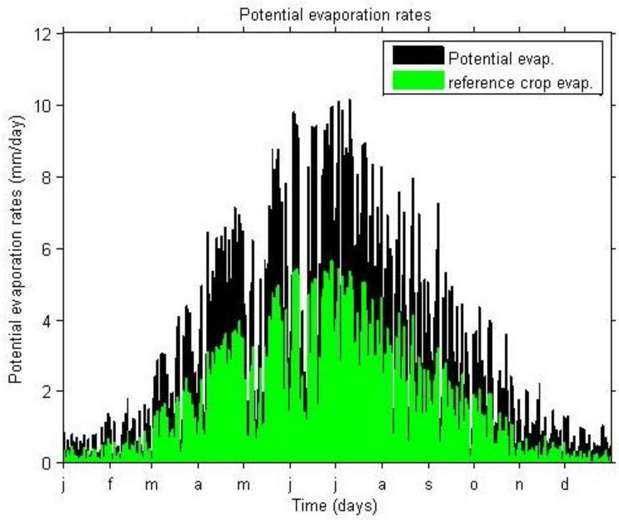

Figure 4.7. Potential evaporation (Penman, Eq. 4.3) and reference crop evaporation (Makkink, Eq. 4.2) in the year 2010. The ticks on the x-axis indicate the first day of the month.

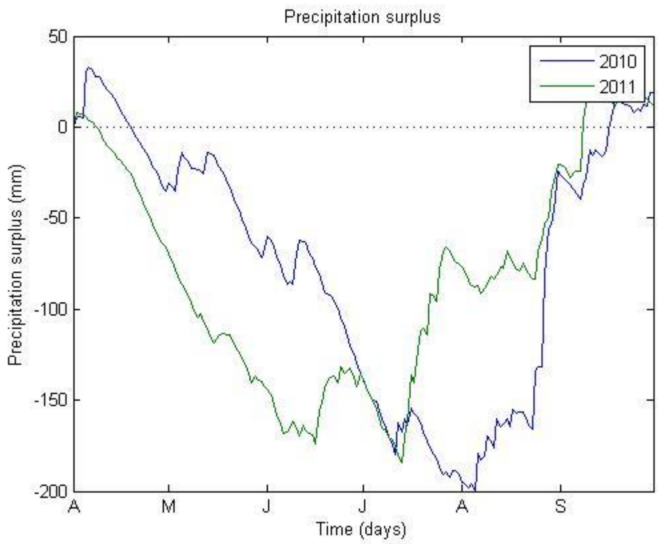

Figure 4.8. The precipitation surplus for the years 2010 and 2011. The precipitation surplus is defined as the cumulative precipitation exceeding the reference crop evaporation since the first of April. The ticks on the x-axis indicate the first day of the month.

4.1.5 Drinking water supply

The drinking water supplied to the Prinseneiland was not measured directly. Waternet made a time series of the drinking water supply to the city of Amsterdam available to allow for an estimation of the drinking water supply. The estimation was made by taking a fraction of the measured supply as the base flow of the sewer discharges. The fraction was taken such that the simulated base flow did not exceed the measured base flow too often. The estimated drinking water supply is shown in Figure 4.9. The average daily supply is equivalent to a 3.5 mm layer of water over the entire study area. This is equal to 119 m^3 of water. The available data did not include the year 2013. Therefore, the drinking water supply was assumed to be 3.5 $mm.day^{-1}$ for the remainder of the study period.

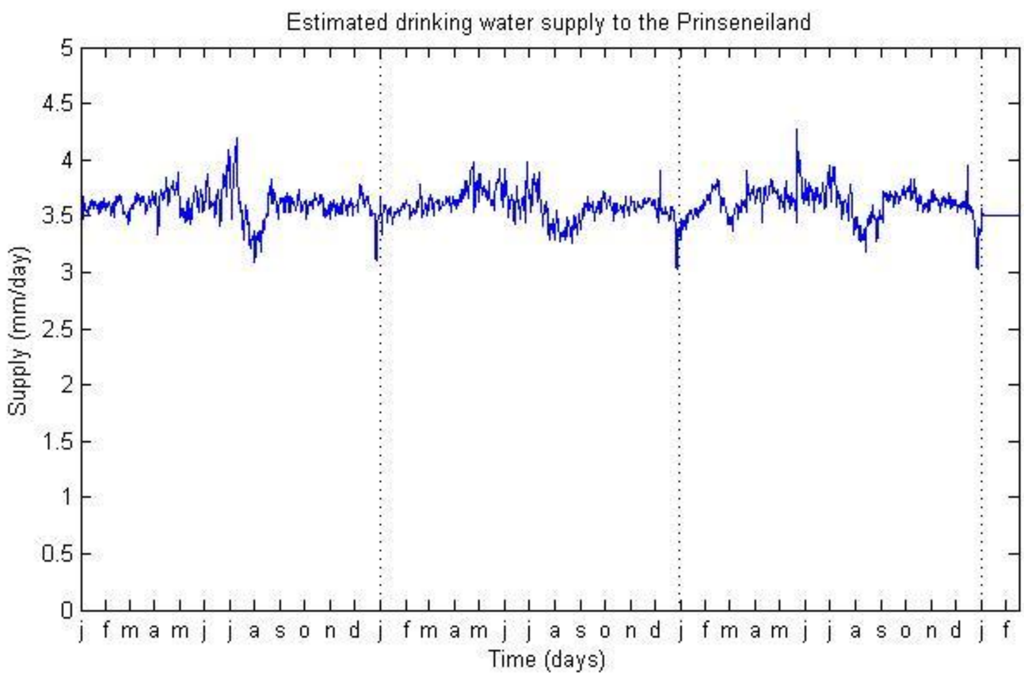

Figure 4.9. Estimated drinking water supply to the Prinseneiland (mm/day) over the period Jan. 2010 – Feb. 2013. The supply is based on the daily totals of the drinking water supply to the city of Amsterdam.

4.2 Other available information

4.2.1 Land use data sources

To determine the land uses and its distributions over the area a GIS of a base map (Grootschalige Basiskaart Amsterdam or GBKA) was used. This map was used with knowledge of the area to determine the land uses in the area. The map with land use types assigned to the features is shown in Figure 3.3.

Next to the map an aerial photograph of the island from 2011 was provided by Waternet (shown in Figure 3.1).

4.2.2 Additional information about the sewer system

Next to the sewer discharges Waternet also provided additional information regarding the sewer system. Firstly, the design of the sewer system was made available. In this design the dimensions and the layout of the system are shown. The system has about 160 m^3 of storage. The pumping station on the island has a maximum pumping capacity of 40 m^3/hour.

The sewer was constructed in 1988. Due to its relative young age, little to no leakage is expected. Inspection reports of video inspections done in 2005 were also provided by Waternet. These reports indicated that on three locations in the system superficial damage to the concrete was spotted and that the joint between the pipe and the manhole had rotated. These damages are not reported as serious and are located in an upstream section of the system where the groundwater level fluctuates around the bottom of the pipe. It is therefore assumed that any leakages are within the uncertainty limits of the sewer inflow and outflow and of the fluxes to and from the groundwater.

4.2.3 Additional information about the drinking water supply system

Note on the estimated drinking water supply discharge
The average estimated drinking water supply discharge is about 119 m^3 per day. When the daily water use per capita per day is estimated at 0.134 m^3/cap.day (average water use in Amsterdam), the estimated discharge indicates a population of about 888 person equivalents on the island.

The drinking water supply system on the island has about 350 house connections. With an average household size of about 1.5 - 2 persons[9], this amounts to a population between 525 and 700 persons. The exact number of people living on the island was not examined during the study, because of the limited value of such information for estimating the drinking water supply. For a check on the performance of the sewer system in 2008 the number of inhabitants was estimated at 530.

It should be noted though, that the number of inhabitants is not the only influence on the supply to an area. The water use in offices and companies has to be added to the discharge to the island. Another important factor affecting the discharge is the amount of water used per capita by the inhabitants. The value that was used for the above calculation may not be representative for the water use by the inhabitants of the Prinseneiland.

Leakage of the drinking water supply system
The unaccounted for water from the drinking water supply to the city of Amsterdam as a whole is about 3.5%[10] of the total amount supplied to the city. Because the drinking water supply system of the Prinseneiland is relatively young compared with the rest of the city, it is assumed that the leakage of the system is between 0 and 2% of the total supply to the island.

[9] Source: Centraal Bureau voor de Statistiek, http://www.cbs.nl/nl-NL/menu/themas/bevolking/publicaties/bevolkingstrends/archief/2012/2012-bevolkingstrends-huishoudensgrootte-steden-art.html
[10] Personal correspondence with a senior asset manager of the drinking water branch of Waternet.

4.2.4 Soil surveys on the island

A couple of reports of soil surveys performed on the island were provided by Waternet. With the reports of these surveys the section about the subsurface of the Prinseneiland was drawn up. In appendix 13 some of the schematisations from these surveys are shown. The legends of these figures are in Dutch. A table containing the translation of the most important words has been added.

4.2.5 Representativeness of the years 2010, 2011 and 2012

In order to cover ground quickly in setting up and testing the model meteorological data of the past few years was used (mostly 2010 and 2011). To determine the representativeness of these data qualitative statements made by the KNMI about the season averaged precipitation, sunshine duration and temperature are used. These statements describe the deviations of the season averaged data from the data averaged over the last thirty years. The results are summarized in Table 4.3.

Table 4.3. Indication of representativeness of season averages of precipitation, sunshine and temperature. Winter: Dec.-Feb., Spring: Mar.-May, Summer: June-Aug., Autumn: Sep.-Nov. Source: KNMI[11] (Royal Dutch Meteorological Institute) website

Season	Precipitation	Sunshine	Temperature
Winter 2009-2010	Wet (snowy)	Normal	Coldest since 1996
Spring	Dry	Very sunny	Coldest since 1996
Summer	Wet	Sunny	warm
Autumn	Normal	Normal	Quite cold
Winter 2010-2011	Quite dry	Normal	Quite cold
Spring	Driest in recorded history	Sunny	Warm
Summer	Exceptionally wet	Clouded	Quite cool
Autumn	Dry	Very sunny	Very warm
Winter 2011-2012	Relatively wet	Sunny	Warm (cold end)
Spring	Dry	Sunny	Warm
Summer	Wet	Normal	normal
Autumn	Dry	Sunny	normal

Judging from the indications in the table, the years 2010 till 2012 - in terms of season averaged precipitation, sunshine duration and temperature - may not be the most representative for the Dutch climate. They do, however, provide a good opportunity to see the effects of variations in weather conditions on the urban water balance.

The first part of the year 2011 was exceptionally dry and the resulting moisture deficit was even worse than the drought of 1976, which turned out to be the worst drought of the twentieth century. The exceptionally wet summer of 2011 made up for the deficit and prevented or diminished further damage.

[11] 2010:
http://www.knmi.nl/klimatologie/maand_en_seizoensoverzichten/seizoen/win10.html
http://www.knmi.nl/klimatologie/maand_en_seizoensoverzichten/seizoen/len10.html
http://www.knmi.nl/klimatologie/maand_en_seizoensoverzichten/seizoen/zom10.html
http://www.knmi.nl/klimatologie/maand_en_seizoensoverzichten/seizoen/her10.html
2011:
http://www.knmi.nl/klimatologie/maand_en_seizoensoverzichten/seizoen/win11.html
http://www.knmi.nl/klimatologie/maand_en_seizoensoverzichten/seizoen/len11.html
http://www.knmi.nl/klimatologie/maand_en_seizoensoverzichten/seizoen/zom11.html
http://www.knmi.nl/klimatologie/maand_en_seizoensoverzichten/seizoen/her11.html
2012:
http://www.knmi.nl/klimatologie/maand_en_seizoensoverzichten/seizoen/win12.html
http://www.knmi.nl/klimatologie/maand_en_seizoensoverzichten/seizoen/len12.html
http://www.knmi.nl/klimatologie/maand_en_seizoensoverzichten/seizoen/zom12.html
http://www.knmi.nl/klimatologie/maand_en_seizoensoverzichten/seizoen/her12.html

5 The urban water balance model

5.1 Introduction

5.1.1 The model concept

The urban water cycle is modelled as a conceptual model in which the main processes of the urban water cycle are modelled on a daily basis. The model treats an area as a homogeneous entity with parameter values and variables representing a sort of 'average' over the area. The daily time step results in the model calculating (with) daily averages.

Considerations
This approach has been chosen to ensure short calculation times, which allow one to see the effects of changes made to the model input very quickly. The model generates limited output, which makes it easier to interpret the effects of changes in the model input on the urban water cycle.

Next to that, due to the limited number of measuring locations and the high heterogeneity of an urban environment a distributed model would only generate a lot of uncertain output. This uncertainty is caused by the limited opportunity for validation on measurements and limited information on the heterogeneities that need to be modelled to get consistent output.

The disadvantages of this model set up are the loss of information on the extremes in both space and time. The lumped results for instance do not show the groundwater varying with the distance to nearby surface waters. The time step of one day results in the loss of information on for example the effects of high intensity precipitation events. Furthermore, a lumped model misses out on the effects of land use on for instance groundwater recharge, due to the averaging over the area.

The disadvantages with respect to averaging over a larger area can be countered by modelling only a small part of the study area. That way it is possible to study the effects of land use and distance to a nearby surface water. It should be noted though that the most reliable results are obtained when the model of the smaller area can be calibrated, for instance on groundwater levels.

5.1.2 Model contents

The urban water cycle
In the urban water balance model the urban water cycle is modelled. The urban water cycle can be thought of as the hydrological cycle of an urban area supplemented with the urban water system.

The urban hydrological cycle
The hydrological cycle in an urban area is more or less the same as in a rural area. The same processes take place in both areas. In the urban areas there is a shift from infiltration to surface runoff as the main process following precipitation. Next to this difference the heterogeneity in an urban area is larger than that of a rural area. In an urban area more functions need to be fulfilled in closer proximity to each other. This means that in an urban area more different land uses occur, which need to be taken into account.

The small urban water cycle
The small urban water cycle consists of the drinking water supply system and the wastewater collection (and treatment) system. In the wastewater collection system water coming from the households - used drinking water - and precipitation runoff are collected separately or combined and pumped out of the urban area.

5.1.3 Boundaries of the model

The boundaries of a research area that is to be modelled should be chosen with care. Features that can be used to form a boundary of the area should have a known or easy to measure head or flow. To the sides of the area a known head can be given by a water body that penetrates to a confining layer. An example of a known flow boundary is a sheet pile wall, which can be assumed to block any flow of water. To below one can place the boundary at the top of a soil layer with a high resistance to flow that is between the phreatic groundwater and a deeper groundwater body. The boundary is then modelled as a known or knowable flow.

In the case of the Prinseneiland the boundaries to the side are formed by the canals surrounding the island. The water level in the canals is assumed to be 0.4 metres below N.A.P., which is the water level of the adjacent lake IJ. Further it is assumed that variations over the day are averaged out and that higher water levels in wet periods are controlled enough to have little impact.

The boundary to the bottom is formed by the clay and peat layers discussed in section 3.3.4. The resistance to flow of these layers is assumed to be 8,000 days, which is a little lower than the 10,000 days resistance used in most groundwater models of Amsterdam. A lower resistance was chosen due to the influence of the IJ estuary in earlier times, which caused sand to be deposited in the layers. The head in the deeper groundwater body is assumed to be the same as the head measured at the Planciusstraat in Amsterdam (see section 4.1.3).

5.1.4 Definitions used in the model description

Urban groundwater:	The phreatic groundwater body of the modelled area
Regional groundwater:	The deeper groundwater body underneath, outside the modelled area
Urban surface water:	Surface water bodies within the boundaries of the modelled area
Regional surface water:	Surface water bodies outside the boundaries of the model, but with an influence on the modelled area. It is best to keep surface water bodies that discharge a lot of water outside the boundaries of the model.

5.2 Model structure and processes

5.2.1 Model structure

A visualisation of the model structure is shown in Figure 5.1. The **atmosphere** is shown at the top of the figure, outside the model boundaries. From the atmosphere part of the *precipitation* is routed to the **trees**, where a part of the precipitation is *intercepted* and the rest becomes *throughfall*. The other part of the precipitation is routed together with the throughfall to the **surfaces** or to an **urban water body**.

The surfaces are divided in the three land use types from which part of the precipitation is *intercepted* and the rest of the precipitation becomes *infiltration*, *sewer inflow* or *runoff*. The infiltration is routed to the **unsaturated zone** reservoir from which *transpiration* by vegetation takes place. When the storage in the reservoir is higher than field capacity, *percolation* of water to the **urban groundwater** occurs. When the storage is lower than field capacity, *capillary rise* from the urban groundwater occurs. From the urban groundwater *drainage* of water to or from the **regional surface** water and *seepage* to or from the **regional groundwater** takes place. Water stored in the urban surface water reservoir partly *evaporates* and may flow to or from the urban or regional groundwater.

The inputs to the **sewer**(**s**) consist of the *sewer inflow*, *dry weather flow* and potentially groundwater *leaking* into the sewer. Outflow consists of pumping/flowing of wastewater outside the model boundaries (*WWTP*), *overflows* or *outflows* and potentially *leakage* to the unsaturated zone.

In the following subsections the processes incorporated in the model are described. The descriptions do not include how the process is modelled. Information on the modelling can be found in section 5.3.

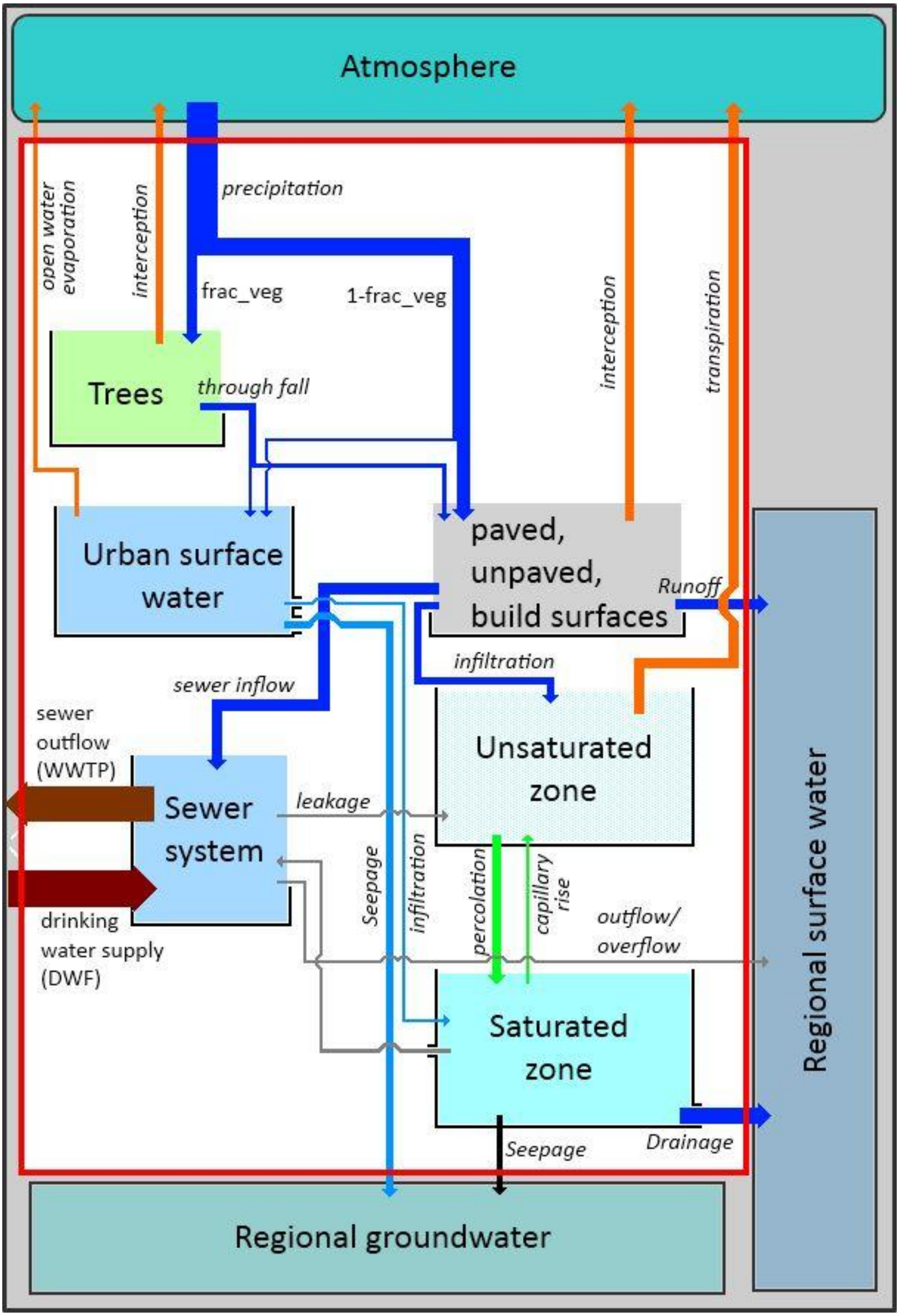

Figure 5.1. Structure of the model showing the storages and fluxes and some simplified relations. The thicknesses of the arrows are for illustrative purposes only. They should not be interpreted as the size of the fluxes. The red line indicates the model boundary.

5.2.2 Interception evaporation

Interception evaporation
"[…] interception represents a loss of rainfall which would otherwise be available to the soil." (Horton, 1919, pp. 1) Horton posed this definition of interception for use in rural areas. For an urban area this definition should be expanded with; 'or would runoff to a storm water collection system or a surface water body.'. Thus the 'loss of rainfall' consists of interception by surfaces above the terrain and moisturising losses and depression storage on the terrain.

Interception by vegetation
Interception in a narrow sense is the part of the precipitation that stays on vegetation (or other surfaces above the terrain) it fell on and from which that part is evaporated before it has a chance of reaching the surface. Interception in this sense mainly takes place on tree canopies and on vegetation, which is concentrated on unpaved surfaces.

Moisturising losses on the terrain surface
Moisturising loss is the part of the precipitation that stays on the terrain it fell on. The terrain in this sense consists of the top layer of the soil, paved surfaces, walls and roofs of buildings. This part of the precipitation moistening the terrain is later evaporated.

Depression storage evaporation
When precipitation exceeds the moisturising capacity runoff is generated. Part of this runoff may end up in depressions on the terrain surface. From these depressions stored water can evaporate (or infiltrate into the subsoil or become external runoff or sewer inflow).

Routing of remaining precipitation
The precipitation that is left after the interception evaporation processes flows to a combined or separated sewer, infiltrates into the soil or flows directly outside the model boundaries. The framework that is used for the division of the precipitation over the four pathways has been discussed in sections 3.3.2 and 3.3.3. The fractions of the precipitation that follow a specified pathway are determined per land use type and are used by the model to rout the available precipitation over the pathways.

5.2.3 The urban surface water

The urban surface water is modelled as a reservoir with inflow from precipitation on the surface classified as 'water' and outflow from open water evaporation. Furthermore, the surface water can exchange water with the urban groundwater, when the boundaries of the surface water body are permeable. When the surface water touches the confining layer between the urban and the regional groundwater, there can also be a flow between the urban surface water and the regional groundwater.

5.2.4 The unsaturated zone

The unsaturated zone is the part of the soil profile that is in between the surface and the urban groundwater. Inflow into the unsaturated zone comes from the infiltration of precipitation, leakage from sewer pipes and/or the drinking water supply system and irrigation. Vegetation on the surface extracts water from the unsaturated zone for transpiration. The energy that is used for the transpiration is deducted from the available potential evaporation. There is also an exchange of water between the unsaturated and the saturated zone. Downward flow of water is called percolation and upward flow capillary rise.

5.2.5 The urban groundwater

The urban groundwater is recharged by percolation of water from the unsaturated zone and is partially depleted by capillary rise. The urban groundwater can further exchange water with the sewer through leakage, urban surface waters, regional surface waters and the regional groundwater. The driving force for all these exchanges of water is the difference in water level or head. A potential outflow of the urban groundwater is groundwater abstraction. Furthermore, the urban groundwater can receive water from the leaking drinking water mains. In extreme circumstances the urban groundwater may lose water to the drinking water mains.

5.2.6 The sewer system

The sewer system consists of the storm water collection systems (gully pots, etc.), the connections to the households and businesses, the sewer pipes, outflow/overflow structures and in some cases a pumping station. The sewer system in an area can be a combined or separate system or a combination of both.

The combined system is a one pipe system in which both the storm water as the household water are collected. In case of extreme precipitation the system may not be able to store and discharge all the received water and overflow into a surface water body.

The separated system is a two pipe system. This means that the storm water and the household water have a pipe of their own. The household water is discharged to a wastewater treatment plant (WWTP). The (relatively) clean storm water flows out of the sewer into a nearby surface water body. The model also incorporates the simulation of 'first flush' systems. These 'first flush' (or 'improved') systems capture the first part of a precipitation event and pump the water over to the wastewater pipe.

5.3 Modelling of the model processes

In this section of the report a short description on how the processes described in section 5.2 are modelled is given. In section 5.4 the model parameters and their values for the modelling of the Prinseneiland are discussed.

5.3.1 Interception by trees

In the model the interception by trees is modelled as a separate process, because of the large interception capacity of trees. Another reason for modelling it as a separate process is the possibility of investigating the impact of the interception by trees on the urban water cycle.

The interception by trees is modelled as a threshold process from which throughfall ('*Pnet*') is generated when the precipitation exceeds the interception capacity of the trees (*'SIntTree*') [L]. The intercepted precipitation stored (*'S_tree*') on the surfaces can then be evaporated. The evaporation (*'Eint_tree*') can never exceed the potential (open water) evaporation ('*Ep*'). General values for the interception capacity of a wide variety of plants can be found in Breuer et al., 2003.

The fractions of the land use types overhung by tree canopies is specified with the parameters (*'frac_veg_paved', 'frac_veg_unpaved', 'frac_veg_water' and 'frac_veg_build'*). The sum of these fractions is the parameter ('*frac_veg'*).

$$Pnet = \max(P - SIntTree, 0) \quad \text{Eq. 5.1}$$

$$E\text{int\_}tree = \min(S\_tree, Ep) \quad \text{Eq. 5.2}$$

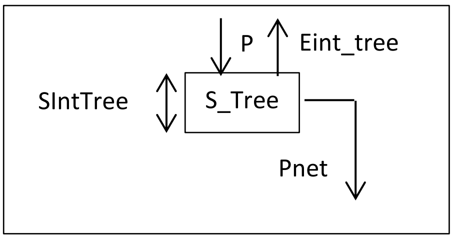

The amount of energy that is used for the interception evaporation is deducted from the potential evaporation to ensure that not more evaporation is simulated than possible.

Routing of the throughfall
The precipitation that reaches the surface consists of precipitation that fell next to a tree (direct) and the throughfall. The amount of precipitation reaching the surface of land use type ('_x') is calculated with Eq. 5.3.

The first term represents the direct precipitation and the second term the throughfall. The direct precipitation (‘*P*’) falls on the areal fraction of the land use type (‘*frac*_x’) minus the fraction that is overhung by trees. The throughfall on the land use type is a fraction of the total throughfall. This fraction is the fraction of the by tree canopy overhung area belonging to the land use type (‘*frac_veg_x*’ / ’*frac_veg*’). So, when for instance 20% of the tree canopy is above paved surface, 20% of the trough fall is routed to the paved surface.

$$Pnet\_x = P \times \left(frac\_x - frac\_veg\_x \right) + Pnet \times \frac{frac\_veg\_x}{frac\_veg} \qquad \text{Eq. 5.3}$$

5.3.2 Interception evaporation from the surface

Part of the precipitation that reaches the surface is evaporated before it can take part in other processes. This evaporation consists of interception from vegetation on unpaved area, evaporation of moisturising losses and from depression storages. This interception evaporation on the surface is also modelled as a threshold process. The amount of water evaporated is calculated with Eq. 5.4. The evaporation is the minimum of the amount of precipitation that reached the surface (‘*S_x*’); the potential evaporation (‘*Ep*’) times a correction factor (‘*ec_x*’) and the fraction of land use involved (‘*frac_x*’); the height of the threshold (‘*S_x_int*’). The amount of energy that is used for this evaporation is deducted from the potential to ensure a closed energy balance.

$$E\,\mathrm{int}\_x = \min(S\_x, Ep \times ec\_x \times frac\_x, S\_x\_\mathrm{int}) \qquad \text{Eq. 5.4}$$

The correction factor ‘*ec_x*’ is used to compensate for differences in potential evaporation at the measuring location and the modelled area. This difference is caused by more storage of heat and a reduction in evaporative cooling in urban environments. This causes an urban environment to be warmer than a rural environment (‘Urban heat island, Oke 1982) and thus potentially higher potential evaporation. Next to that, Van de Ven (1985) identified the heating of surfaces by solar radiation prior to evaporation as a process that enhances the amount of evaporation. For this study the model is run at a daily timescale, which makes corrections for temporary storage of heat in urban surfaces unnecessary.

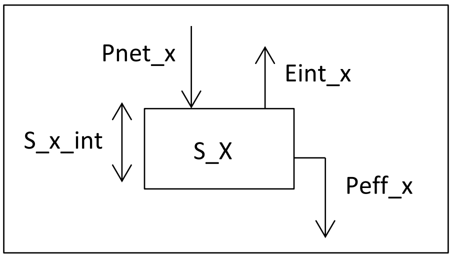

5.3.3 Precipitation routing over the pathways

The precipitation remaining after the evaporation processes can flow to a combined or a separated sewer, infiltrate into the soil or flow directly outside the model boundaries. The precipitation on the land use types is divided with the parameters ‘*c_x*’, ‘*s_x*’, ‘*i_x*’ and ‘*r_x*’. These parameters represent the land use type averaged fractions of the precipitation that follow the above mentioned pathways. The values of these parameters are arrived at by taking the land use type average of similar parameters for the combination of land use types and precipitation discharge modes.. Eq. 5.5 forms the law of conservation of mass for the division of the precipitation.

$$c\_x + s\_x + r\_x + i\_x = 1 \qquad \text{Eq. 5.5}$$

Combined sewer inflow

A part of the precipitation that is not intercepted flows to the combined sewer. The total inflow into the combined sewer (‘*Qcs*’) is the sum of the not evaporated precipitation on the land use surfaces (‘*S*_x’) times the fractions of the precipitation that flow to the combined sewer (‘*c_paved*’,’*c_unpaved*’,’*c_build*’).

$$Qcs = \sum c\_x \times S\_x \qquad \text{Eq. 5.6}$$

Separated sewer inflow

A part of the precipitation that is not intercepted flows to the storm water part of the separated sewer. The total inflow into the separated sewer (‘*Qss*’) is the sum of the not evaporated precipitation on the land use surfaces (‘*S*_x’) times the fractions of the precipitation that flow to the separated sewer (‘*s_paved*’, ‘*s_unpaved*’, ‘*s_build*’).

$$Qss = \sum s\_x \times S\_x \qquad \text{Eq. 5.7}$$

Infiltration into the soil

A part of the precipitations that is not intercepted infiltrates into the soil. The total infiltration into the soil (‘*I*’) is the sum of the not evaporated precipitation on the land use surfaces (‘*S_x*’) times the fractions of the precipitation that infiltrates into the soil (‘*i_paved*’,’*i_unpaved*’,’*i_build*’).

$$I = \sum i\_x \times S\_x \qquad \text{Eq. 5.8}$$

Flow directly outside the boundaries

A part of the precipitation that is not intercepted flows directly outside the model boundaries. The total flow (‘*R*’) is the sum of the not evaporated precipitation on the land use surfaces (‘*S_x*’) times the fractions of the precipitation that flows directly outside the model boundaries (‘*r_paved*’,’*r_unpaved*’,’*r_build*’).

$$R = \sum r\_x \times S\_x \qquad \text{Eq. 5.9}$$

5.3.4 The urban surface water

From the urban surface water reservoir evaporation takes place and (potentially) an exchange of water with the urban and/or regional groundwater. The evaporation from the urban surface water is the minimum of the amount of water available (‘*S_water*’) and the potential open water evaporation (‘*Ep*’) times a correction factor (‘*ec_water*’) times the fraction of the area classified as urban surface water (‘*frac_water*’) (Eq. 5.10).

The exchange of water between the urban surface water and groundwater is calculated with Eq. 5.11. In this equation the first term is the difference between the surface and groundwater level. This term is multiplied with a recession value (‘*i_water_ugw*’) [T^{-1}] that represents the connectivity between the surface and groundwater bodies and with the fraction of the area classified as urban surface water (‘*frac_water*’).

The exchange of water between the urban surface water and the regional groundwater is calculated with Eq. 5.12. In this equation the first term is the difference between the urban surface water and regional groundwater level. This term is multiplied with a recession value (‘*i_water_rgw*’) [T^{-1}] that represents the connectivity between the surface and groundwater bodies and with the fraction of the area classified as urban surface water (‘*frac_water*’).

$$Ea\_water = \min(S\_water, Ep \times ec\_water \times frac\_water) \qquad \text{Eq. 5.10}$$

$$I\_water\_ugw = (H\_ugw - H\_water) \times i\_water\_ugw \times frac\_water \qquad \text{Eq. 5.11}$$

$$I\_water\_rwg = (H\_rgw - H\_water) \times i\_water\_rgw \times frac\_water \qquad \text{Eq. 5.12}$$

5.3.5 The unsaturated zone

The inflow into the unsaturated zone consists of infiltration (both natural and from infiltration systems), irrigation (garden watering) and leakage from the sewer and/or drinking water mains. The influx then flows down to the saturated zone through the pore matrix or through macro pores.

The distribution of the influx over the matrix and the macro pores is done with Eq. 5.13. This equation is taken from the FLEX model described in Fenicia et al. 2006. The equation assumes an S-shaped relation between the moisture content in the unsaturated zone (‘*S_uz*’/‘*UZmax*’) [-] and the proportion of the influx becoming macro pore flow. This schematisation results in a large fast flux during high moisture contents and a small fast flux during low moisture contents. The difference in the proportion between high and low moisture contents is controlled with the parameters ‘gamma’ and ‘*beta*’.

$$Cr = \frac{1}{1+e^{\frac{\frac{S\_uz}{UZ\max}+gamma}{beta}}}$$ Eq. 5.13

The part of the influx that flows into the pore matrix (1 – Cr) is either held in the unsaturated zone against gravity or slowly percolates to the saturated zone depending on the moisture content. When the amount of water stored in the unsaturated zone is higher than '*UZmax*' [L], water can percolate down to the saturated zone. When the stored amount is lower than '*UZmax*', some water flows from the saturated zone to the unsaturated zone due to capillary rise. This slow percolation/capillary rise process is schematised with Eq. 5.14. The parameter '*c_ugw*' [$L.T^{-1}$] denotes the maximum amount of flow. The term between brackets determines the direction of flow and to what extend the maximum flow is reached. Please note that the maximum flow is reached when the amount of storage in the unsaturated zone is either double of '*UZmax*' or zero.

$$C\_ugw = c\_ugw \times \left(1 - \frac{S\_uz}{UZ\max}\right)$$ Eq. 5.14

Transpiration
Transpiration of water from the root zone by plants ('*Et*') is modelled with Eq. 5.26 (partially from Fenicia et al., 2006). The amount of transpiration depends on the reference crop evaporation available ('*Ecrop*'), a crop factor '*ec_crop*', a relation with the soil moisture content and the fraction of the area classified as unpaved or overhung by tree canopy.

$$Et = Ecrop \times ec\_crop \times \min\left(\frac{S\_uz}{UZ\max} \times \frac{1}{Lp}, 1\right) \times \left(frac\_unpaved + frac\_veg\right)$$ Eq. 5.15

The reference crop evaporation is determined with the Makkink equation (Eq. 4.2). The crop factor is used to convert the reference crop evaporation into the potential crop evaporation of the vegetation in the study area. The transpiration also depends on the moisture content of the unsaturated zone. When the moisture content is higher than the parameter '*Lp*', there is no reduction in transpiration. Below this value the transpiration reduction linearly decreases with rising moisture content. The transpiration is calculated over the area of the unpaved terrain and the area overhung by tree canopies as transpiration occurs from both areas.

5.3.6 The urban groundwater

The urban groundwater can exchange water with the urban surface water ('*I_water_ugw*'), the regional surface water ('*Drain_ugw_*rw'),the regional groundwater ('*seep_*inf') and the sewer ('*Drain_ugw_sewer*'). The exchange with the urban surface water is modelled with Eq. 5.11.

The flow to the regional surface water is modelled as a linear reservoir (Eq. 5.16). The part between brackets is the difference in level between the urban groundwater ('*H_ugw*') and the regional surface water ('*H_rw*'), which is the driving force of the flow.
The influence of the driving force on the amount of water flow is increased with the power 1 + '*alfa*'. When the parameter '*alfa*' [-] is close to zero, the flow resembles the outflow of a slowly reacting groundwater body. When the parameter '*alfa*' is closer to one, the flux mimics the outflow of a fast reacting groundwater body.
The parameter '*k_ugw_rw*' [T^{-1}] is the recession value of the linear reservoir and determines the resistance to flow. The formula resembles the Darcy-Weisbach formula, when one assumes the recession value to be the same as the hydraulic conductivity [$L.T^{-1}$] divided by the distance of flow [L].

$$Drain\_ugw\_rw = (H\_ugw - H\_rw)^{1+alfa} \times k\_ugw\_rw$$ Eq. 5.16

The flow to the sewer is modelled in the same way as the flow to the regional surface water(Eq. 5.17). The part between brackets is the difference in level between the urban surface water and the average level of the underside of the leaking sections of the sewer ('*SEWER*'). The power 1 + 'alfa' determines the response between a change in level difference and the amount of flow between the urban groundwater and the sewer.

The parameter '*k_ugw_sewer*' [T^{-1}] is the recession value of the linear reservoir and determines the resistance to flow.

$$Drain\_ugw\_sewer = (H\_ugw - SEWER)^{1+alfa} \times k\_ugw\_sewer \qquad \text{Eq. 5.17}$$

The exchange between the urban groundwater and the deeper groundwater can be a predefined flux or a predefined head in the deeper layer and a resistance to flow. In the latter case the flux ('*seep_inf*') is determined with Eq. 5.18. The head difference between the urban ('*H_ugw*') and regional groundwater ('*H_rgw*') is calculated in the nominator. In the denominator the resistance to flow ('*res_sf*') [T] is specified. The flux is positive in the upward direction.

$$seep\_\inf = \frac{H\_rgw - H\_ugw}{res\_sf} \qquad \text{Eq. 5.18}$$

5.3.7 The separated sewer

The inflow of precipitation into the separated sewer ('*Qss*') is led into the storm water section of the system. When (a part of) the sewer is connected to a 'first flush' (or 'improved') system, that part of the inflow - specified with the parameter '*frac_sep_imp*' – is led into a separate bucket ('*S_sep*'). This bucket has a maximum storage capacity ('*D_SSO*'), which leads to an outflow of the water exceeding this capacity to a regional surface water ('*Q_SSO*'). The amount of water that is pumped to the wastewater section of the sewer is determined with Eq. 5.19. The amount being pumped over is the minimum of the inflow into the separate bucket, the capacity with which the water can be pumped over ('*k_clean_dirty*') and the amount of water that can be temporarily stored.

The outflow of the separated sewer to a nearby surface water is calculated with Eq. 5.20. The first part is the outflow from the 'improved' section of the sewer. The second part is the outflow of the 'normal' section of the sewer, which is the same as the inflow.

$$Q\_clean\_dirty = \min(S\_sep, k\_clean\_dirty, D\_SSO) \qquad \text{Eq. 5.19}$$

$$Q\_SSO = \max(S\_sep - D\_SSO, 0) + (1 - frac\_sep\_imp) \times Qss \qquad \text{Eq. 5.20}$$

The discharge of the wastewater section of the separated sewer to the wastewater treatment plant ('WWTP') is determined with Eq. 5.21. The first term is the wastewater from the households ('*Qdry*'). The fraction of the households in the area that are connected to a separated sewer is specified with the parameter '*frac_DWF_sep*'. The second term is the amount of storm water pumped to the wastewater section of the separated sewer.

$$WWTP = Qdry \times frac\_DWF\_sep + Q\_clean\_dirty \qquad \text{Eq. 5.21}$$

5.3.8 The combined sewer

With Eq. 5.22 the inflow into the combined sewer is calculated. The first term is the wastewater flux from the remaining fraction of households in the area (1 – '*frac_DWF_sep*') collected in the combined sewer. The second term is the inflow of precipitation into the combined sewer '*Qcs*'. The third term is the leakage of urban groundwater into the combined sewer *'Drain_ugw_sewer'*.

When the inflow into the combined sewer exceeds the storage ('*D*_overflow') [L] and the discharge capacity ('*k_wwtp*') [$L.T^{-1}$], the exceeding amount of water is discharged onto a nearby surface water ('*Q_CSO*') [$L.T^{-1}$].

The discharge of the wastewater from the combined sewer to the wastewater treatment plant ('*WWTPcomb*') is determined with Eq. 5.24. The total discharge of wastewater from an area is the sum of '*WWTP*' and '*WWTPcomb*'.

$$S\_comb = Qdry \times (1 - frac\_DWF\_sep) + Qcs + Drain\_ugw\_sewer \quad \text{Eq. 5.22}$$

$$Q\_CSO = \max(S\_comb - D\_Overflow, 0) \quad \text{Eq. 5.23}$$

$$WWTPcomb = \min(S\_comb, k\_wwtp) \quad \text{Eq. 5.24}$$

5.4 Model parameter descriptions and values

Most of the parameters used by the model can be measured or estimated from available information as shown in the descriptions of the model parameters and their values. The values of the model parameters that are used for the simulation of the Prinseneiland are shown in bold. The units of the values are also shown for parameters that have a unit. The main units of the parameter values are millimetres (mm.) and days (d). Parameters with an asterisk (*) are calibrated.

frac_paved: **0.31**, *frac_unpaved*: **0.20**, *frac_build*: **0.49**, *frac_water*: **0.00**

The fractions of the surface of an area belonging to a land use type. The values of these parameters can easily be determined with a detailed land use map and some knowledge on the area.

frac_veg_paved: **0.044**, *frac_veg_unpaved*: **0.037**, *frac_veg_build*: **0.004**, *frac_veg_water*: **0.00**, *frac_veg*: **0.09**

The fractions of the land use types overhung by tree canopy. The values of these parameters can be determined by combining a land use map with an aerial photograph in a GIS system.

ec_paved, *ec_unpaved*, *ec_build*, *ec_water*: all **1**

Correction factors for the potential evaporation. It is assumed that the difference in potential (open water) evaporation between the Prinseneiland and Schiphol Airport are negligible. Therefore the values of the parameters are all assumed to be 1.

S_paved_int: **1.5 mm**, *S_unpaved_int*: **2 mm**, *S_build_int*: **1 mm**

The 'interception capacities' of the land use types are a summation of the interception capacity above the surface, the potential moisturizing losses and depression storage of the land use type.

The value for the paved area was arrived at by assuming a moisturising loss of 0.5 mm. and a depression storage of 1 mm. Both values were found in Van de Ven, 2007, pp. 71.

The interception capacity of the unpaved areas is assumed to be 2 mm., which is based on averaging measured interception capacities of grasses, shrubs and understory found in table 1 and the medians in table 7 of Breuer, 2003.

The interception capacity of areas classified as build is assumed to be lower than that of paved area, due to the fact that about 90% of the roofs in the area is sloping. This mainly affects the amount of depression storage that can take place on the roof. It is therefore assumed that the interception capacity of the build area is 1mm.

DATUM: **-2800 mm**

The parameter '*DATUM*' specifies the distance between the reference plane that is used in the model and a standard reference plane. The model needs its own reference plane as the levels in the urban groundwater and surface water reservoirs cannot become negative. Using the standard reference plane could result in the reservoirs being empty part of the time, which does not correspond with reality.

In the case of the Prinseneiland, the model datum has been put 2800 mm below N.A.P.. This corresponds roughly with the bottom of the phreatic groundwater body and the bottom level of the nearby canals.

PerSIntTreeN1: **100 d**, *PerSIntTreeN2*: **180 d**, *SIntTreeN1*: **0 mm**, *SIntTreeN2*: **2 mm**, *ec_crop1*: **0.6**, *ec_crop2*: **0.9**

In the model the effect of the shedding of leaves by the vegetation is simulated with a simple block function. This function allows for specifying two periods with lengths '*PerSIntTreeN1*' and '*PerSIntTreeN2*' with different interception capacities ('*SIntTreeN1*', '*SIntTreeN2*') and crop factors ('*ec_crop1*', '*ec_crop2*'). The two specified periods do not need to cover the entire year. The part of the year that is not covered by the periods is assigned the values of the first period. Figure 5.2 shows a visualisation of the resulting vegetation properties over the year.

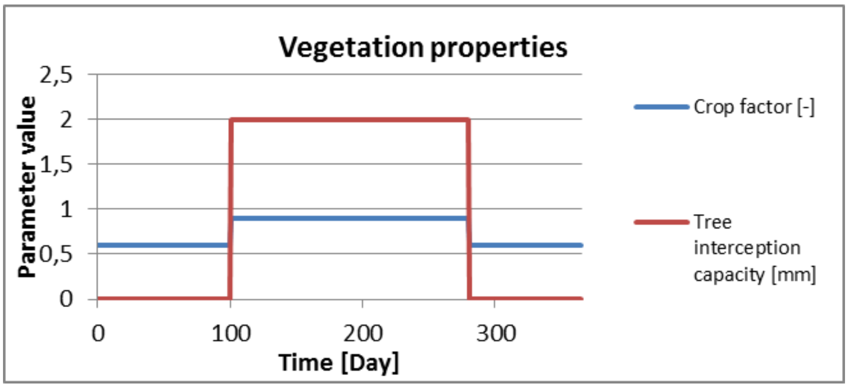

Figure 5.2. Vegetation properties over the year.

The interception capacity of the trees in the 'leaf off' period is assumed to be 0 mm. The interception capacity of the trees in the 'leaf on' period is assumed to be 2 mm. (based on Horton, 1919).

Gerrits (2010, pp. 3020) states that "[…] the effect of the storage capacity on canopy interception evaporation is limited. On average, the increase or decrease is about 5% with an average coefficient of variation in the storage capacity of 56%. Hence, a large variation in the storage capacity has a low impact on the evaporation predictions, and thus canopy interception is more driven by the number of rain days and the potential evaporation than by the storage capacity."

"The impact of uncertainties in the storage capacity (which can be as high as ±100%) on the total interception evaporation is about 11% and the difference in the lower or upper storage capacity is 15% and 8%, respectively. This indicates that interception is more influenced by the rainfall pattern than by the storage capacity. Hence, in interception modelling, the value of the storage capacity is of minor concern."

The crop factors '*ec_crop1*' and '*ec_crop2*' are based on the crop factors of fruit trees in table 12 of Allen et al., 1998.

'*i_water_ugw*': **0 d^{-1}**
The value of the parameter is set at zero, as there is no urban surface water present on the island.

'*i_water_rgw*': **0 d^{-1}**
The value of the parameter is set at zero, as there is no urban surface water present on the island.

'*n*': **0.27***
Porosity of the soil

Davis (1969) found ranges of typical porosity values:
Narrowly graded silt, sand, gravel: 30-50%
Widely graded silt, sand, gravel: 20-35%
Most piezometers are placed in medium fine sand with silt and some debris. The value obtained from the calibration is low, but within the boundaries that were found.

'*wp_uz*': **0.05**
Residual soil moisture in the unsaturated zone.

'*fc_uz*': **0.14**
The depth average of the equilibrium soil moisture content ('θ') of the unsaturated zone.
The value is based on a depth average of an integration of the Mualem – Van Genuchten formula (Eq. 5.25). The depth ('h') = 1400 mm. 'n' = 2, 'α' = 0.02 (values for sandy soil), θ_r = '*wp_uz*', θ_s = '*n*' (the porosity of the soil).

$$\theta = \theta_r + \frac{\theta_s - \theta_r}{\left(1+(\alpha h)^n\right)^{1-\frac{1}{n}}} \qquad \text{Eq. 5.25}$$

The specific yield (indirectly) used in the model (*'n'* – *'fc_uz'*) is 0.13. Johnson (1967) found the following values:
Silt: 0.03-0.19
Fine sand: 0.10-0.32
Medium sand: 0.15-0.32
Since most of the piezometers are placed in medium fine sand with some silt, the value that is used seems reasonable.

'gamma': **0.31***, *'beta'*: **0.5***
Shape parameters that determine the fraction of the inflow into the unsaturated zone that is routed through the macro pores.

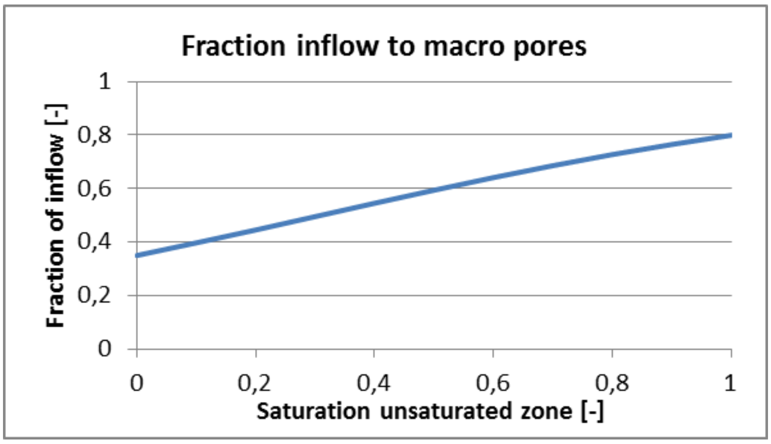

Figure 5.3. Fraction of the inflow into the unsaturated zone that is routed to through the macro pores as a function of the saturation of the unsaturated zone bucket.

'Lp': **0.8**
The parameter 'Lp' forms a limit for the transpiration. When the saturation of the unsaturated zone reservoir drops below the value of *'Lp'*, the simulated transpiration is reduced linearly to zero at a saturation of zero.

'k_ugw_rw': **0.000049* d^{-1}** (Point in Galgenstraat), **0.000098 d^{-1}** (Whole of the Prinseneiland)
The recession value for the flow from the urban groundwater to the regional surface water. Calibrated

'c_ugw': **2 mm.d^{-1}**
Magnitude of the slow flow component between the unsaturated zone and the urban groundwater. Calibrated

'alfa': **0.87***
Parameter determining the response of the groundwater outflow as a result of a change in storage in the saturated zone.

'frac_DWF_sep': **0**
Fraction of the households connected to a separated sewer system. 1 – *frac_DWF_sep* is the fraction of the households connected to a combined sewer system. Since the Prinseneiland does not have a separated sewer system, the value of the parameter has been set to 0.

'frac_sep_imp': **0**
The fraction of the total inflow of precipitation into a separated sewer that flows to a 'first flush' structure. Since the Prinseneiland does not have a separated sewer, the value of the parameter has been set to 0.

'*k_ugw_sewer*': **0* d^{-1}**

The recession value for the flow from the urban groundwater to the sewer system. Calibrated

Leakage of groundwater into the sewer system may contribute for a large part to the base flow of the sewer. Eiswirth and Hötzl (1997) found that 52% of the sewer discharge of Pflittersdorf, Germany stems from groundwater infiltration. This example shows that leakage of groundwater into the sewer system may contribute a lot to the sewer discharge. It should therefore be investigated whether groundwater leaking into the sewer is possible and/or significant.

Leakage of the connections of the buildings to the sewer is a blind spot. Rutsch et al. (2006, pp. 143) states that " […] field investigations on the magnitude of this phenomenon are scarce and models are lacking completely." Ballweg (2002) found during a large measuring campaign in Göttingen, Germany that 92% of the investigated house connections did not meet the criteria on pressure testing. This does not imply that all the connections would leak during normal operation, but it shows that leakage from house connections may be present at a large scale.

'*k_sewer*': **0 d^{-1}**

The recession value for flow from the sewer system to the unsaturated zone. Calibrated

'*k_wwtp*': **14 mm/d**

The parameter '*k_wwtp*' simulates the pumping capacity (or maximal gravitational outflow) of the sewer system. The maximum pumping capacity of the sewer system on the Prinseneiland is 40 m^3/hour. This is equivalent to a layer of water of about 1.2 mm. over the entire island (34,000 m^2). When the pumping station is operated at maximum capacity during an entire day, it can pump 28 mm. (or 960 m^3.) out of the area. Since most extreme precipitation events happen over shorter periods of time and since the storage capacity of the sewer is limited, the parameter has been given a value half that of the theoretical maximum pumping capacity.

The data on the sewer discharges from the pumping station show that this assumption is reasonable. The pumping station discharged water for 12 to 16 hours at maximum capacity during the most extreme precipitation events over the years 2010 till 2012. An assumed maximum pumping capacity of 14 mm. will result in underestimations on sewer discharge peaks resulting from long, low intensity precipitation events. The model will probably overestimate the sewer discharge peaks resulting from short, high intensity precipitation events.

'*k_clean_dirty*': **0 mm/d**

The parameter '*k_clean_dirty*' simulates the discharge of storm water caught by a 'first flush' system to the wastewater section of the separated sewer. Since the Prinseneiland does not have a separated system, the value of the parameter has been set to 0.

'*D_Overflow*': **18.6 mm**

The parameter '*D_Overflow*' simulates the maximum amount of water the combined sewer system can store or discharge. This amount of water consists of the amount of storage in the system and the pumping capacity of the combined sewer system. The amount of inflow into the combined sewer system exceeding this threshold is discharged onto a nearby surface water via a combined sewer overflow (CSO).

'*D_SSO*': **0 mm**

The parameter '*D_SSO*' simulates the amount of storm water inflow into a separated system that can be temporarily stored in a 'first flush' structure. The amount of water that is stored in the reservoir cannot flow to a nearby surface water ('*Q_SSO*', Eq. 5.20) and is pumped to the wastewater section of the separated system.

'*SEWER*': **2600 mm**

The parameter '*SEWER*' denotes the average bottom level of leaking sewer sections with respect to the model reference level ('*DATUM*'). The value of this parameter for the Prinseneiland has been arrived at by combining information from sewer inspections with information on the bottom level of the sewer pipes.

'*Leak_Drink*': **0.01 –**
Fraction of the drinking water supply discharge to the model area that leaks into the unsaturated zone.

Garcia-Fresca (2005) found via a literature review that typical values for leakage of drinking water mains are around 20 to 30% averaged over a city. The most efficient cities lose about 10% of the input into the supply system. In less developed countries losses may be as high as 30 to 60%.

Leakage of the drinking water supply system in the city of Amsterdam has already been discussed in section 4.2.3.

'*res_sf*': **8000 d**
Resistance of the confining layer below the urban groundwater body to flow. In combination with measured or assumed heads in the regional groundwater body the seepage flux can be modelled.

5.4.1 Precipitation routing parameters

In Table 5.1 the values of the precipitation routing parameters are shown. The precipitation routing parameters specify the fractions of precipitation fallen on a land use type with a certain precipitation discharge mode that follow a specified pathway. The pathways are indicated with the letters 'c', 's', 'r' and 'i', which stand for the combined sewer, separated sewer, external discharge and infiltration respectively.

The numbers in the table specify the fraction of precipitation on combinations of land use types and precipitation discharge modes following a specific pathway. As can be seen, this leads to 64 combinations which is too much to implement in a model. Therefore, the fractions are summed per land use type with a weight for the area of each combination of land use and discharge mode. Taking the weighted sum results in the values shown in Table 5.2.

The highlighted value of this table means that 41% of the precipitation on the paved area on the island flows to a combined sewer. This value is the sum of the highlighted values in Table 5.1 with the fractions in the top row of Table 3.3 (divided with the fraction of the island classified as paved, 0.31) as weights. Since only water from features classified as 'Combined' flows to a combined sewer, the 41% is a result of multiplying the fraction of 0.63 with the percentage of the paved area that is connected to a combined sewer 0.65 (0.2/0.31).

Further it is assumed that all precipitation on buildings follows the allocated precipitation discharge mode. Since most of the buildings are connected to the combined sewer, the largest fraction of precipitation on buildings flows to the sewer.

For unpaved areas it is assumed that all precipitation that reaches the soil surface infiltrates into the subsoil.

Table 5.1. Values for the precipitation routing parameters for the main discharge modes of the land use types.

		Precipitation discharge mode															
		Combined				Separated				Not connected				External			
		c	s	r	i	c	s	r	i	c	s	r	i	c	s	r	i
Land use class	Paved	0,63	0	0	0,37	0	0,63	0	0,37	0	0	0	1	0	0	1	0
	Unpaved	0	0	0	1	0	0	0	1	0	0	0	1	0	0	0	1
	Build	1	0	0	0	0	1	0	0	0	0	0	1	0	0	1	0
	Water	-	-	-	-	-	-	-	-	-	-	-	-	-	-	-	-

Table 5.2. Land use type averaged precipitation routing parameters

		Land use type average			
		Combined			
		c	s	r	i
Land use type	Paved	0,41	0	0,02	0,57
	Unpaved	0	0	0	1
	Build	0,81	0	0,18	0,01
	Water	-	-	-	-

5.5 Calibration of model parameters and validation

5.5.1 Introduction in calibration

Not all parameters in the model could be measured or estimated a priori. The values of these parameters need to be determined by calibration. During a calibration run the model is fed with sets of differing parameter values, which cause the model to give different results. These results are then compared with measurements from the area to determine which sets of parameter values give good model results. The set of parameters that gives the best results is then chosen as the optimal parameter set. The performance of this parameter set is then tested on another time series to test its predictive qualities (as suggested by e.g. Klemeš, 1986)

In this research calibration of the model has been carried out using a Monte-Carlo simulation. In a Monte-Carlo simulation a large number of parameter sets are constructed with the values of the parameters being varied randomly between specified boundaries. With this method the model is tested with parameter sets that cover the entire parameter space between specified boundaries.

Details of the performed calibration

For this research Monte-Carlo simulations were performed with 10.000 sets with varying parameter values. Due to the large number of parameters and the option of determining most of them a priori only the parameters ‘c_paved’, ‘k_ugw_rw’, ‘alfa’, ‘beta’, ‘gamma’ and ‘n’ were calibrated. The first two are key parameters governing the simulated groundwater levels and the other four also influence the groundwater levels, but to a lesser extent. For calibration on the sewer discharges the values of the parameters ‘c_paved’, ‘k_ugw_rw’ and ‘k_ugw_sewer’ were varied.

The performance of the parameter sets are determined by comparison with groundwater measurements from the Galgenstraat and sewer discharge measurements. For this the Nash-Sutcliffe (Eq. 5.26) and the Log Nash-Sutcliffe coefficient (Eq. 5.27) were used. The Nash-Sutcliffe coefficient focusses more on the peaks in the measured and modelled variables and the Log Nash-Sutcliffe coefficient focusses more on the base of the variables.

$$F_{NS} = 1 - \frac{\sum \left(y_o - y_m \right)^2}{\sum \left(y_o - \overline{y_o} \right)^2} \qquad \text{Eq. 5.26}$$

$$F_{LogNS} = 1 - \frac{\sum \left(\log(y_o) - \log(y_m) \right)^2}{\sum \left(\log(y_o) - \log(\overline{y_o}) \right)^2} \qquad \text{Eq. 5.27}$$

In which

F_{NS} = Nash-Sutcliffe (efficiency) coefficient (Nash and Sutcliffe, 1970)

F_{LogNS} = Log Nash-Sutcliffe (efficiency) coefficient

y_o = observed variable y at time t

y_m = modelled variable y at time t

$\bar{y}_0$ = average of the observed value y over the period one is interested in

Calibration periods

The calibration has been performed over two different periods with distinct differences in data availability. The first period spans the years 2010 and 2011 in which only a few groundwater level measurements are available for the measuring location in the Galgenstraat. The sewer discharge data over the same period has more frequent measurements.

The second calibration period is from the tenth of October 2012 till the fifteenth of February 2013. For the largest part of this period data is available for each day. The sewer discharge data has the same frequency as over the years 2010 and 2011, but contains some erroneous data, which hamper calibration.

The model is calibrated on the groundwater level measurements of both periods. The merit of the 'optimal' parameter values that are found is validated by simulating the groundwater levels over the other period. Further the model is calibrated on the sewer discharges over the years 2010-2011.

The results of the calibration on data over the years 2010 and 2011 are shown in appendix 12. In sections 5.5.2 and 5.5.3 the resulting 'optimal' parameter sets for the calibration runs on the groundwater levels in the Galgenstraat are discussed. In section 5.5.4 the resulting optimal parameter sets for the calibration on the sewer discharges are discussed. The set of parameter values that was chosen for the model runs is discussed in section 5.5.5.

5.5.2 Calibration on groundwater levels over the years 2010-2011

For the calibration of the parameters 'c_paved', 'k_ugw_rw', 'alfa', 'beta', 'gamma' and 'n' the groundwater level measurements from the measuring point in the Galgenstraat over the period 2010-2011 are used.

In section 12.1 a figure showing the parameter values leading to a low to good model performance that were found with the Monte-Carlo simulation are shown. The optimal values are shown in Table 5.3. In the left column the calibrated parameters are listed. In the second column the values of the parameters that give the highest performance according to the Nash-Sutcliffe coefficient are shown. In the third column the best parameter values according to the Log Nash-Sutcliffe coefficient are shown.

In the second and third part of the table the performance of the model with the parameter values from the first part of the table are shown. It can be seen that the model performs a lot better in the calibration period than in the validation period. Judging from the numbers the model seems to behave quite well over both periods. This impression is confirmed by Figure 5.4 for the simulation of the groundwater levels over the calibration period.

When one looks at Figure 5.5, however, it turns out that the model does not simulate the dynamics in the measured groundwater levels over the period October 2012 till February 2013 properly. The missing out on the extent of the groundwater dynamics could be caused by the relatively high porosities that are found with the calibration. A lower porosity leads to a larger fluctuation in groundwater levels, which might simulate the dynamics in the groundwater better.

Table 5.3. Optimal parameter values from the calibration over the years 2010 and 2011 and their performance

Parameter	Values Nash-Sutcliffe	Values Log Nash-Sutcliffe
'c_paved'	0.7599	0.7599
'k_ugw_rw'	0.000036	0.000036
'alfa'	0.7454	0.7454
'beta'	0.0741	0.0741
'gamma'	0.2451	0.2451
'n'	0.3468	0.3468
Calibration performance indicators		
NS	0.7922	0.7922
Log NS	0.9386	0.9386
RMSE		
Validation performance indicators		
NS	0.3969	0.3969
Log NS	0.2296	0.2296
RMSE	36.9693	36.9693

Calibration

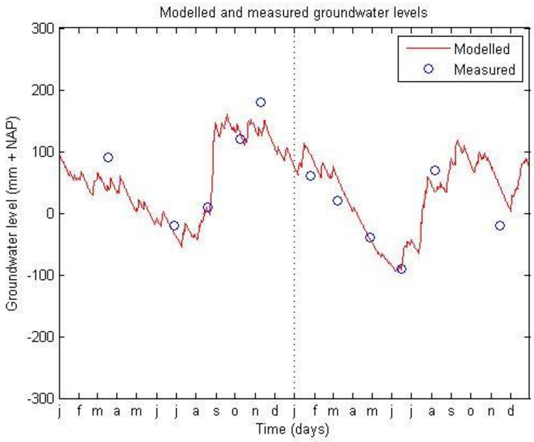

Figure 5.4. Simulated groundwater levels at the Galgenstraat with the optimal parameter values according to both performance indicators over the years 2010-2011.

Validation

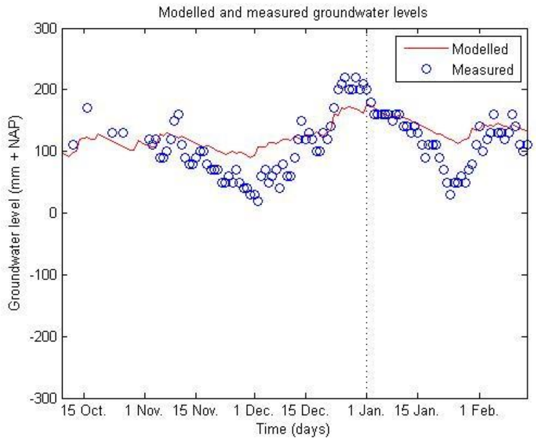

Figure 5.5. Simulated groundwater levels at the Galgenstraat with the optimal parameter values according to both performance indicators from Oct. 2012-Feb. 2013.

5.5.3 Calibration on groundwater levels over the period Oct. 2012-Feb. 2013

For the calibration of the parameters 'c_paved', 'k_ugw_rw', 'alfa', 'beta', 'gamma' and 'n' the groundwater level measurements from the measuring point in the Galgenstraat over the period October 2012 – February 2013 are used.

In section 12.2 a figure showing the parameter values leading to a low to good model performance that were found with the Monte-Carlo simulation are shown. The 'optimal' parameter values that were found are shown in Table 5.4. The table has the same lay-out as Table 5.3. The simulated groundwater levels with the found parameter values are shown in Figure 5.6 for the calibration period and in Figure 5.7 for the validation period.

From these figures it can be seen that the found parameter values seem to be able to simulate the groundwater dynamics quite well during wet(ter) periods. The groundwater levels during the dry periods in the years 2010 and 2011 shown in Figure 5.7 are underestimated by the model. This is confirmed by the Log Nash-Sutcliffe performance indicator for the validation period, which is even negative. It should be noted though, that this number is mainly based on only three groundwater level measurements during the dry periods, which reduces the significance of the indicator.

Table 5.4. Optimal parameter values from the calibration over the period Nov. 2012-Feb. 2013 and their performance

Parameter	Values Nash-Sutcliffe	Values Log Nash-Sutcliffe
'c_paved'	0.6285	0.6285
'k_ugw_rw'	0.000049	0.000049
'alfa'	0.8718	0.8718
'beta'	0.5035	0.5035
'gamma'	0.3078	0.3078
'n'	0.2719	0.2719
Calibration performance indicators		
NS	0.7884	0.7884
Log NS	0.7402	0.7402
RMSE	21.8974	21.8974
Validation performance indicators		
NS	0.4864	0.4864
Log NS	-2.0358	-2.0358
RMSE	53.4862	53.4862

Calibration

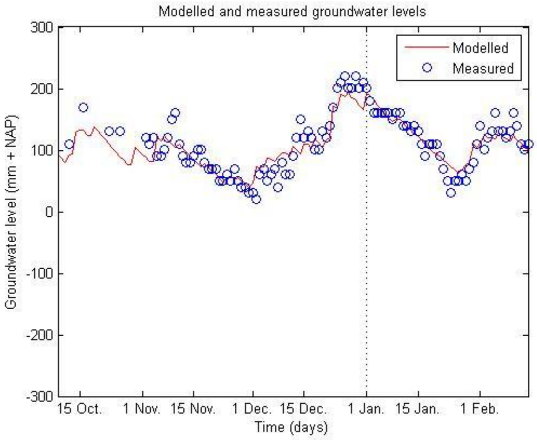

Figure 5.6. Simulated groundwater levels at the Galgenstraat with the optimal parameter values according to both performance indicators from Oct. 2012-Feb. 2013.

Validation

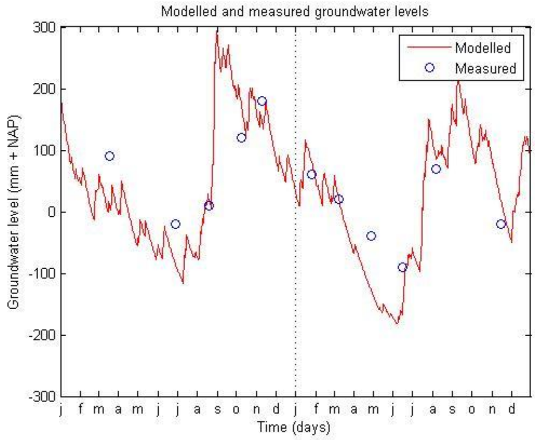

Figure 5.7. Simulated groundwater levels at the Galgenstraat with the optimal parameter values according to both performance indicators over the years 2010-2011.

5.5.4 Calibration on sewer discharges over the years 2010-2011

For the calibration of the model parameters 'c_paved', 'k_ugw_rw' and 'k_ugw_sewer' the sewer discharges measured over the period 2010-2011 were (also) used. In Table 5.5 the values of the other parameters are shown. The figures showing the results of the calibration are shown in appendix 12.3.

Table 5.5. Used parameter values

Parameter	Value
'alfa'	0.87
'beta'	0.3
'gamma'	0.5
'n'	0.27

In Table 5.6 the optimal values that were found with the Monte-Carlo simulation are shown. In the left column the calibrated parameters are listed. In the middle column the values of the parameters that give the highest performance according to the Nash-Sutcliffe coefficient are shown. In the right column the best parameter values according to the Log Nash-Sutcliffe coefficient are shown. As it happens, one parameter set achieves the highest performance for both the Nash-Sutcliffe and the Log Nash-Sutcliffe coefficient.

Table 5.6. Parameter sets with highest performance indicators

Parameter	Value NS	Value Log NS
'c_paved'	0.5199	0.5199
'k_ugw_rw'	0.000012	0.000012
'k_ugw_sewer'	0.000087	0.000087
Calibration performance indicators		
NS	0.6338	0.6338
Log NS	0.6090	0.6090

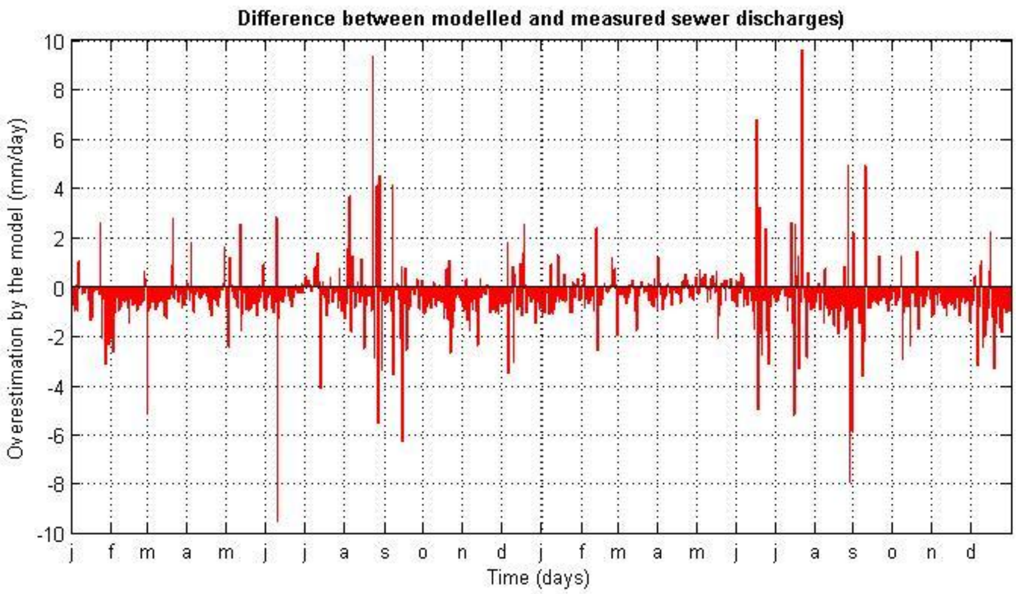

Figure 5.8. Difference between modelled and measured sewer discharges over the years 2010 and 2011. Positive values represent an overestimation by the model.

Influence of the dry weather flow on low sewer discharges
In model runs where the dry weather flow is not taken into account (and subtracted from the measured discharges) the Log Nash-Sutcliffe coefficient is always negative. This indicates that the model is not able to simulate the base flow in the sewer discharges accurately. Groundwater leaking into the sewer also does not explain the gap between the measured and modelled base flow, as can be seen fromFigure 12.3.

In Figure 5.8 the measured sewer discharges minus the assumed dry weather flow and the modelled sewer discharges are plotted. The modelled discharges in this figure are a result of the 'optimal' parameter set indicated in Figure 12.3 with the red crosses. In the parameter set the 'optimal' value for the parameter 'k_ugw_sewer' is set at about 0.03. This leads to a relatively large leakage flux into the sewer. As can be seen from **Fout! Verwijzingsbron niet gevonden.** the modelled base flow does not show the same pattern as the measured base flow. This is a clear indication that the pattern in the measured base flow cannot be explained by a leakage flux to the sewer.

The only process left that can cause the pattern in the base flow of the sewer discharges is the dry weather flow. The current dry weather flow put into the model does not have the same pattern as the base flow, but this can be caused by the time series used as the dry weather flow not being representative for the actual dry weather flow.

Remark on the dry weather flow input used

The time series that was used to represent the dry weather flow is based on the drinking water supply to the whole of Amsterdam. Since most of the drinking water supplied to households leaves the homes again as dry weather flow, using drinking water supply data as an estimate is relatively accurate. The problem with using data from a larger area is that the pattern of the smaller area has little influence on the pattern of the larger area. This results in the pattern of the smaller area not being introduced into the model. For further research into the water balance of this or any other area it is advised to measure the dry weather flow flowing to the research or a slightly larger area as it has a large temporal impact on the sewer discharges.

5.5.5 Chosen parameter values

The results of the calibration runs on the groundwater levels over the two periods show quite some different parameter values. These differences are partly caused by the dissimilarities in data availability between the two periods. In the last period with more frequent data available, the calibration process resulted in parameter values that are more capable of simulating groundwater level changes over shorter periods of time. In the first period the less frequent data available resulted in parameter values that are less capable of following the groundwater dynamics over short periods of time.

The parameter values found with the calibration run on the groundwater levels over the period October 2012 till half of February 2013 give the best results over both periods. It was attempted to improve the model performance by manual fine-tuning, but this did not result in a parameter set that was better able to simulate the groundwater levels over both periods. Therefore, the values found with the calibration are rounded off and used for further model runs. The rounded off values of the parameters and the performance of the model over both periods are shown in Table 5.7.

Table 5.7. Chosen parameter values and resulting model performance.

Parameter	Chosen parameter values
'c_paved'	0.63
'k_ugw_rw'	0.000049
'alfa'	0.87
'beta'	0.50
'gamma'	0.31
'n'	0.27
Performance indicators 2010 - 2011	
NS	0.7872
Log NS	0.7325
RMSE	21.9620
Performance indicators Oct. 2012 - Feb. 2013	
NS	0.4224
Log NS	-1.9500
RMSE	56.7217

The value for the parameter '*c_paved*' is about the same as similar values found in literature. Van de Ven (1989, pp. 241) for instance found values of 0.68 and 0.65 for two residential areas and a value of 0.68 for a parking lot in Lelystad, the Netherlands. Lerner (2002) stated that 50% of the impermeable surface should be treated as permeable.

The values that were found for the other parameters seem to be realistic.

The average distance between all locations on the Prinseneiland to the nearest canal is about half of the distance between the measuring point in the Galgenstraat to the nearest canal. So, the ratio in resistance to flow between the urban groundwater and the regional surface water is also a half. This results in a twice as high value of '*k_ugw_rw*' (0.000098) for the whole of the Prinseneiland.

6 Presentation and discussion of model results

In this section of the report some of the results of the model run for the Prinseneiland over the year 2011 are shown. After that, the results of the model runs for the Prinseneiland and the Galgenstraat are compared. Next the effects of land use on the urban water cycle are investigated, followed by an investigation on the effects of drought on the Prinseneiland. Lastly the effects of climate change on the Prinseneiland are discussed.

6.1 Results of the model run for the Prinseneiland

From the results in Figure 6.1 the correlation between the groundwater recharge and the precipitation can easily be seen. In the summer the recharge in between precipitation becomes negative due to low soil moisture contents in the unsaturated zone, which causes capillary rise and a depletion of the groundwater.

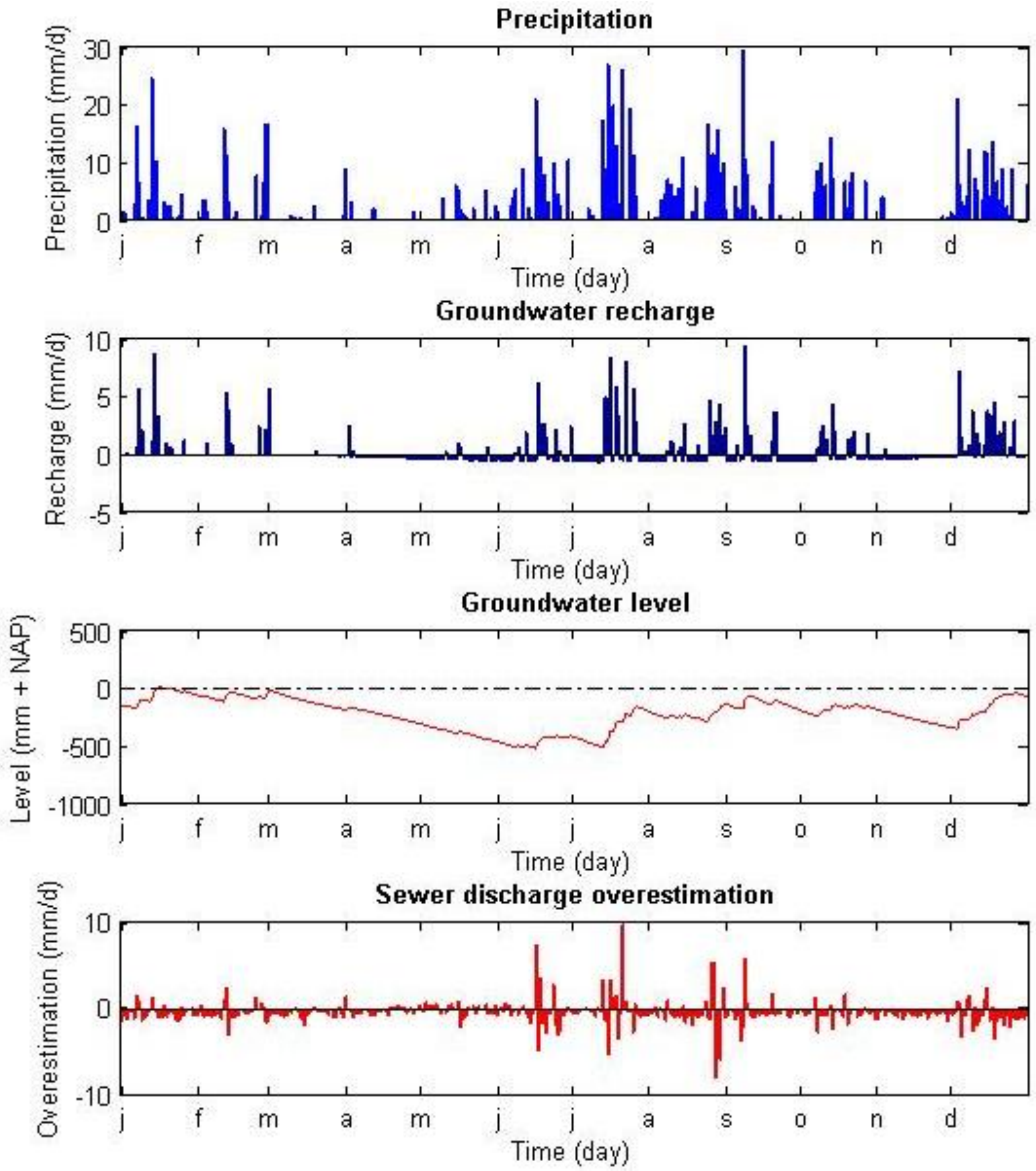

Figure 6.1. The main results of the model run for the Prinseneiland over the year 2011.

The differences between the measured and modelled sewer discharges are shown in the last subfigure. The figure shows a general underestimation of the sewer discharges by the model, which is caused by the lack of measured drinking water inputs to the region. The larger differences are caused by lags in sewer discharges relative to the moment of the precipitation event. In the model an event late in the day may be discharged that same model day, while in reality most of the discharge took place the next day. This way the model overestimates the sewer discharges on the first and underestimates them on the next day.

Next to that some differences are caused by the fact that the model does not take precipitation intensity into account. High intensity precipitation is more likely to enter the sewer system, as the water does not get the time to infiltrate and is thus forced to start flowing. Low intensity precipitation is more likely to infiltrate, as water in small depressions may not flow to the sewer at all. All this results in a model that performs reasonably, but does not simulate the sewer discharges of high intensity events quite well.

Table 6.1. Cumulative sums (mm) and fractions of the precipitation sum (-) of the fluxes on the Prinseneiland over the year 2011.

		Prinseneiland 2011	
Process	Precipitation	927	1
	Evaporation	170	0,18
	Transpiration	146	0,16
	Runoff	75	0,08
	Infiltration	276	0,30
	Recharge	128	0,14
	Drainage	65	0,07
	Sewer inflow	406	0,44
	DWF	1314	-
	WWTP	1720	-
	Overflow/Outflow	0	0,00
	Seepage	-60	-0,06
	Storage	-5	-0,01

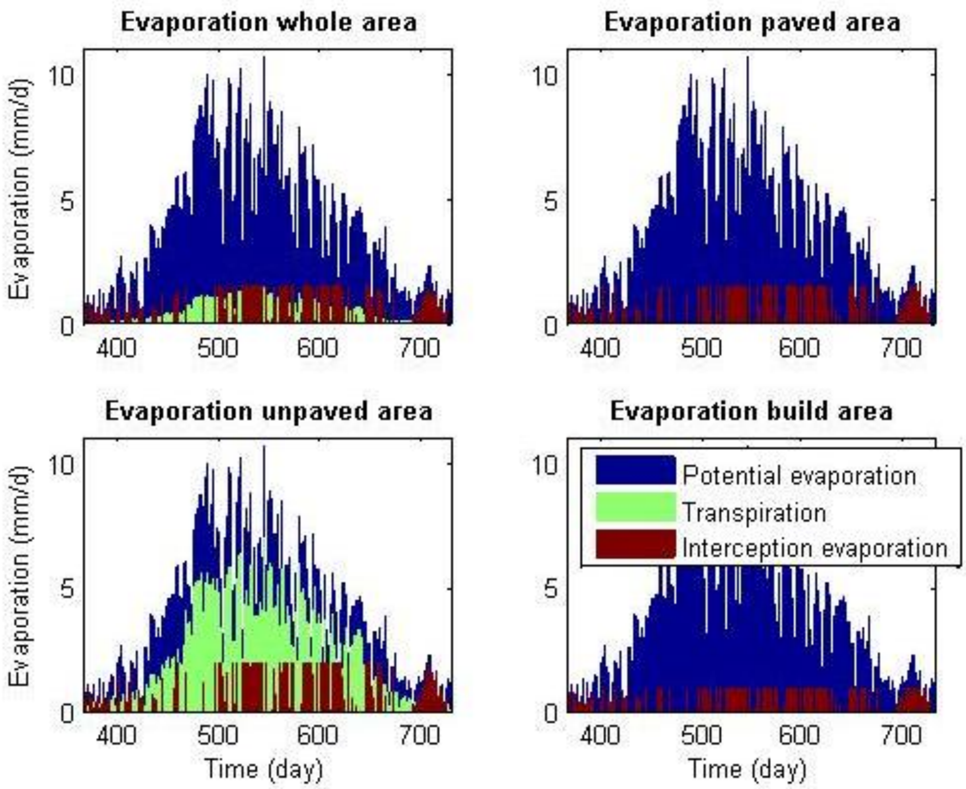

Figure 6.2. Potential, transpiration and interception evaporation over the whole, paved, unpaved and build up area of the Prinseneiland over the year 2011.

6.2 Comparing the Galgenstraat with the whole of the Prinseneiland

In Table 6.2, Figure 6.3 and Figure 6.4 the most important results of the simulations of the Galgenstraat and the whole of the Prinseneiland with the model are shown. The simulation was run for the years 2010 and 2011.

6.2.1 Discussion of the results of the comparison

The difference in the cumulative precipitation surplus (precipitation - evaporation) is caused by a higher evaporation in the Prinseneiland case, due to the higher transpiration and interception from unpaved areas, which makes up 20% of the island.

The differences between the groundwater levels are caused by a lower groundwater recharge on the whole island. This may be counterintuitive, but can be explained by the high fraction of the island which is build up (49%). In the model it is assumed that no precipitation on build up area infiltrates into the subsurface. So, in the case of the Prinseneiland, there is only a relatively small fraction of the area that attributes to groundwater recharge. Of the water that infiltrates into the subsurface about half is transpired again by the vegetation, reducing the recharge.

Another difference in the groundwater levels are the deeper dips in level during dry periods for the Prinseneiland case. This is caused by the vegetation in the area transpiring the water from the unsaturated zone, which is then replenished by capillary rise from the groundwater lowering the groundwater level. The effect of transpiration by the vegetation can also be seen in the simulated soil moisture contents. During the dry period the soil moisture in the Prinseneiland case is clearly reduced by the transpiration.

Due to the lower groundwater levels in the Prinseneiland case, there is less groundwater draining to the nearby surface waters and less seepage to the deeper groundwater. From Figure 6.4 it can be seen that over the years 2010 and 2011 very little surface water flowed to the urban groundwater. The model suggests that the only period in which the urban groundwater was naturally replenished with surface water is in July 2011. It should be noted, however, that the model is a lumped schematisation of the area and that local deviations from the average could result in local groundwater replenishing by the surface water. The model is not capable of simulating this. If one wants to investigate this, a distributed model is better suited.

6.2.2 Results of the comparison

Table 6.2. Cumulative sums (mm) and fractions of the precipitation sum (-) of the fluxes in the scenarios over the years 2010 and 2011

		Scenario			
		Prinseneiland		Galgenstraat	
Process	Precipitation	1869.00	1	1869.00	1
	Evaporation	330.00	0,18	338.00	0,18
	Transpiration	289.00	0,15	0.00	0,00
	Runoff	152.00	0,08	0.00	0,00
	Infiltration	563.00	0,30	566.00	0,30
	Recharge	272.00	0,15	555.00	0,30
	Drainage	151.00	0,08	416.00	0,22
	Sewer inflow	823.00	0,44	964.00	0,52
	DWF	2625.00	-	2625.00	-
	WWTP	3431.00	-	3567.00	-
	Overflow/Outflow	17.00	0,01	22.00	0,01
	Seepage	-122.00	-0,07	-140.00	-0,07
	Storage	2.00	0,00	11.00	-0,01

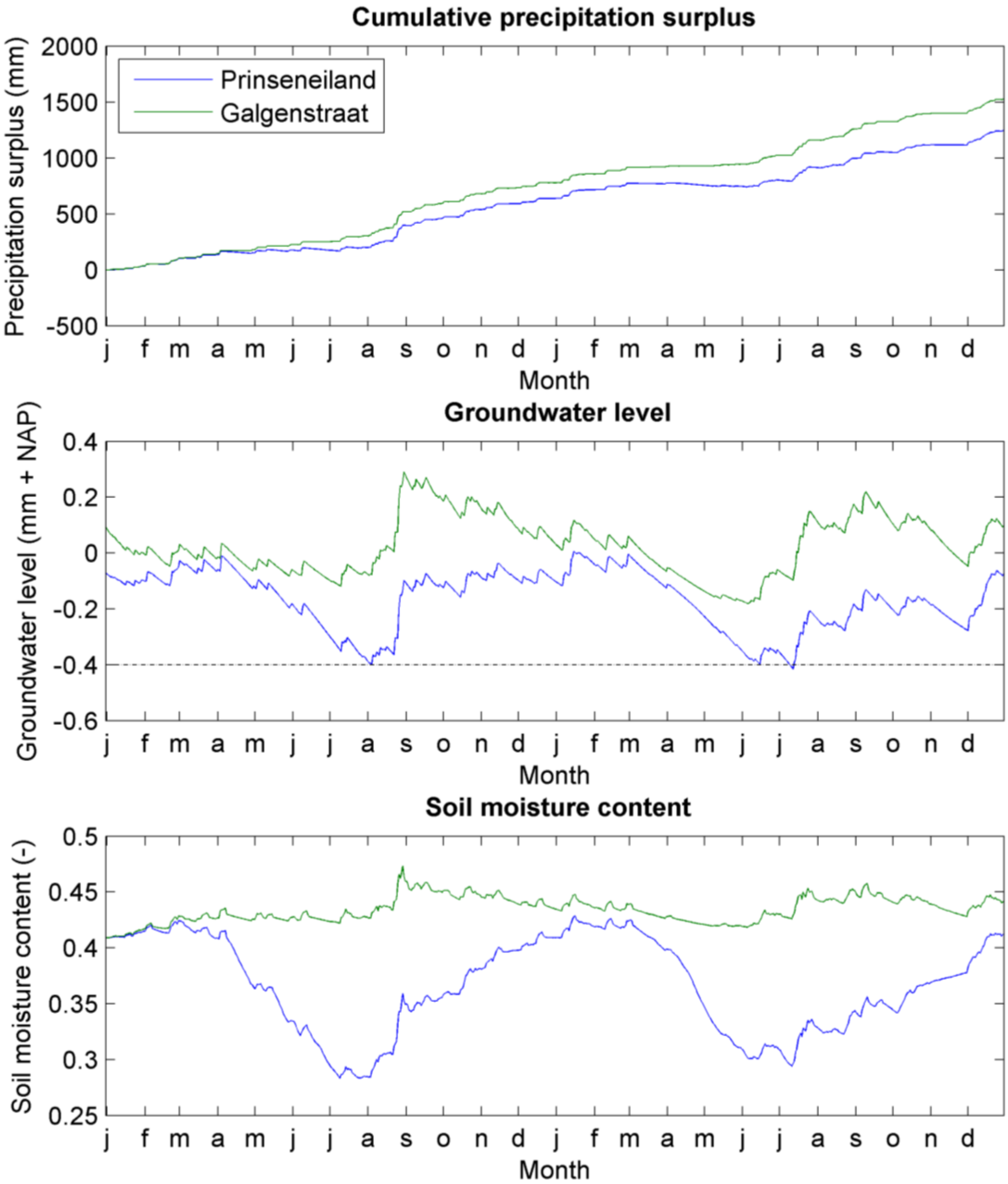

Figure 6.3. The simulated cumulative precipitation surplus (precipitation - evaporation), groundwater levels and soil moisture content over the years 2010 and 2011 for the entire Prinseneiland (blue) and at the measuring point at the Galgenstraat (green). The dotted line in the middle graph indicates the surface water level.

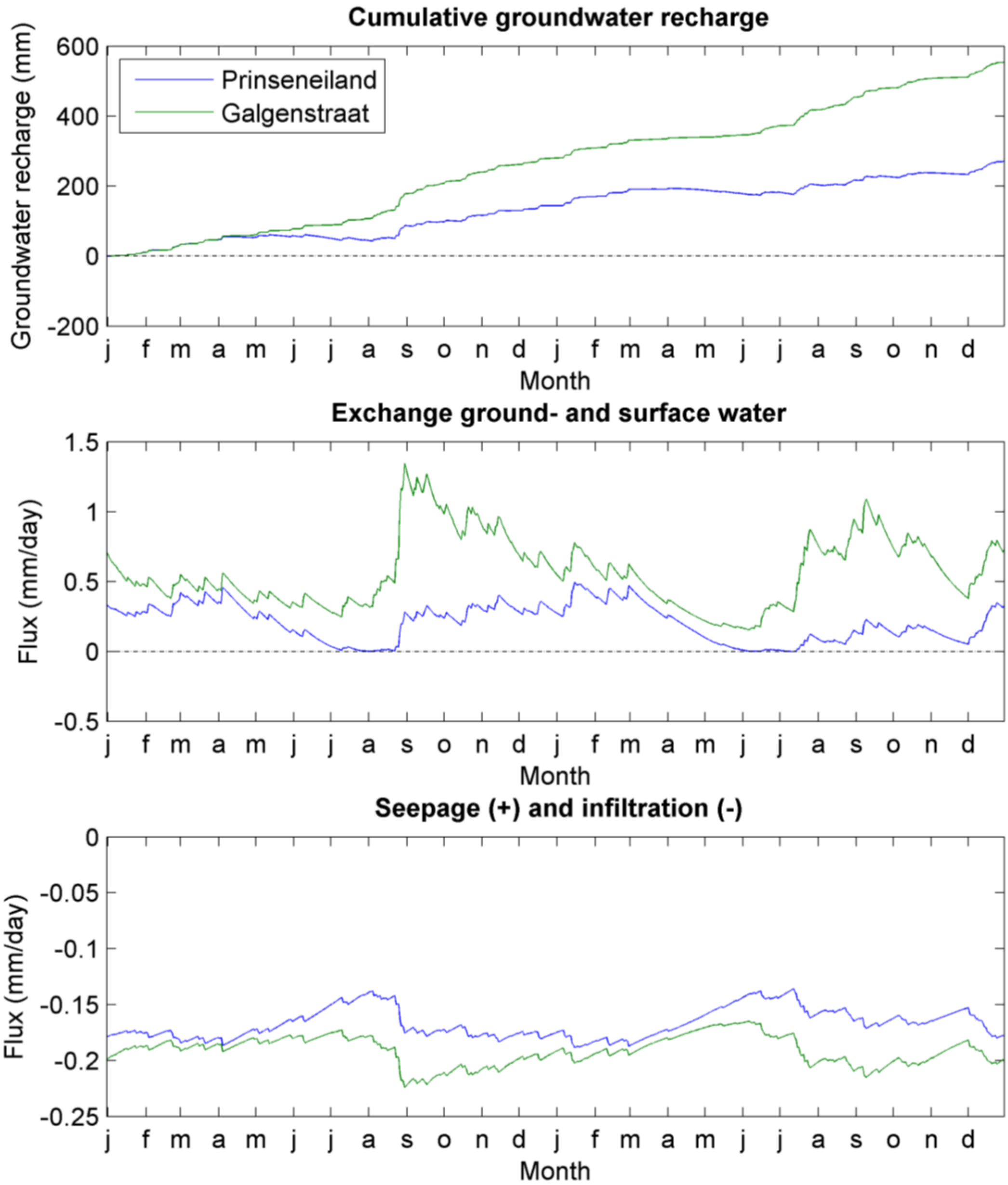

Figure 6.4. The simulated groundwater recharge, the flow of water between the urban ground- and the regional surface water and the flow between the urban and regional groundwater bodies over the years 2010 and 2011 for the Prinseneiland and the measuring location at the Galgenstraat.

6.3 The effects of land use differences

6.3.1 The land use type scenarios

With the model the influence of differences in land use were investigated. For this the Prinseneiland was also modelled as being completely paved (with bricks) and completely unpaved or vegetated (see Table 6.3 for the chosen land use type fractions). A hypothetical completely build up Prinseneiland is not shown, because all precipitation left the area through the sewer, resulting in rather dull results in the urban hydrological cycle.

For the simulations only the land use type fractions were changed whilst all other parameters kept their original values. In Table 6.4, Figure 6.5, Figure 6.6 and Figure 6.7 the most important results of these simulations are shown together with the results for the normal simulation of the Prinseneiland.

6.3.2 Discussion of the results of the land use type scenarios

The differences between the cumulative precipitation surpluses are caused by the differences in the amounts of water being evaporated due to interception and/or transpiration. Due to the low amount of evaporation from paved surface, the highest precipitation surplus is found on paved surface. The lowest surplus is on an entirely unpaved area.

The highest and lowest groundwater levels are found in the simulation of an entirely unpaved Prinseneiland. The high groundwater levels are caused by the large fraction of precipitation infiltrating into the subsoil, resulting in a large recharge and thus high groundwater levels. During dry periods the vegetation takes too much moisture from the unsaturated zone, resulting in capillary rise which in turn lowers the groundwater level. In the Prinseneiland and the paved Prinseneiland case the infiltration and transpiration are lower, resulting in smaller groundwater level fluctuations. Since the Prinseneiland does have unpaved areas, the groundwater level is lowered during dry periods, but the effects of transpiration are reduced due to the paved and build up areas. The groundwater level in the paved Prinseneiland case fluctuates less, because of the lower infiltration and the absence of vegetation.

Quite surprisingly, the groundwater recharge on the Prinseneiland is smaller than the paved Prinseneiland case. This is surprising, as intuitively one might think that having some unpaved areas gives a higher groundwater recharge in a city compared to a completely paved area like a parking lot. The lower groundwater recharge in the Prinseneiland can be explained by the high fraction of build-up area (49%) from which no water infiltrates into the subsurface.

6.3.3 Answers to research questions

1.1 What are the dominant processes in the urban water cycle on the Prinseneiland?

From the values in Table 6.3 and Figure 6.7 it can be concluded that sewer inflow and infiltration are the largest fluxes. A further inspection reveals that a third of the precipitation on the island is evaporated or transpired. The other processes are not less important for the urban water cycle, but their fluxes are smaller.

1.1 What are the dominant processes in the urban water cycle?

1.2 How much does paved area reduce groundwater recharge compared to unpaved area?

In answer to research question it can be seen from Table 6.4 that the simulated unpaved area has 1472 mm of infiltration over two years, whereas the simulated paved area only has 566 mm, which is 38% of the infiltration of unpaved area. The difference in groundwater recharge is smaller though, due to transpiration that takes place from unpaved areas, but not from paved areas. This transpiration accounts to 742 mm over two years.

The recharge of the groundwater on unpaved areas amounts to 721 mm against 555 mm from paved areas. This means that paved areas generate 23% less groundwater recharge compared to unpaved areas. It should be noted though that this is valid for paved area that consists of ordinary bricks. In case of asphalt, concrete slabs or permeable pavements, the difference changes.

1.3 How much does an urban environment reduce groundwater recharge compared to a hypothetical 'natural' state (unpaved) of the same area?

The main difference between an urban environment and its hypothetical 'natural' state are caused by the sealing of surfaces in the area. Surface sealing decreases the amount of infiltration due to lower infiltration capacities of paved and built-up surfaces. Next to that there is little to no vegetation on sealed surfaces, which reduces the amount of transpiration from those surfaces.

The lower infiltration capacity of the sealed surfaces on the Prinseneiland causes the infiltration to be reduced by two thirds compared to the completely unpaved scenario. This is mainly caused by the large fraction of the island being built-up, which is assumed to result in no infiltration. Most of the water that does infiltrate is precipitation that fell on unpaved area (52%) or paved surfaces that are not connected to a sewer (27%). The remaining infiltration stems from semi-pervious areas connected to the sewer (19%).

Since only 20% of the Prinseneiland consists of unpaved area and only 10% of the island has tree cover, transpiration has become a relatively small flux in the water cycle of the Prinseneiland. Compared with the 'natural' situation there is 60% less transpiration from the Prinseneiland.

The groundwater recharge of the Prinseneiland is reduced with 60% compared with the 'natural' state, due to the surface sealing. This difference is lower than the reduction in infiltration due to the lower loss of water through transpiration. It should be noted though that these results are valid for the Prinseneiland, which is a densely built-up part of Amsterdam. In areas with a lower building density groundwater recharge is probably higher, since more water may infiltrate into the soil. Also areas in which more surfaces are disconnected from the sewer groundwater recharge may be higher than in the Prinseneiland case.

6.3.4 Results of the land use type scenarios

Table 6.3. Land use type fraction of the schematisations

		Simulation run		
		Prinseneiland	Paved	Unpaved
Land use type fraction	Paved	0.31	1	0
	Unpaved	0.2	0	1
	Build	0.49	0	0

Table 6.4. Cumulative sums (mm) and fractions of the precipitation sum (-) of the fluxes in the scenarios over the years 2010 and 2011. In Figure 6.7 an these values are visualized for easier interpretation.

		Scenario					
		Prinseneiland		Paved		Unpaved	
Process	Precipitation	1869.00	1	1869.00	1	1869.00	1
	Evaporation	330.00	0,18	338.00	0,18	397.00	0,21
	Transpiration	289.00	0,15	0.00	0,00	742.00	0,40
	Runoff	152.00	0,08	0.00	0,00	0.00	0,00
	Infiltration	563.00	0,30	566.00	0,30	1472.00	0,79
	Recharge	272.00	0,15	555.00	0,30	721.00	0,39
	Drainage	151.00	0,08	395.00	0,21	527.00	0,28
	Sewer inflow	823.00	0,44	964.00	0,52	0.00	0,00
	DWF	2625.00	-	2625.00	-	2625.00	-
	WWTP	3431.00	-	3567.00	-	2625.00	-
	Overflow/Outflow	17.00	0,01	22.00	0,01	0.00	0,00
	Seepage	-122.00	-0,07	-138.00	-0,07	-141.00	-0,08
	Storage	2.00	0,00	33.00	-0,02	62.00	-0,03

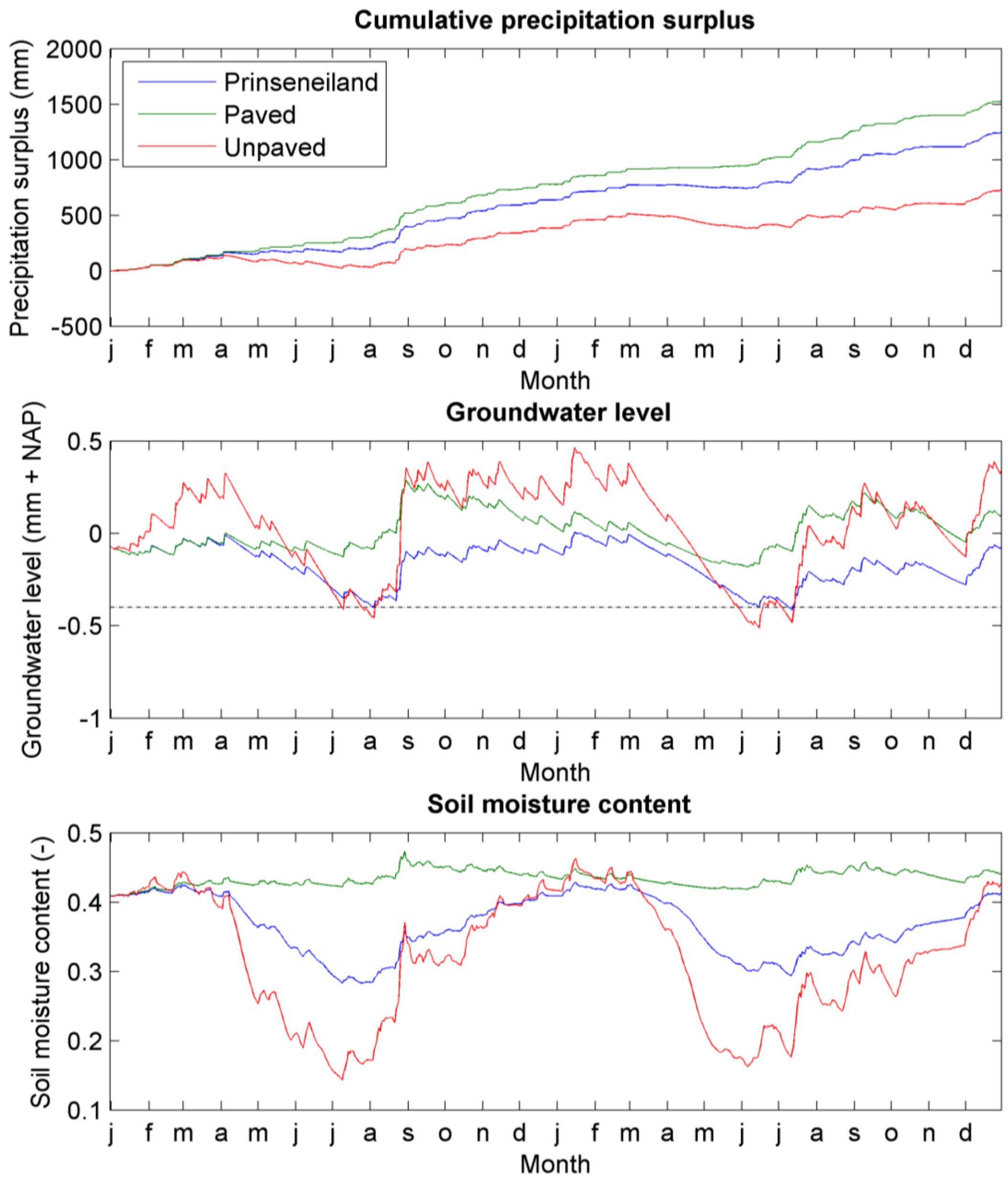

Figure 6.5. The simulated cumulative precipitation surplus (precipitation - evaporation), groundwater levels and soil moisture content over the years 2010 and 2011 for the Prinseneiland (blue line) and a completely paved (green) and unpaved Prinseneiland (red). The dotted line in the middle graph indicates the surface water level.

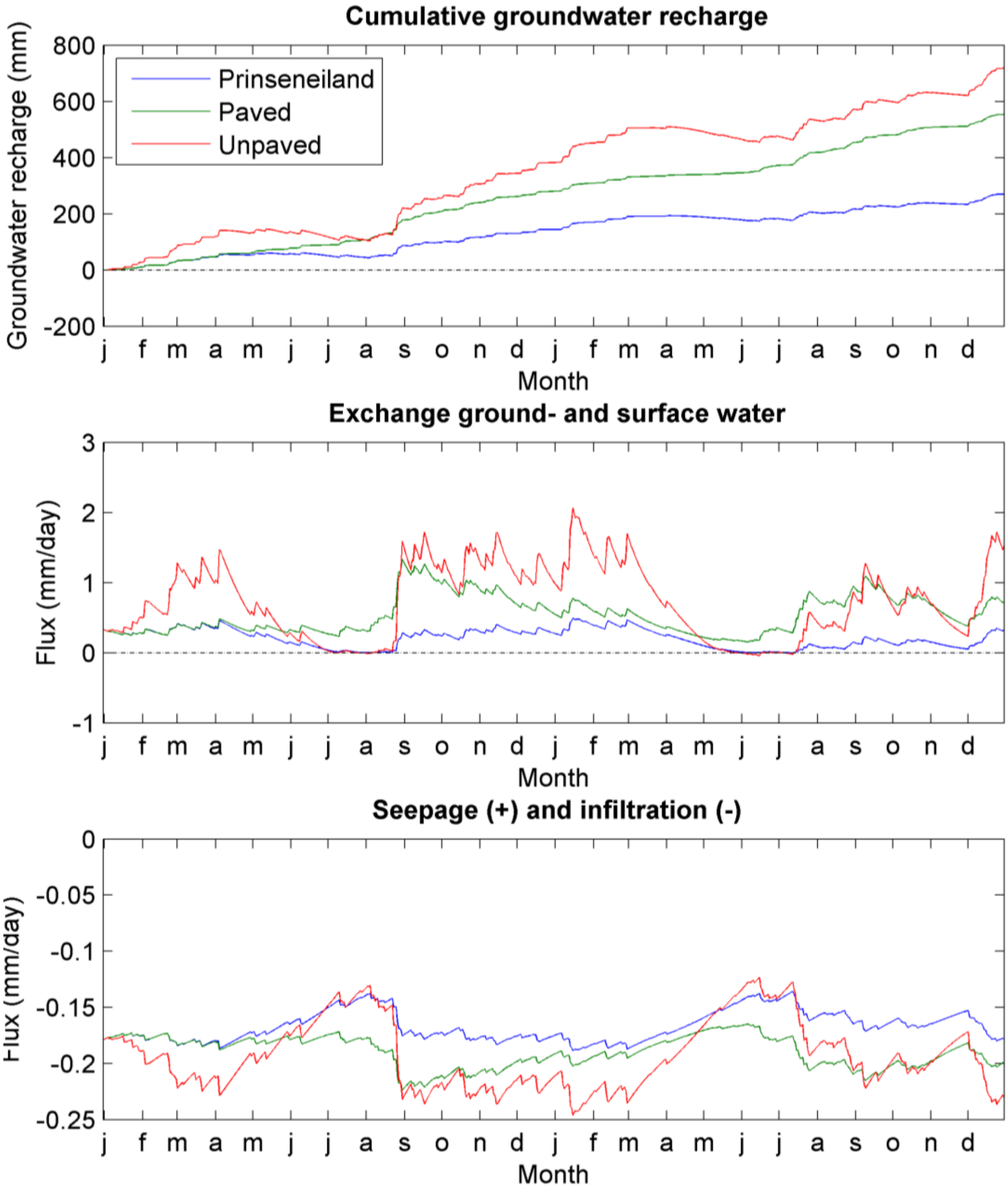

Figure 6.6. The simulated groundwater recharge, the flow of water between the urban ground- and the regional surface water and the flow between the urban and regional groundwater bodies over the years 2010 and 2011 for the Prinseneiland and a completely unpaved (green) and a completely paved Prinseneiland (red).

Prinseneiland

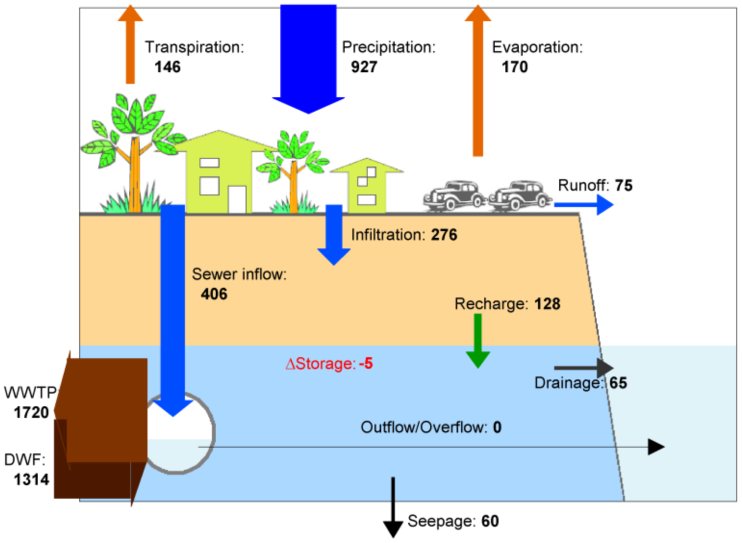

Paved

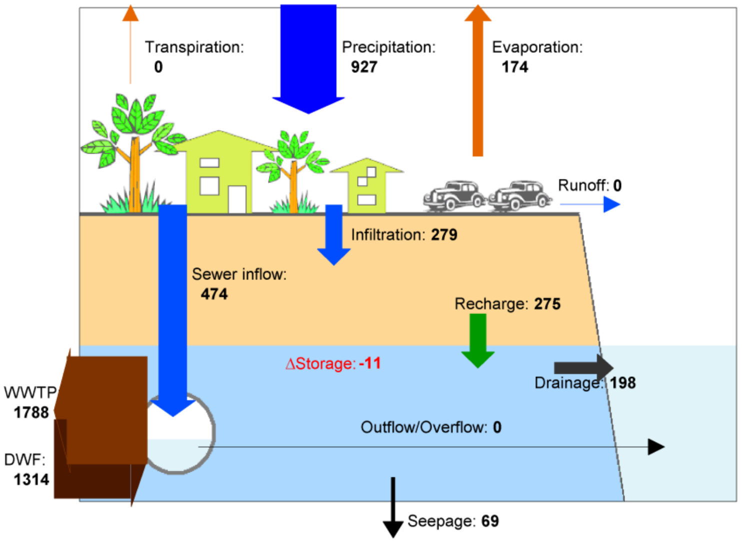

Unpaved

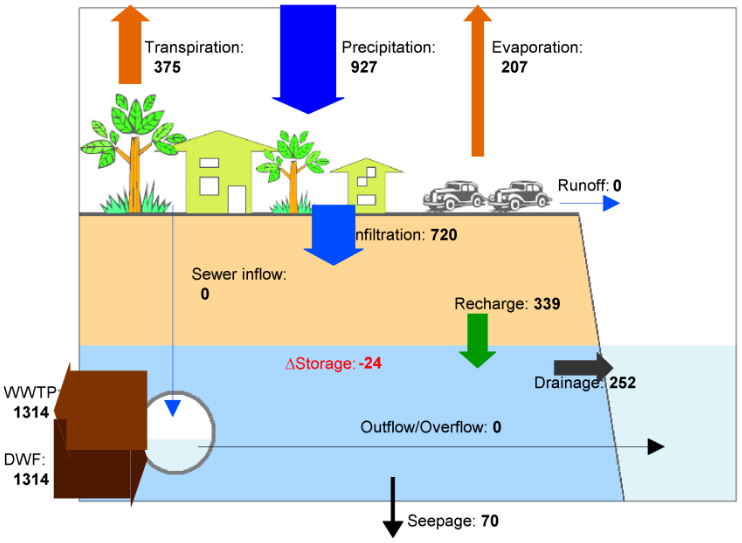

Figure 6.7.Overviews of the year sums of the fluxes over the year 2011 for the three land use scenarios

6.4 The effects of drought

6.4.1 The drought scenarios

The effects of drought on the water cycle of the Prinseneiland were investigated by using historical meteorological data. These years are 1967, 1976 and 1989. These years were selected by the Delta programme Fresh Water ('Deltaprogramma Zoet Water', DPZW) on the basis of the return periods of the lowest river discharges in those years. These return periods are 1 (1967), 10 (1989) and 100 years (1976).

The return periods of the meteorological data in those years is closely linked to the return periods of the lowest river discharges, but are not the same. Therefore, the mentioned return periods are not used, but the meteorological data of these years are denoted to as 'Normal' (1967), 'Dry' (1989) and 'Extremely dry' (1976). There has been no analysis performed on these data to check whether this is correct, but the results of the simulations do not give a pressing reason to check.

The meteorological data of these years was obtained from the Netherlands Hydrological Instrument (NHI, Nationaal Hydrologisch Instrumentarium).For the simulation runs the scenario year was preceded by a 'Normal' year to ensure that the results are not affected by improper initial conditions. The results of the simulation are shown in Table 6.5, Figure 6.8, Figure 6.9 and Figure 6.10.

6.4.2 Discussion of the results of the drought scenarios

From the simulated precipitation surpluses it can be seen that using different years for the drought scenarios does have an influence on the results. From the graph it can be seen that the year 1989 which was used for the 'Dry' scenario is almost the same as the 'Normal' year (1967) for the first eight months of the year. Only in autumn and early winter the year starts being dry. In the 'Extremely dry' scenario (1976) on the other hand the drought starts in early spring and continues for most of the rest of the year. The differences in timing of the onset of drought makes it more difficult to compare the results of the model.

The numbers in Table 6.5 show that the 'Extremely dry' year of 1976 received more than 40% less precipitation compared to the 'Normal' year. The transpiration by the vegetation remained the same as in the 'Dry' scenario, resulting in a much lower recharge of the urban groundwater with respect to the 'Normal' and 'Dry' scenarios.

Due to the lower recharge and the lowering of the groundwater level by capillary rise, the groundwater levels in both the 'Dry' and 'Extremely dry' scenarios drop significantly compared to the 'Normal' scenario. This reduces the amount of groundwater being drained by the nearby canals and as they drop below the surface water level lead to an inflow of surface water into the urban groundwater. For the 'Dry' scenario the difference in drainage with the 'Normal' year mainly takes place in the last four months of the year, due to the lower amount of precipitation at that time.

6.4.3 Answers to research questions

2.1 How much less precipitation is there in a dry or extremely dry year compared to a normal year

In a normal year there is about 990 millimetres of precipitation in Amsterdam. In a dry year this becomes 700 millimetres, so about 200 millimetres less than in a normal year. It should be noted though that this reduction in precipitation is mostly concentrated in a short period of time causing the drought. In a very dry year precipitation is about 350 millimetres less than in a normal year of which most is concentrated in a 'short' period of time.

2.2 How much further does the groundwater table drop due to drought compared to an normal year?

In a 'Normal' year the lowest, simulated groundwater level is about 0.41 metres below N.A.P.. In a 'Dry' year the groundwater levels drops to about 0.51 metres below N.A.P. and in an 'Extremely dry' year to 0.65 metres below N.A.P..

So, these numbers indicate that in a dry year the lowest area averaged groundwater level is about 10 centimetres lower than in a normal year. In an extremely dry year the area averaged groundwater level is about 15 centimetres lower at the time of the lowest groundwater levels compared to the normal situation.

These numbers, however, do not take any differences in groundwater level over the area into account. In reality the groundwater levels near a surface water body will deviate less from the level in the surface water due to groundwater replenishing from the surface water. In case of a drought the groundwater levels will thus be less affected. At locations further away from the surface waters the effects of drought will be greater, due to the larger distance and thus lower replenishment.

In the simulation the regional surface water level remained the same even during the peak of the drought. In reality it is likely that the desired water level cannot be maintained during dry spells. This is not so much the case for Amsterdam, as there is plenty of water stored in the nearby lake Ijssel for dry periods. In other locations where there is no or not enough water stored for dry spells the boundary condition should be altered to account for a drop in regional surface water level. Determining a reasonable boundary condition for dry and extremely dry years may be difficult, but quite important for arriving at a good prediction of groundwater levels and other parts of the urban water cycle.

6.4.4 Results of the drought scenarios

Table 6.5. Cumulative sums (mm) and fractions of the precipitation sum (-) of the fluxes in the drought scenario years. In Figure 6.10 an these values are visualized for easier interpretation.

		Scenario					
		Normal		Dry		Extremely dry	
Process	Precipitation	988	1	701	1	551	1
	Evaporation	162	0,16	123	0,18	100	0,18
	Transpiration	113	0,11	129	0,18	130	0,24
	Runoff	81	0,08	56	0,08	44	0,08
	Infiltration	305	0,31	215	0,31	167	0,30
	Recharge	192	0,19	97	0,14	47	0,09
	Drainage	127	0,13	88	0,13	55	0,10
	Sewer inflow	439	0,44	307	0,44	239	0,43
	DWF	1098	-	1098	-	1098	-
	WWTP	1537	-	1405	-	1337	-
	Overflow/Outflow	0	0,00	0	0,00	0	0,00
	Seepage	-64	-0,06	-59	-0,08	-54	-0,10
	Storage	2	0,00	-61	-0,09	-72	-0,13

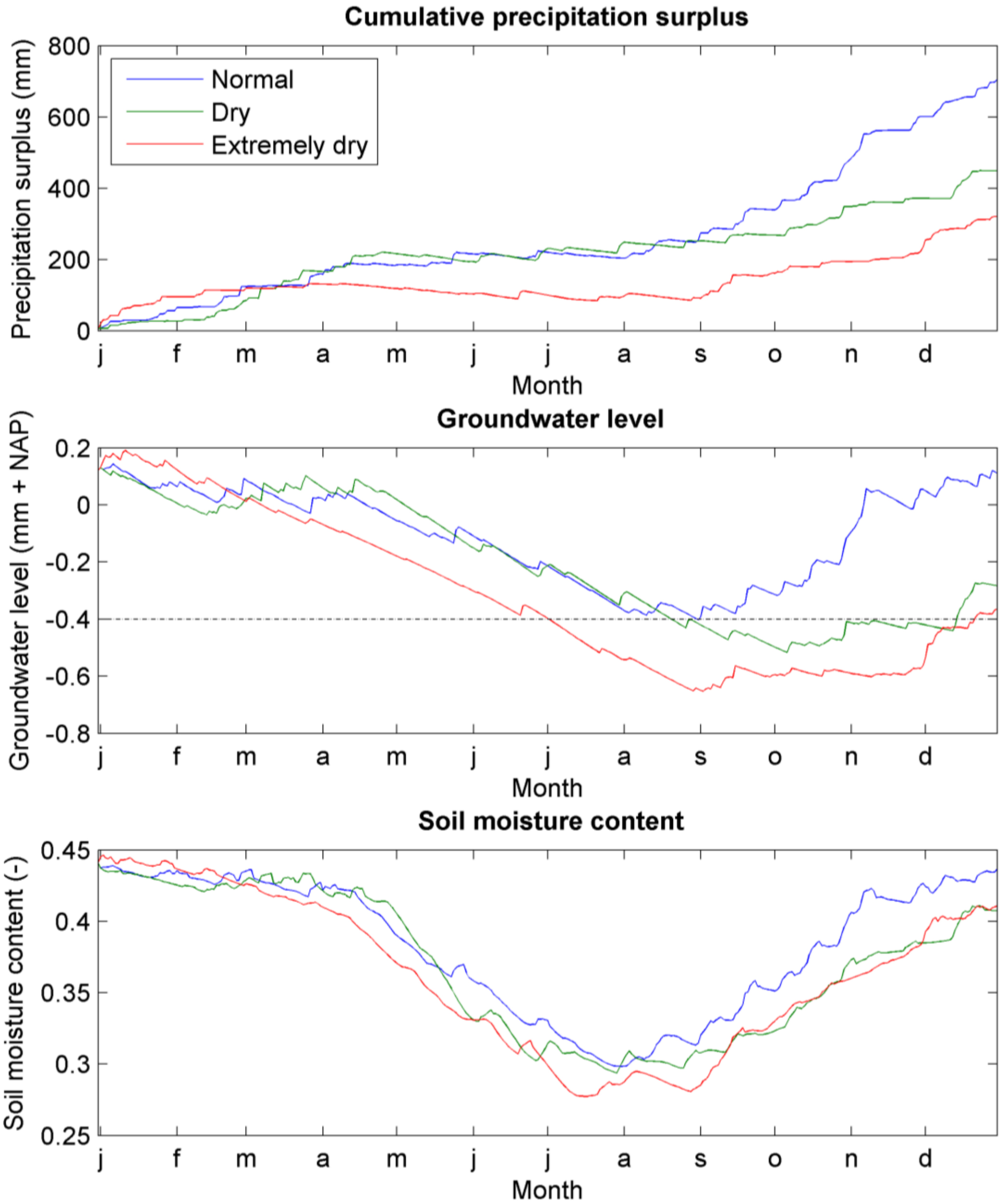

Figure 6.8. The simulated cumulative precipitation surplus (precipitation - evaporation), groundwater levels and soil moisture content over the scenario years 'Normal' (blue line), 'Dry' (green) and 'Extremely dry' (red) for the Prinseneiland. The dotted line in the middle graph indicates the surface water level.

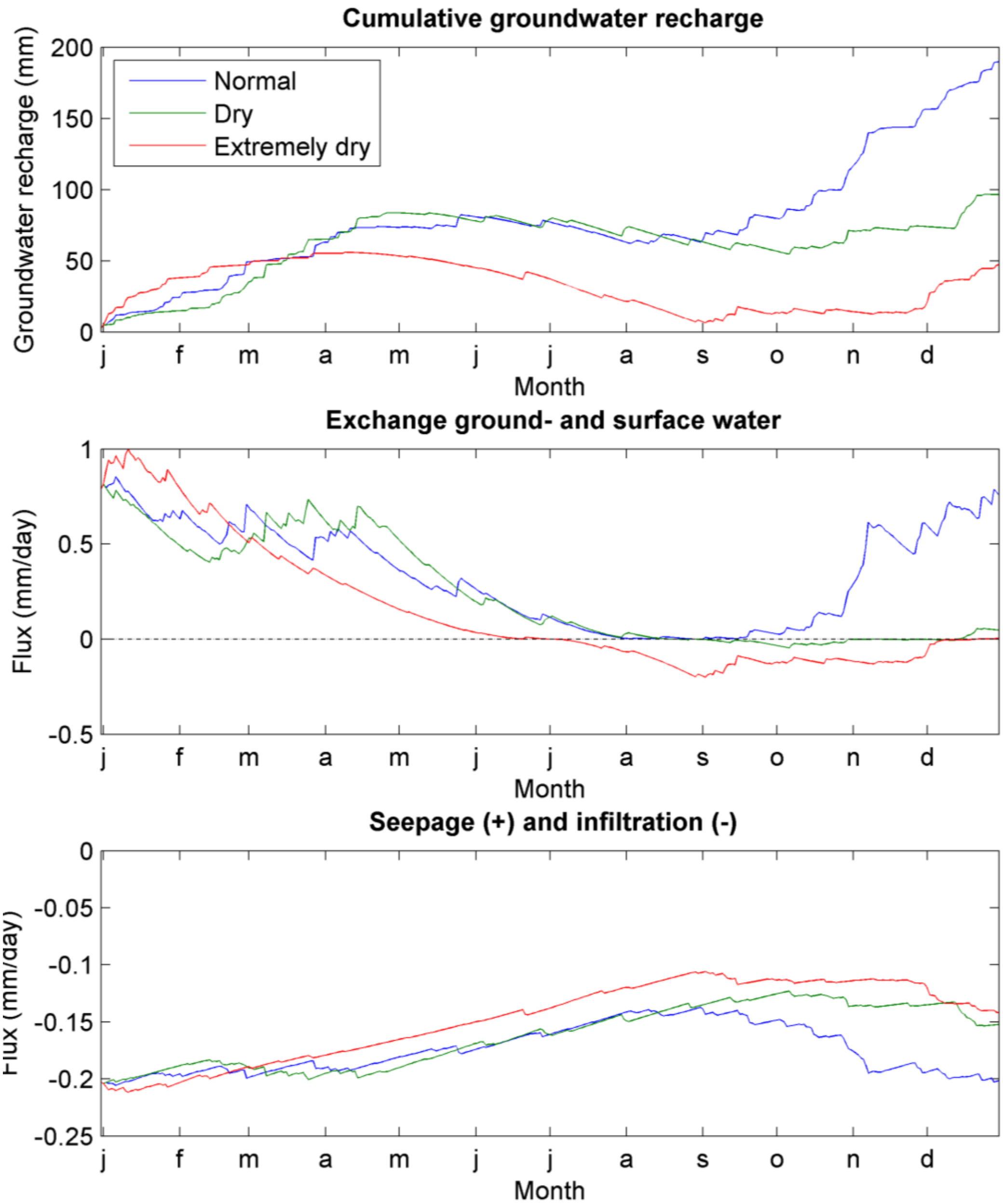

Figure 6.9. The simulated groundwater recharge, the flow of water between the urban ground- and the regional surface water and the flow between the urban and regional groundwater bodies over the scenario years 'Normal' (blue line), 'Dry' (green) and 'Extremely Dry' (red) for the Prinseneiland.

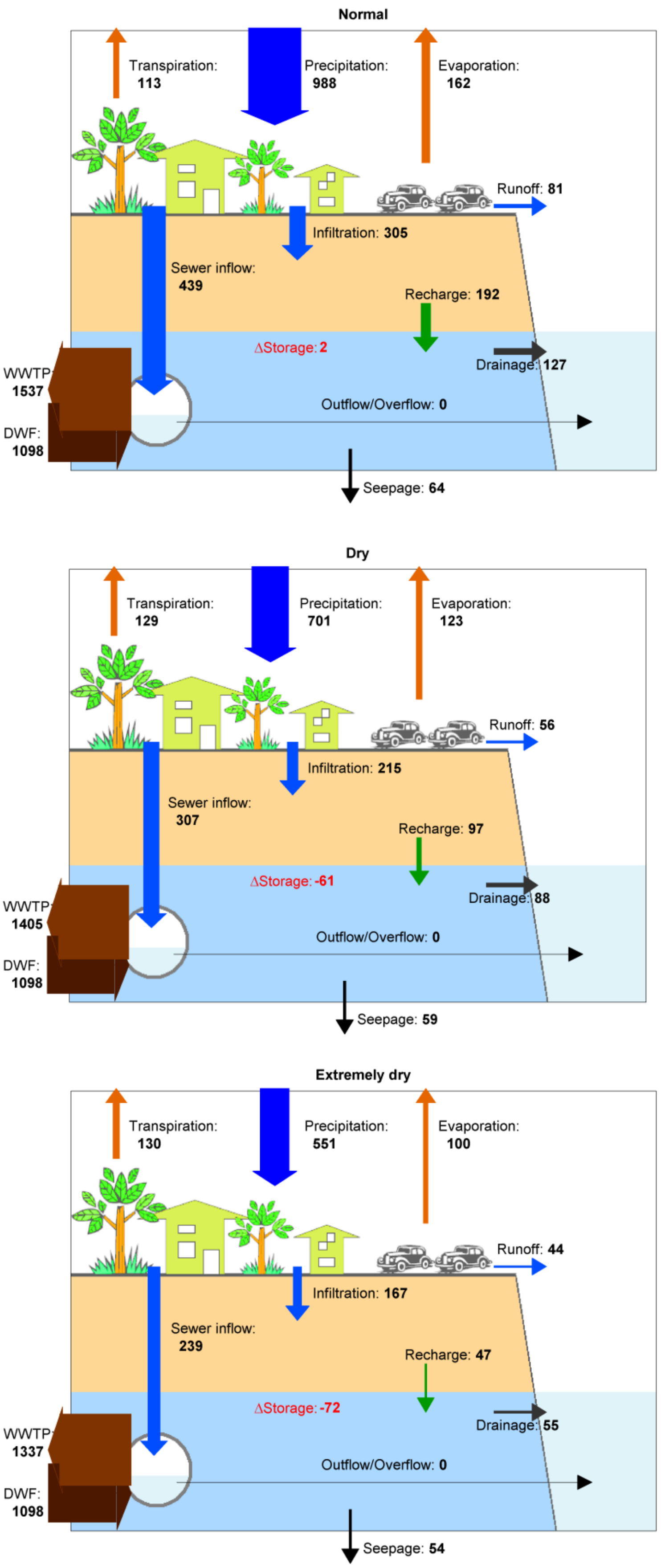

Figure 6.10. Overviews of the year sums of the fluxes over the three drought scenario years.

6.5 The effects of climate change

6.5.1 The climate scenarios

The effects of climate change in combination with drought on the water cycle of the Prinseneiland were investigated by using climate scenario's devised by the KNMI for the year 2050. The KNMI came up with four scenario's (Figure 6.11) that simulate the effects of one or two degrees Celsius warming of global temperatures in combination with changes or no changes in overall air circulation patterns.

Of these four climate scenarios the scenarios 'W+' and 'G' were selected for this study, as they capture the range in which the four evenly likely scenarios lie. So, by simulating only two scenarios it becomes possible to provide a range for the potential effects of a changed future climate. What the actual effects of climate change will be is uncertain, but probably within the range that the scenarios give.

The meteorological data that was used to simulate climate change were obtained from the NHI. The data consists of measured meteorological data over the three drought scenario years that was corrected to account for the effects of climate change. A 'Reference' scenario comprising of uncorrected data (the same as for the drought scenarios) was used to be able to compare the results of the scenarios. The results of the simulations are shown in sections 13.2, 13.4 and 13.6. In the following sections the results of the 'Reference' and 'W+' scenario for the 'Normal' and 'Extremely dry' drought scenarios are shown, as these combinations of scenarios are the most informative. The results and the discussion for the 'G' climate and 'Dry' drought scenario can be found in the appendix.

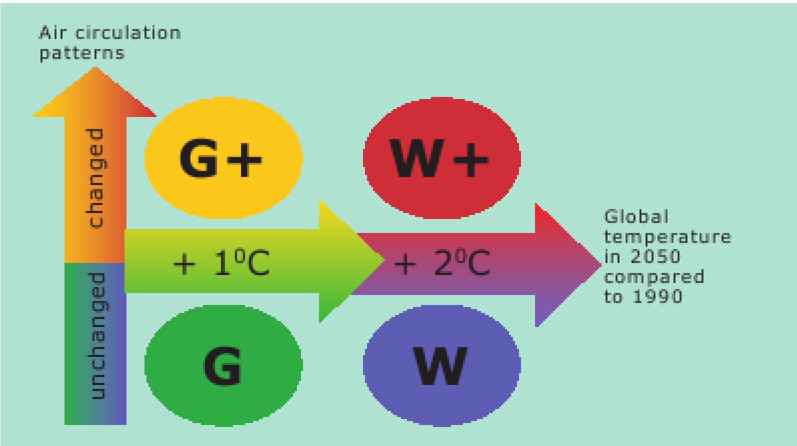

G	Moderate*	1°C temperature rise on earth in 2050 compared to 1990 no change in air circulation patterns in Western Europe
G+	Moderate +	1°C temperature rise on earth in 2050 compared to 1990 + milder and wetter winters due to more westerly winds + warmer and drier summers due to more easterly winds
W	Warm	2°C temperature rise on earth in 2050 compared to 1990 no change in air circulation patterns in Western Europe
W+	Warm +	2°C temperature rise on earth in 2050 compared to 1990 + milder and wetter winters due to more westerly winds + warmer and drier summers due to more easterly winds

Figure 6.11. KNMI'06 climate scenarios for the year 2050[12].

[12] Source: http://www.knmi.nl/climatescenarios/knmi06/index.php

6.5.2 Discussion of the results of the selected climate scenarios

In a normal year the ‘W+’ scenario the precipitation sum over the year is slightly higher compared with the ‘Reference’ scenario. The higher precipitation sum is a result of more precipitation during the winter months and less precipitation during the summer months compared to the ‘Reference’ scenario. Due to higher temperatures more water is transpired by vegetation. The combination of higher transpiration and lower precipitation during summer results in less groundwater recharge and thus groundwater levels that drop more compared to the ‘Reference’ situation.

In an ‘Extremely dry’ year the ‘W+’ scenario results in an even worse drought. This is caused by there being even less precipitation and still some more transpiration during the summer. This results in lower groundwater recharge and thus lower groundwater levels during summer. In the winter the groundwater recharge is higher groundwater levels at the start of summer, but this is not enough to compensate for the worse drought during summer.

6.5.3 Answers to research questions

3.1 On which parts of the urban hydrological cycle does a changing climate have the most impact?

In the ‘G’ scenario the precipitation is slightly higher than in the ‘Reference’ scenario. As a result all other fluxes in the urban hydrological cycle are also slightly higher. The differences, however, are not significantly large to worry about the effects of this climate scenario.

There are quite significant differences between the ‘Reference’ and ‘W+’ scenarios. Precipitation is about 10% lower over the whole year in the ‘W+’ scenario. It should be noted that there is actually more precipitation during the winter months compared to the current climatic conditions. This means that the summer months have an even larger reduction in precipitation than the 10%. As a result of the changes in precipitation pattern, the interception evaporation pattern also changes.

Due to the higher temperatures transpiration increases with about 10% compared to the ‘Reference’ scenario. As a result of the lower precipitation and the higher transpiration, the groundwater recharge decreases with 30 mm. (35%). In the winter months groundwater recharge becomes higher due to the higher precipitation amounts. In summer groundwater recharge is reduced dramatically due to lower precipitation and higher transpiration.

As a result the interception evaporation is also about 10% smaller. It should be noted that most of the precipitation falls in the winter months and that the summer months are even dryer than 10% compared to the ‘Reference’ scenario. Transpiration, is about 10% larger due to the higher temperatures. As a result of the smaller precipitation and higher transpiration, the groundwater recharge have dropped by about 35% or 30 mm. The smaller recharge results in lower groundwater levels, which in turn result in less seepage and more replenishing of the groundwater by the regional surface water during the drought.

6.5.4 Results of the selected climate scenarios

Table 6.6. Cumulative sums (mm) and fractions of the precipitation sum (-) of the fluxes in the drought scenario years. In Figure 6.14 an these values are visualized for easier interpretation.

		Scenario							
		Ref. Normal		Ref. Extremely dry		W+ Normal		W+ Extremely dry	
Process	Precipitation	988	1	551	1	1004	1	497	1
	Evaporation	162	0,16	100	0,18	157	0,16	90	0,18
	Transpiration	113	0,11	130	0,24	129	0,13	144	0,29
	Runoff	81	0,08	44	0,08	83	0,08	40	0,08
	Infiltration	305	0,31	167	0,30	314	0,31	151	0,30
	Recharge	192	0,19	47	0,09	182	0,18	15	0,03
	Drainage	127	0,13	55	0,10	120	0,12	37	0,07
	Sewer inflow	439	0,44	239	0,43	450	0,45	216	0,43
	DWF	1098	-	1098	-	1098	-	1098	-
	WWTP	1537	-	1337	-	1548	-	1314	-
	Overflow/Outflow	0	0,00	0	0,00	0	0,00	0	0,00
	Seepage	-64	-0,06	-54	-0,10	-63	-0,06	-52	-0,10
	Storage	-2	0,00	72	0,13	-3	0,00	83	0,17

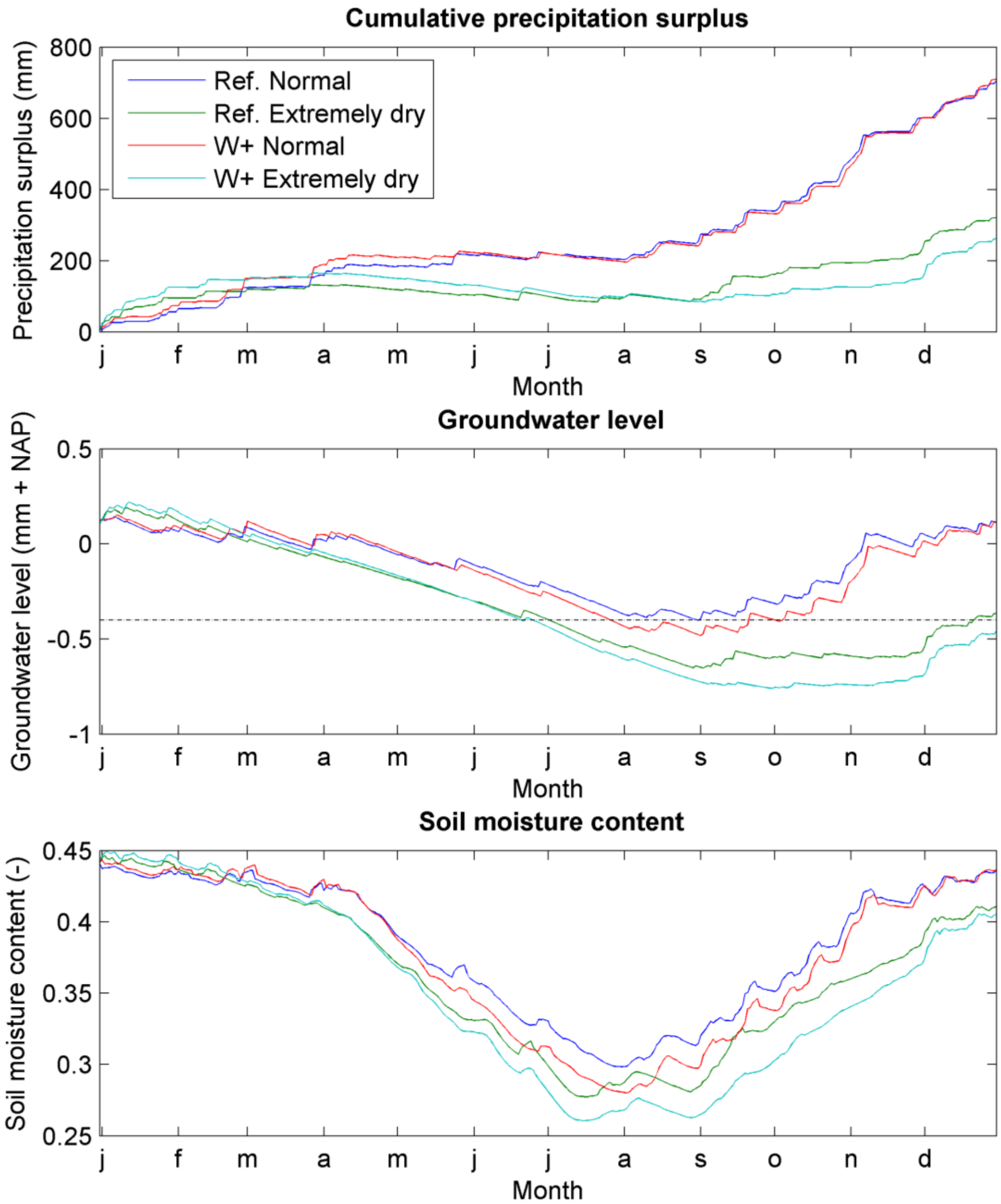

Figure 6.12. The simulated cumulative precipitation surplus (precipitation - evaporation), groundwater levels and soil moisture content over the scenario combinations 'Reference, Normal' (blue line), 'Reference, Extremely dry' (green),'W+, Normal' (red) and 'W+, Extremely dry' (cyan) for the Prinseneiland. The dotted line in the middle graph indicates the surface water level.

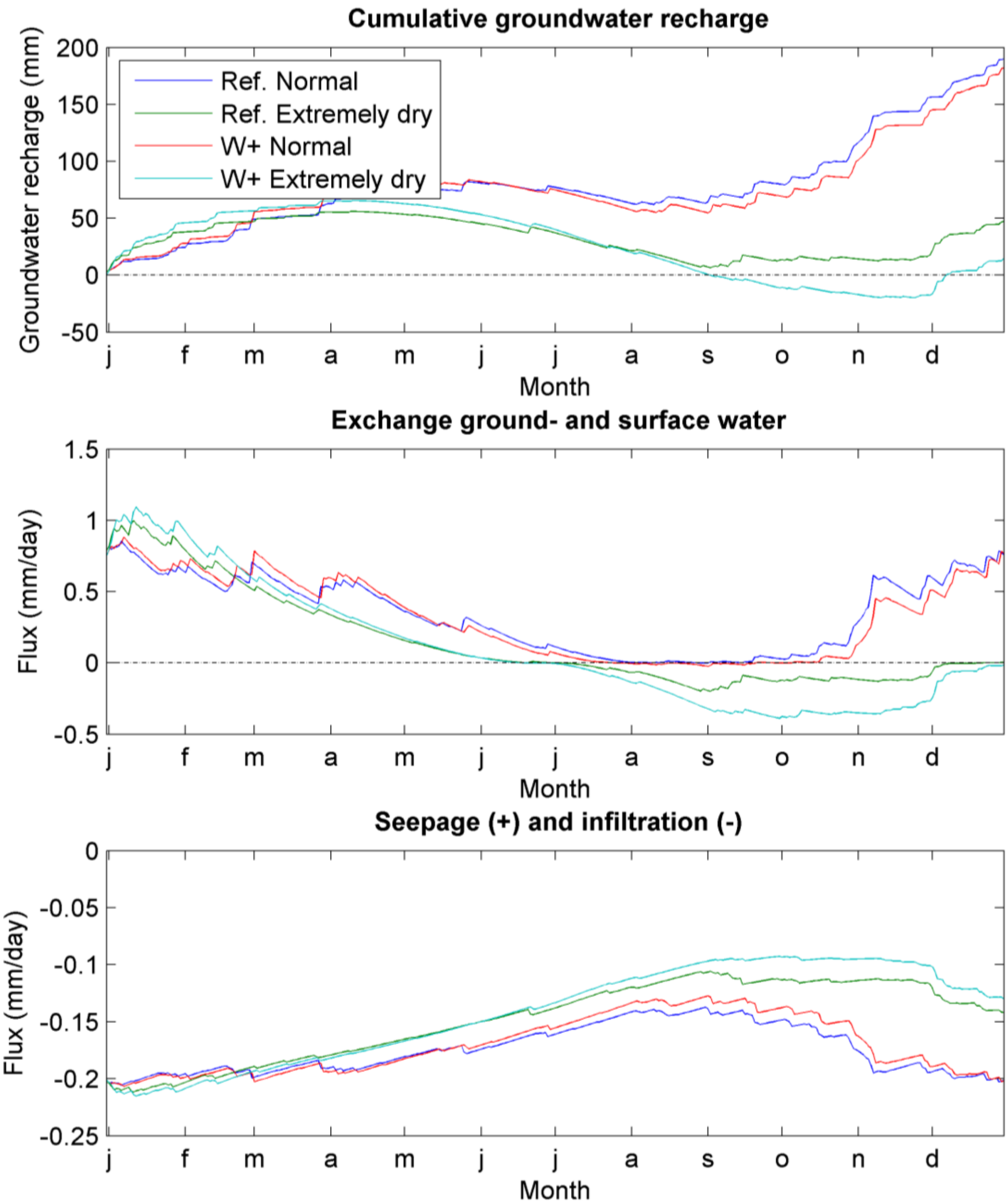

Figure 6.13. The simulated groundwater recharge, the flow of water between the urban ground- and the regional surface water and the flow between the urban and regional groundwater bodies over the scenario years 'Reference, Normal' (blue line), 'Reference, Extremely dry' (green), 'W+, Normal' (red) and 'W+, Extremely Dry' (cyan) for the Prinseneiland.

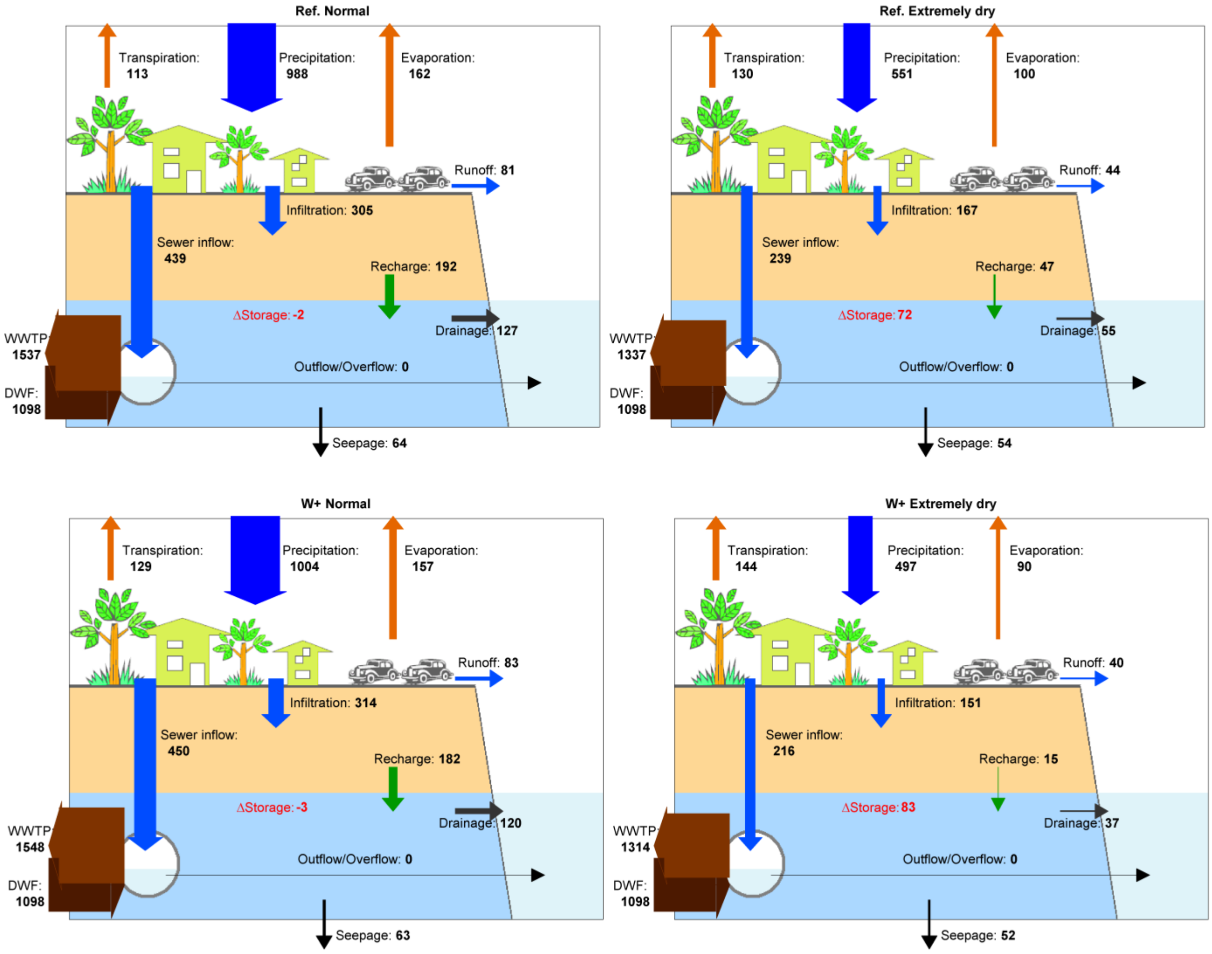

Figure 6.14. Overviews of the year sums of the fluxes over the four selected climate scenarios.

6.6 Uncertainty analysis

6.6.1 Model parameters

The results of the parameter calibration showed that most parameter values were not clearly bounded. This could be an indication of the value of those parameters not being very important for a good simulation of the calibration variable. It could also indicate that a trade-off between parameters is possible, which results in a group of ill-defined parameter values that merely seem to be unimportant.

The values of the parameters that were not calibrated can be estimated by combining information on the study area with parameter values found in literature.

6.6.2 Study area characteristics

The characteristics of the study area are an important aspect in the simulations. The land use classification of the features in the study area (section 3.3.1) should be carried out by combining a land use map of the area with a field survey to verify the information on the map. This way any errors made should not result in a classification with an uncertainty of more than a few per cent.

The precipitation discharge mode classification (section 3.3.2) of the features in the study area should be based on a field survey. This survey should be aimed at determining which pathway(s) precipitation on a feature will follow during normal circumstances. The survey should preferably be undertaken during a precipitation event, which makes it easier to determine the pathways.

6.6.3 Input time series

The precipitation time series that were used during the study originated from a location outside the study area. This means that the data is likely to be different from the actual values, but due to the close proximity the data probably is a good estimate. This is confirmed by the bivariate linear correlation coefficient between the daily precipitation sums of the KNMI stations in Amsterdam and at Schiphol of 0.86. It is assumed that the correlation between the data of the KNMI station in Amsterdam and the actual precipitation in the study area is better due to the closer proximity and since both locations are located nearby the city centre.

The potential evaporation time series were obtained from the KNMI station at Schiphol. The values in the time series are probably lower than the actual values. This is mainly caused by the warmer city environment compared with the rural area of the measuring location.

7 Conclusions

7.1 Data frequency/availability

7.1.1 Groundwater levels

The calibration on the groundwater level measurements over the periods 2010-2011 and October 2012 – February 2013 shows the importance of having high frequency data for calibration. Without the high frequency data available for calibration, the model probably would not have been able to properly simulate the groundwater dynamics.

For the study the groundwater levels were measured every half hour with centimetre accuracy. This set-up, however, resulted in a lot of non-informative data, as shown in Figure 7.1. In the figure it is shown that measuring every 4 till 12 hours already gives enough information to determine the groundwater dynamics.

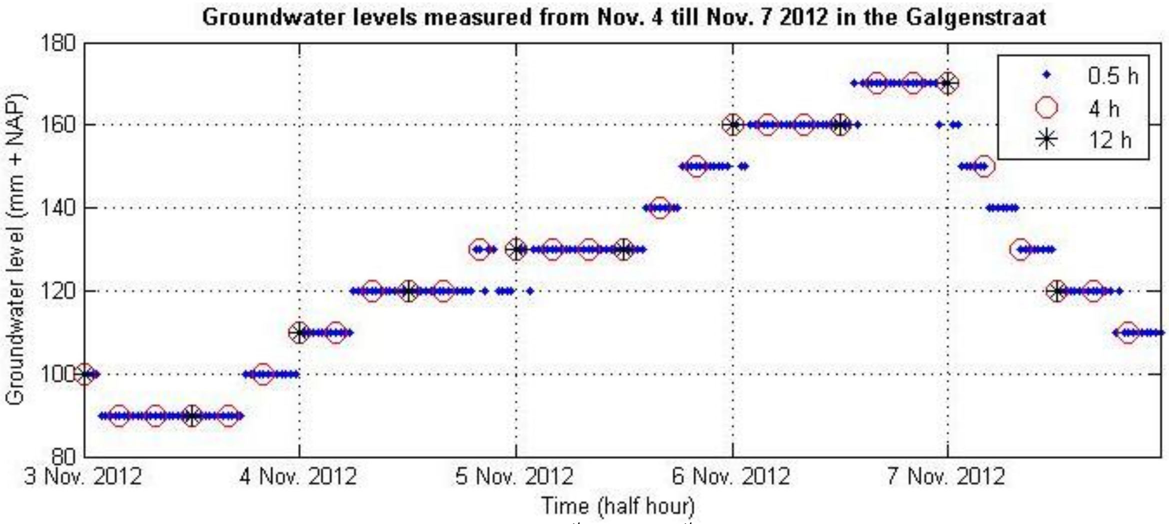

Figure 7.1. Groundwater level measurements from the 4th till the 7th of November 2012 in the Galgenstraat. The blue indicate the actual data. The red circle and black asterisk indicate hypothetical datasets for measurements with a lower frequency of once every 4 and 12 hours respectively.

7.1.2 Precipitation

The precipitation data used for this study was taken from the KNMI station in Amsterdam. The KNMI station at Amsterdam Airport Schiphol could have provided data with a higher measuring frequency. Close examination of the data, however, revealed that the daily precipitation sums of the stations differed too much (see sections 4.1.1 and 11.1) to justify the use of the data from Schiphol for the Prinseneiland case. The potential evaporation data from Schiphol was used for the study, as it was the best available data.

7.2 Model performance

The validation of the model with the optimal parameter values found during calibration showed that the model underestimates the groundwater levels during dry periods. The overall results of the simulations showed patterns that were to be expected. From this it is concluded that the model results seem realistic, but there remains room for improvement of the model.

7.3 General conclusions on droughts

In a 'Dry' year precipitation is about 200 mm less than in a 'Normal' year. This results in a reduction in interception evaporation, infiltration and surface runoff. The potential evaporation is generally higher in 'Dry' years, resulting in an increase in transpiration between roughly 10 and 15 mm of water. The combination of less infiltration and more transpiration results in lower soil moisture contents, followed by higher capillary rise fluxes and consequently in lower groundwater levels. The lower groundwater levels result in lower groundwater drainage and seepage fluxes.

In an ‘Extremely dry’ year precipitation is about 350 mm less than in a ‘Normal’ year (150 mm compared to ‘Dry’), which results in an extra reduction in interception evaporation, infiltration, and surface runoff. Transpiration remains at the same level as during a ‘Dry’ year, due to moisture constraints in the root zone. The reduction in infiltration combined with the lower soil moisture due to transpiration results in an even lower recharge compared to the ‘Dry’ year. The lower recharge results in lower groundwater levels and thus in lower groundwater drainage and seepage fluxes.

7.4 General conclusions on climate change

The ‘G’ scenario has slightly more precipitation than the ‘Reference’ scenario, which results in larger fluxes in the rest of the urban hydrological cycle. The differences, however, are not significant and fall within the uncertainty limits of the model.

The ‘W+’ scenario has about the same amount of precipitation as the ‘G’ scenario. The difference, however, is that there is more precipitation during winter and less during summer. This results in higher infiltration and groundwater recharge and consequently higher groundwater levels during late winter and early spring. During summer precipitation is less, which results in lower infiltration and groundwater recharge rates. Combined with a higher transpiration due to the warmer climate, this results in lower groundwater levels. In late spring and early winter groundwater levels are replenished slower than in the ‘Reference’ scenario due to the lower soil moisture contents.

8 Discussion

8.1 The need for high quality drinking water supply data

The lack of high quality drinking water supply measurements were felt unexpectedly hard during the study. The drinking water supply discharges to the Prinseneiland are not measured. Therefore, discharges to the whole of Amsterdam were used after scaling. The seasonal fluctuations in the used data did not correspond with the fluctuations in the measured sewer discharges. This is to be expected, as the discharges to the whole of Amsterdam is the sum of the discharges to all neighbourhoods in Amsterdam, obscuring the discharge to just the Prinseneiland.

Having the data would have made it possible to determine whether the base flow of the sewer discharges only consists of waste water from the households and businesses on the island or also of intruding groundwater. Combining knowledge on the amounts of groundwater leaking into the sewer with information on groundwater levels and their fluctuations may even have resulted in making an educated guess on which part of the sewer is leaking. Furthermore, such data would have made it possible to set up a water balance for the sewer and determine the inflow of precipitation into the sewer.

8.2 Possible improvements/adaptations of the model

- In the current model structure the fast and slow groundwater flow components are modelled as one process, that forms a sort of average of both components. In future conceptual models it might be better to model these two components as separate processes.
- In the current model set-up only daily precipitation sums are used. This results in a disregard of the intensities of the precipitation event(s). These intensities could be incorporated by using data from KNMI stations with hourly data. Since these measuring stations are probably further away from the study area, it has to be assumed that the measured precipitation durations are representative. Using the data on precipitation duration can be used for making the processes following precipitation intensity dependent. This could result in better estimates of infiltration and surface runoff quantities and more realistic model behaviour.

8.3 Drought scenarios

The drought scenarios used in this study consist of the meteorological data of three years that were chosen on the basis of the return period of the resulting lowest river discharges in the main rivers of the Netherlands. This is not an ideal method for creating drought scenarios, as the differences in precipitation patterns obscure the effects of the drought.

A better way of creating drought scenarios would be to take the meteorological data of a year with an average precipitation sum over the year and which has a precipitation deficit with a return period of one year. In order to determine which year would be appropriate for the study area, an analysis of the available meteorological data is necessary. The meteorological data of the selected year is then to be adapted (manually decrease the precipitation) to increase the maximal precipitation deficit to a level that the precipitation deficit reaches a level of once in N years.

8.4 Climate scenarios

For the investigation of the effects of climate change only the ‘G’ and ‘W+’ KNMI’06 scenarios were used. These two scenarios are likely to cover the potential effects of climate change, as they are the two extremes of the four climate scenario. Since the ‘G+’ and ‘W’ scenarios were not run with the model, the above statement has not been checked and might be invalid. In future research these climate scenarios could be run to make sure that the reported scenarios do give the range in which the results for all scenarios lie.

8.5 The 'water demand' of the Prinseneiland

In this report the possible effects of climate change on the urban water cycle of the Prinseneiland were shown. These effects have not yet been converted into an amount of water the island may need to cancel the effects of drought and climate change. It is quite difficult to make this conversion as it requires more information on the vulnerabilities of an area, to what extend the predicted effects are acceptable and from which point action is required.

In order to provide an example, water demands of the Prinseneiland for the four scenarios selected in section 6.5 were calculated. This was done under the assumption of the groundwater levels not dropping below the (fixed) water level in the nearby canals being the only requirement. The calculation consists of a normal model run with an instantaneous extra water gift that keeps the average groundwater level over the island above the nearby surface water level. The simulated cumulative water demands for the selected scenario years are shown in Figure 8.1. In Table 8.1, Figure 8.2 and Figure 8.3 the effects of the water gifts on the urban water cycle are shown.

From the results it can be seen that the Prinseneiland needs a lot more water during the 'Extremely dry' years than during the 'Normal' years. Further the effect of the changing precipitation pattern on the water demand is not that strong during a 'Normal' year. In an 'Extremely dry' year the changing precipitation pattern does add tremendously to the water need of the area, which nearly doubles.

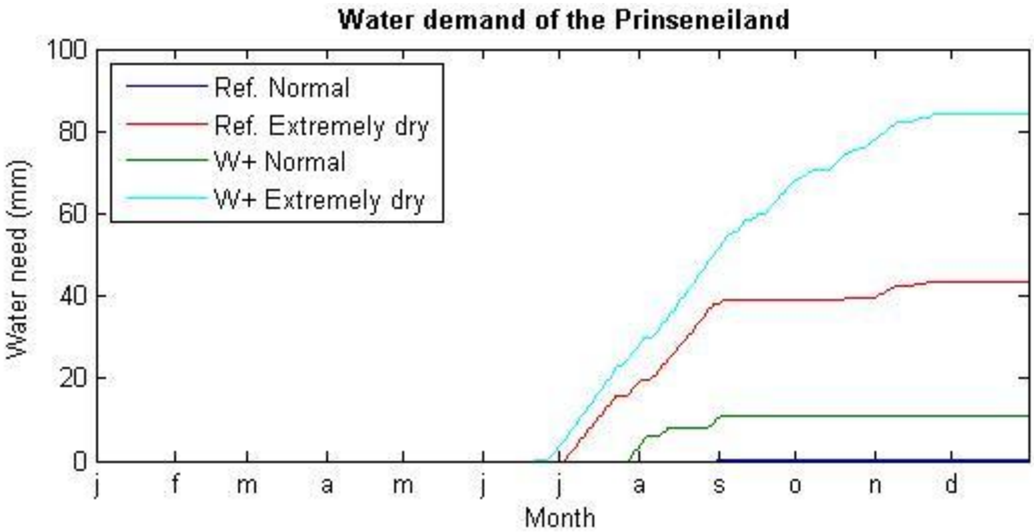

Figure 8.1. Cumulative water need of the Prinseneiland for the four selected scenarios of section 6.5.

Table 8.1. Cumulative sums of the fluxes (mm) and changes in the water cycle due to the extra supply of water (mm) in the selected scenario years.

		Scenario							
		Ref. Normal		Ref. Extremely dry		W+ Normal		W+ Extremely dry	
Process	Water added[13]	0		44		11		84	
	Precipitation	988	0	551	0	1004	0	497	0
	Evaporation	162	0	100	0	157	0	90	0
	Transpiration	113	0	130	0	129	0	144	0
	Runoff	81	0	44	0	83	0	40	0
	Infiltration	305	0	167	0	314	0	151	0
	Recharge	192	0	47	0	182	0	15	0
	Drainage	127	0	74	19	130	10	84	47
	Sewer inflow	439	0	239	0	450	0	216	0
	DWF	1098	0	1098	0	1098	0	1098	0
	WWTP	1537	0	1337	0	1548	0	1314	0
	Overflow/Outflow	0	0	0	0	0	0	0	0
	Seepage	-64	0	-58	-4	-64	-1	-59	-7
	Storage	2	0	-51	21	2	-1	-52	31

[13] In order to arrive at a volume of water, the water needs have to be multiplied with a factor of 34. This results in volumes of 0, 1496, 374 and 2856 m^3 of water needed respectively.

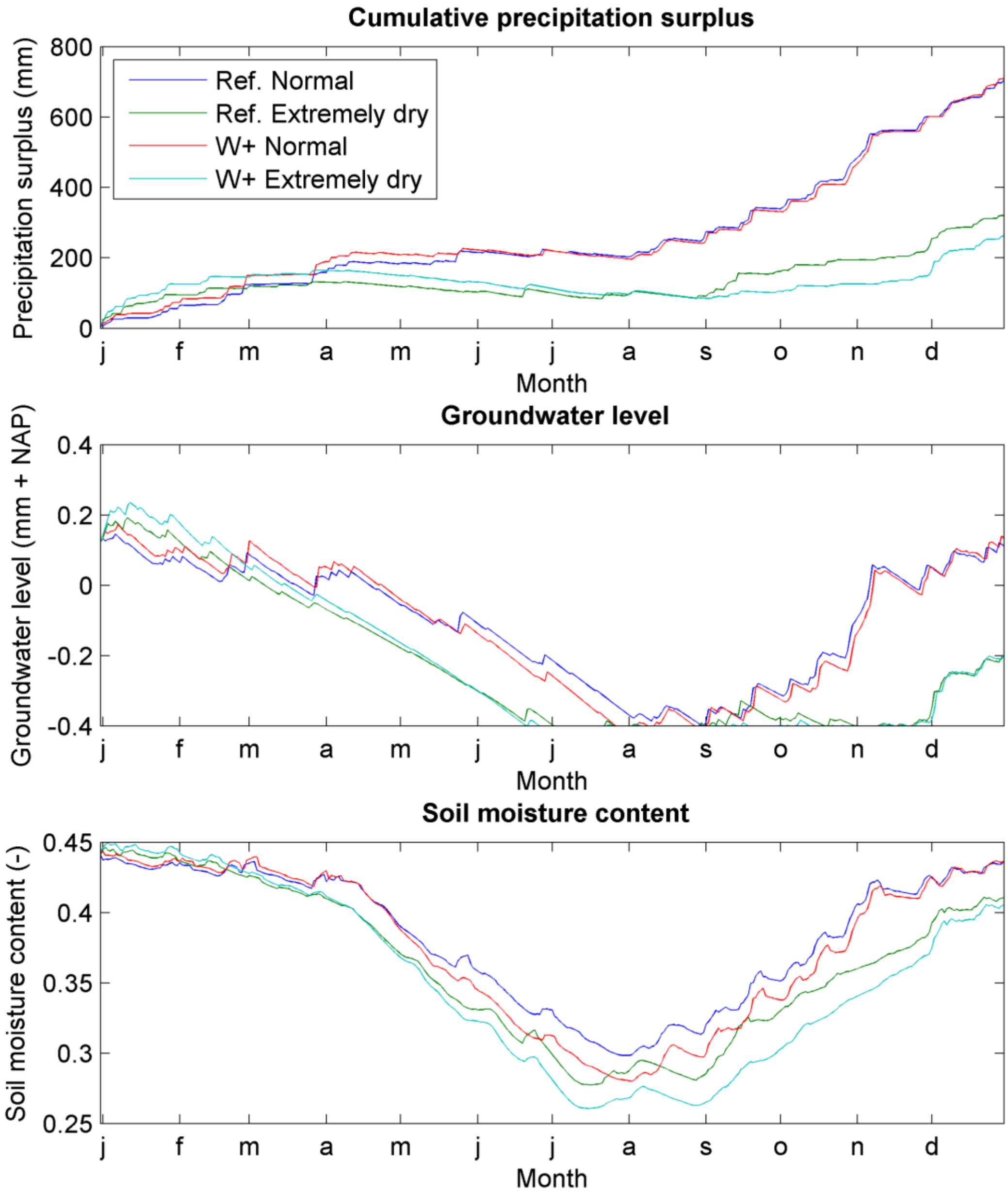

Figure 8.2. The simulated cumulative precipitation surplus (precipitation - evaporation), groundwater levels and soil moisture content over the scenario combinations 'Reference, Normal' (blue line), 'Reference, Extremely dry' (green),'W+, Normal' (red) and 'W+, Extremely dry' (cyan) for the Prinseneiland. The dotted line in the middle graph indicates the surface water level.

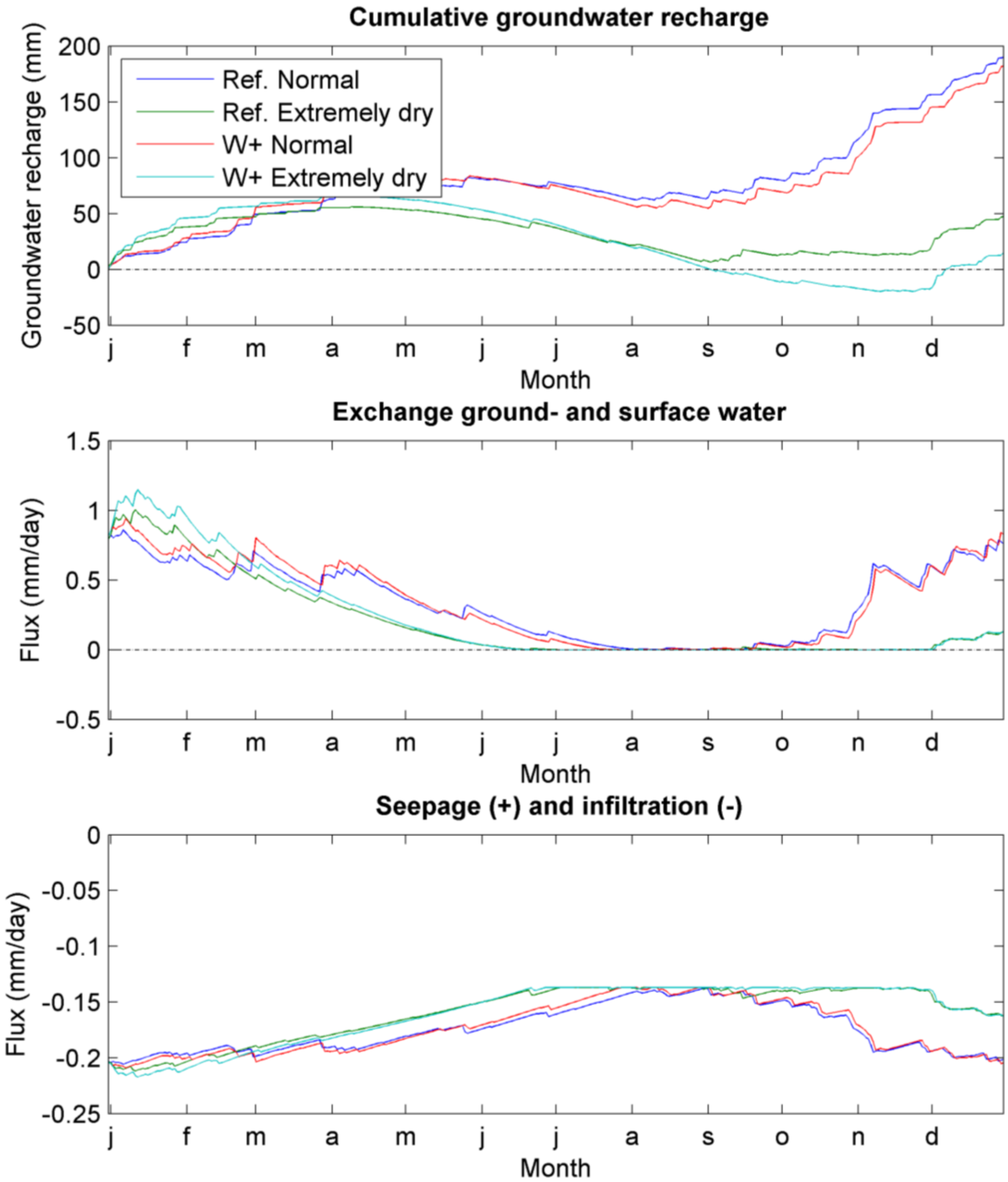

Figure 8.3. The simulated groundwater recharge, the flow of water between the urban ground- and the regional surface water and the flow between the urban and regional groundwater bodies over the scenario years 'Reference, Normal' (blue line), 'Reference, Extremely dry' (green), 'W+, Normal' (red) and 'W+, Extremely Dry' (cyan) for the Prinseneiland.

9 References

Allen, R. G., Pereira, L. S., Raes, D., Smith, M., (1998), Crop evapotranspiration - Guidelines for computing crop water requirements. *FAO IRRIGATION AND DRAINAGE PAPERS,* vol. 56. FAO - Food and Agriculture Organization of the United Nations.

Ballweg, H. (2002), Abenteuer Grundstückentwässerung, *Göttinger Abwassertage*

Breuer, L., Eckhardt, K., Frede, H.G. (2003), Plant parameter values for models in temperate climates, *Ecological Modelling*, vol. 169, no. 2-3, pp. 237–293

Davis, S.N. (1969), Porosity and permeability of natural materials. In: *Flow Through Porous Media,* De Wiest, R.J.M. (ed.), Academic Press, New York, pp. 54-89

Deltares, (2012, maart), Schades door watertekorten en –overschotten in stedelijk gebied. Quick scan van beschikbaarheid schadegetallen en mogelijkheden om schades te bepalen. Deltares projectnummer 1205463.

Deltares, (2012, November), Effect van droogte op stedelijk gebied. Kennisinventarisatie. Deltares projectnummer 1206224

Deltares, (2013, april), Naar een bestendige stedelijke waterbalans. Studie van waterbalansveranderingen, gevoeligheid en maatregelen op wijkniveau. Deltares projectnummer 1206329.

Eiswirth, M., Hötzl, H. (1997), The impact of leaking sewers on urban groundwater. In: *Groundwater in the urban environment*, Chilton, J. (ed.), pp. 399-404, Balkema, Rotterdam

Fenicia, F., Savenije, H.H.G., Matgen, P., Pfister, L. (2006), Is the groundwater reservoir linear? Learning from data in hydrological modelling, *Hydrol. Earth Syst. Sci.*, 10, pp. 139-151

Garcia-Fresca, B. (2006), Urban-enhanced groundwater recharge: review and case study of Austin, Texas, USA. In: *Urban Groundwater, Meeting the Challenge*. *International Association of Hydrogeologists Selected Papers*, Howard, K.W.F. (ed.), Taylor & Francis, London, UK, 2006; pp. 3-18.

Geiger, W.F., Marsalek, J., Rawls, W.J., Zuidema, F.C. (eds.) (1987). Manual on drainage in urban areas. Volume I – Planning and design of drainage systems. In: *Studies and reports in hydrology*, no. 43, UNESCO, Paris, ISBN 92-3-102416-7

Gerrits, A.M.J., Pfister, L., Savenije, H.H.G. (2010), Spatial and temporal variability in canopy and forest floor interception in a beech forrest, *Hydrol. Process.*, vol. 24, no. 21, pp. 3011-3025

Horton, R. E., (1919), Rainfall interception. *Monthly Weather Review*, vol. 47, no. 9, pp. 603–623.

Johnson, A.I. (1967), Specific yield – compilation of specific yields for various materials, *U.S. Geological Survey Water Supply Paper*, 1662-D

Klemeš, V. (1986), Operational testing of hydrological simulation models, *Hydrological Sciences Journal,* vol. 31, no. 1, pp. 13–24.

Lerner, D.N. (2002), Identifying and quantifying urban recharge: a review, *Hydrogeology Journal,* vol. 10, pp. 143-152

Lindström, G., Johansson, B., Persson, M., Gardelin, M., Bergström, S. (1997), Development and test of the distributed HBV-96 hydrological model. *Journal of Hydrology*, 201, pp. 272-288

Marsalek, J. et al. (2006), Urban water cycle processes and interactions, *IHP-VI Technical Document in Hydrology*, no. 78, UNESCO Working Series SC-2006/WS/7

Nash, J.E., Sutcliffe, J.V. (1970), River flow forecasting through conceptual models Part I - a discussion of principles. *Journal of Hydrology*, 10: 282–290.

Oke, T. R., (1982), The energetic basis of the urban heat island, *Quarterly Journal of the Royal Meteorological Society*, vol. 108, no. 455, pp. 1-24

Rutsch, M., Rieckermann, J., Krebs, P. (2006), Quantification of sewer leakage: a review, *Water Science and Technology*, vol. 54, no. 6-7, pp. 135-144

Van de Ven, F.H.M. (1985), From rainfall to sewer inflow; a process with consequences. In: *Water in urban areas*, Hooghart, J. (ed.), TNO Comm. on Hydrol.Res., Proc. and Inform. 33

Van de Ven, F.H.M. (1989) Van neerslag tot rioolinloop in vlak gebied, Dissertation Delft University of Technology

Van de Ven, F.H.M. (1990), Water balances of urban areas, In: *Hydrological processes and water management in urban areas*, Massing, H., Packman, J. and Zuidema, F.C., (eds.), IAHS publ. no. 198, ISBN 0-947571-82-5, pp. 21-32

Van de Ven, F.H.M. (2007), Water management in urban areas, Lecture notes CT5510, Delft University of Technology

Van Genuchten, M. Th. (1980), A closed-form equation for predicting the hydraulic conductivity of unsaturated soils, *Soil science society of America Journal*, vol. 44, no. 5, pp. 892-898

10 Appendix A: Field survey of the Prinseneiland

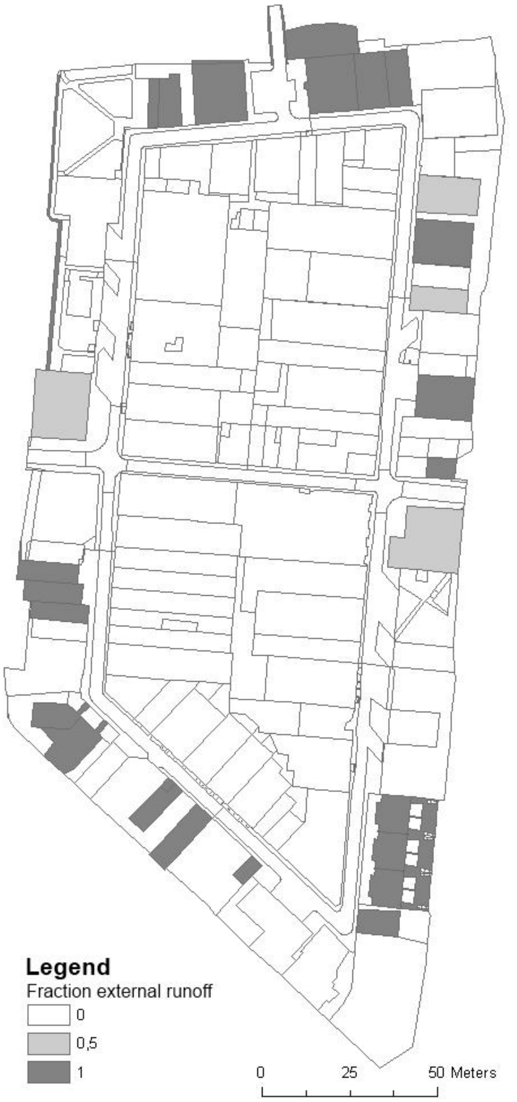

Figure 10.1. The fraction of precipitation on a feature being discharged outside the area boundaries.

Figure 10.2. The locations of the drainpipes from the buildings, gully pots and manholes determined during the fieldwork. The red colour indicates the buildings on the island, whilst the grey shades denote the paved areas and the green the unpaved areas.

11 Appendix B: Data evaluation

11.1 Precipitation data

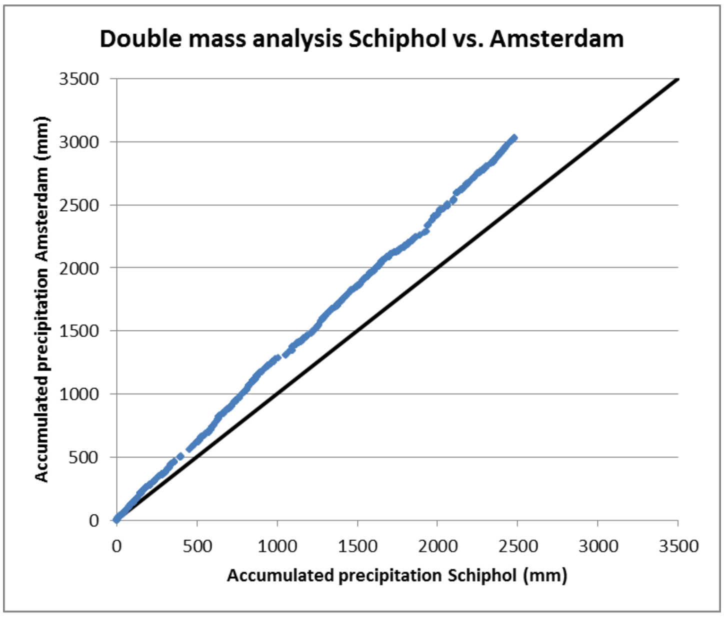

Figure 11.1. Double mass analysis of the precipitation measured at the KNMI stations at Schiphol and Amsterdam over the years 2010 till 2012. The black line indicates perfect correspondence.

As can be seen from Figure 11.1, the KNMI station in Amsterdam measured more precipitation than the station at Schiphol. Over the period 2010 till 2012 the difference in measured totals amounted about 22% of the total precipitation over the three years at Schiphol.

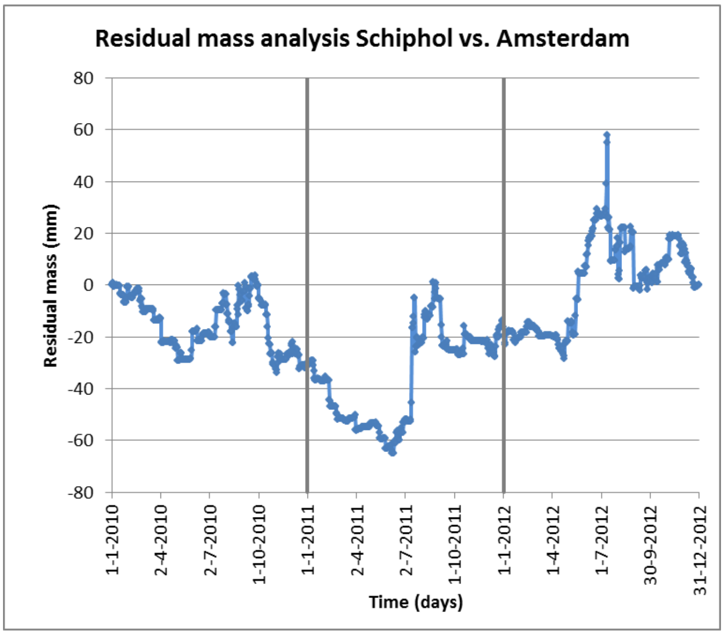

Figure 11.2. Residual mass analysis of the precipitation measured at the KNMI stations at Schiphol and Amsterdam over the years 2010 till 2012.

Figure 11.2 shows the cumulative difference between the precipitation measured at Schiphol and in Amsterdam. A decline indicates more precipitation in Amsterdam than at Schiphol and vice versa. From the figure it can be seen that more precipitation falls at Schiphol from about May/June till September/October than in Amsterdam. In winter and spring more precipitation is measured in Amsterdam than at Schiphol.

12 Appendix C: Model calibration and validation

12.1 Calibration on groundwater levels over the period 2010 – 2011

In the figure below the results of the Monte-Carlo simulation on the groundwater levels in the Galgenstraat over the period 2010-2011 are shown.

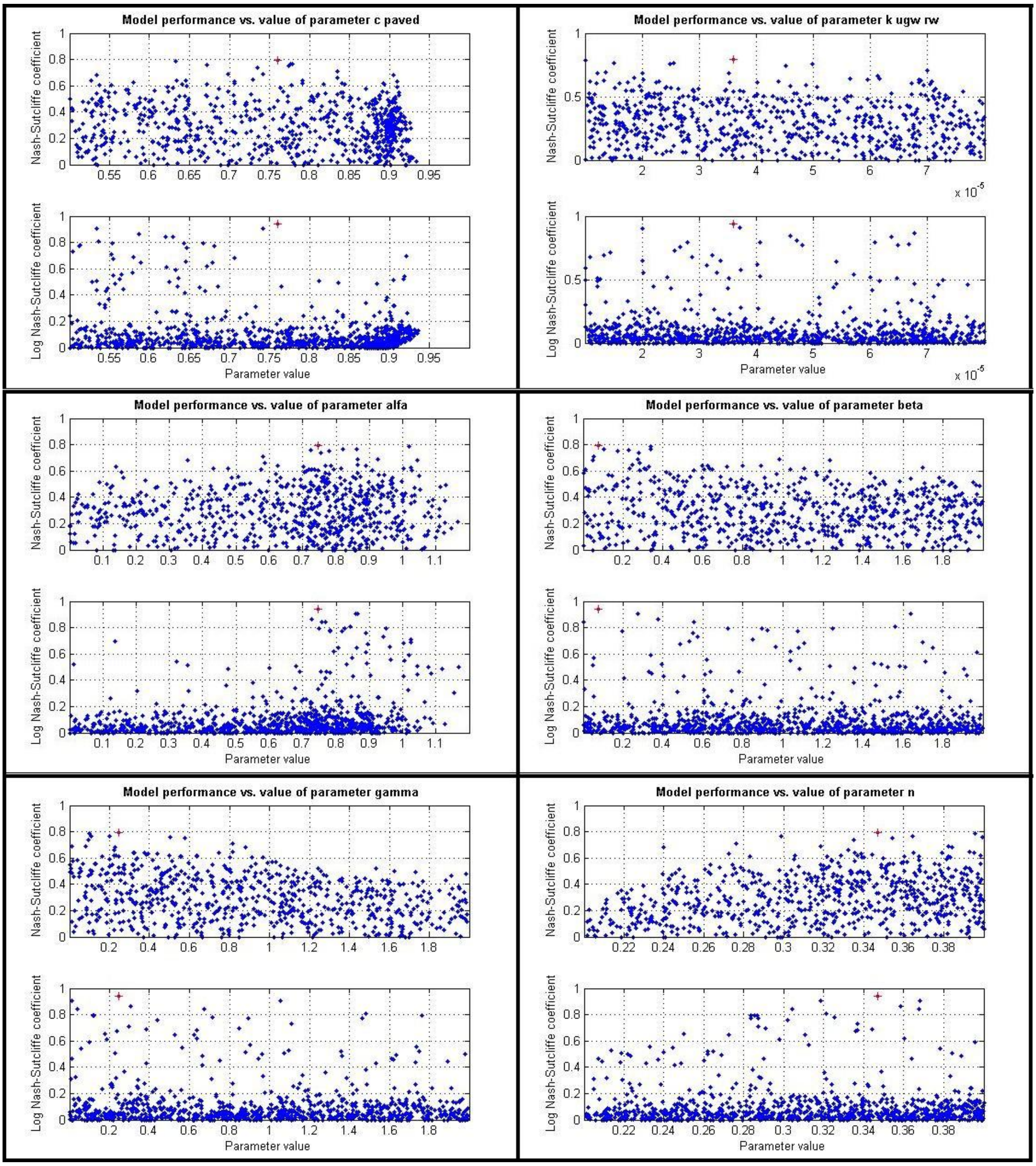

Figure 12.1. Performance of the model as a function of the values of the model parameters. The performance of the model is plotted vs. the values of 'c_paved' (top left pair), 'k_ugw_rw' (top right pair), 'alfa' (middle left), 'beta' (middle right), 'gamma' (bottom left) and 'n' (bottom right). Each blue dot corresponds with the results of one Monte-Carlo run. The red cross indicates the calculated optimal parameter value.

From the subplots in Figure 12.1 it can be seen that the parameters '*alfa*', '*beta*' and '*gamma*' are quite clearly bounded for the Nash-Sutcliffe coefficients. For the Nash-Sutcliffe this is only the case for the parameter '*alfa*'. The other parameters are less clearly bounded.

12.2 Calibration on groundwater levels over the period Oct. 2012 – Feb. 2013

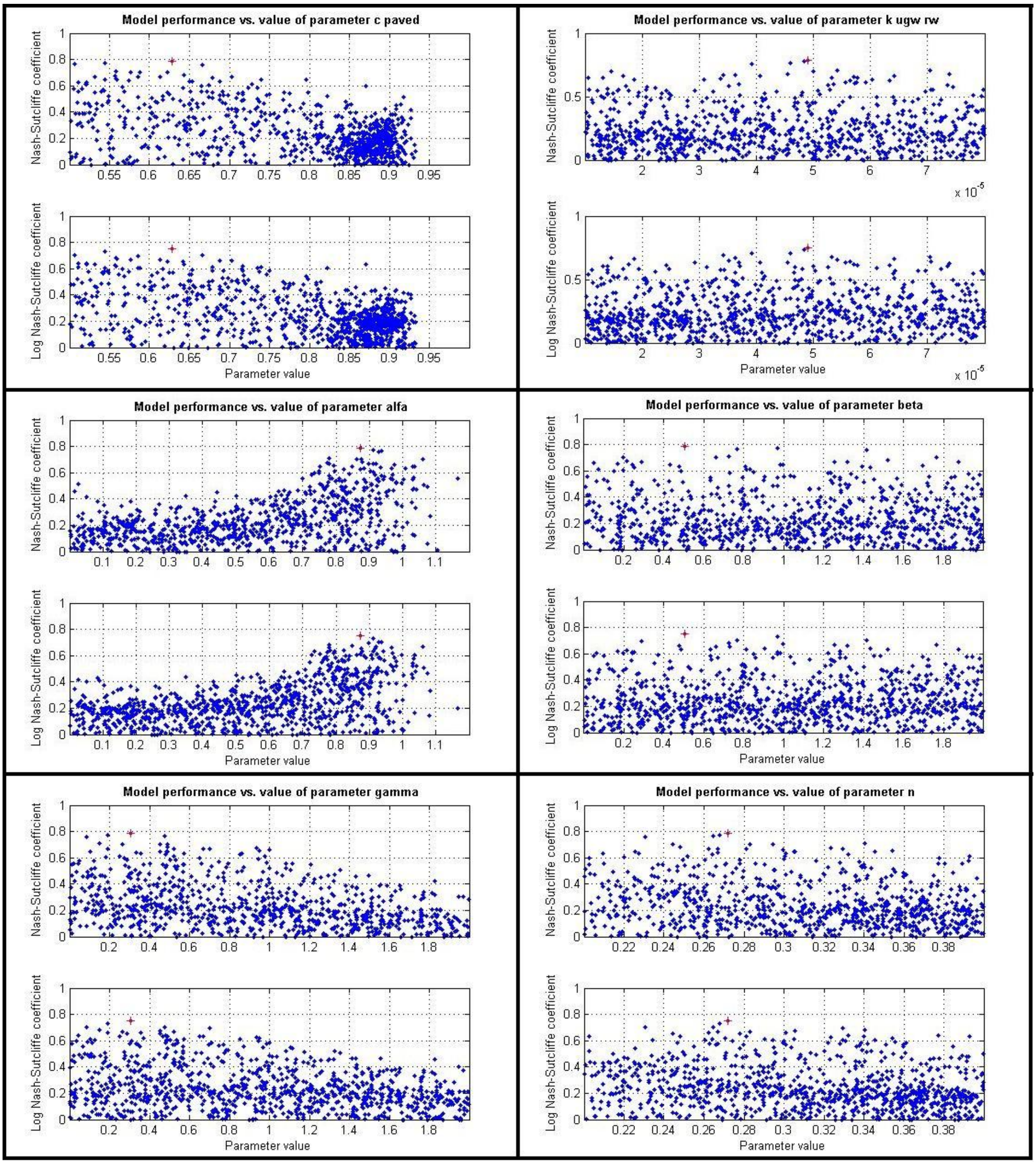

Figure 12.2. Performance of the model as a function of the values of the model parameters. The performance of the model is plotted vs. the values of 'c_paved' (top left pair), 'k_ugw_rw' (top right pair), 'alfa' (middle left), 'beta' (middle right), 'gamma' (bottom left) and 'n' (bottom right). Each blue dot corresponds with the results of one Monte-Carlo run. The red cross indicates the calculated optimal parameter value.

From the subplots in Figure 12.2 it can be seen that the parameters '*c_paved*', '*alfa*' and '*gamma'* are quite clearly bounded for both the Nash-Sutcliffe and Log Nash-Sutcliffe coefficients. The other parameters are less clearly bounded.

12.3 Calibration on sewer discharges from the Prinseneiland 2010-2011

In the figure below the results of the Monte-Carlo simulation on the sewer discharges from the pumping station on the Prinseneiland over the period 2010-2011 are shown. During the simulation the parameters 'c_paved', 'k_ugw_rw' and 'k_ugw_sewer' were calibrated on the precipitation discharge and the dry weather flow.

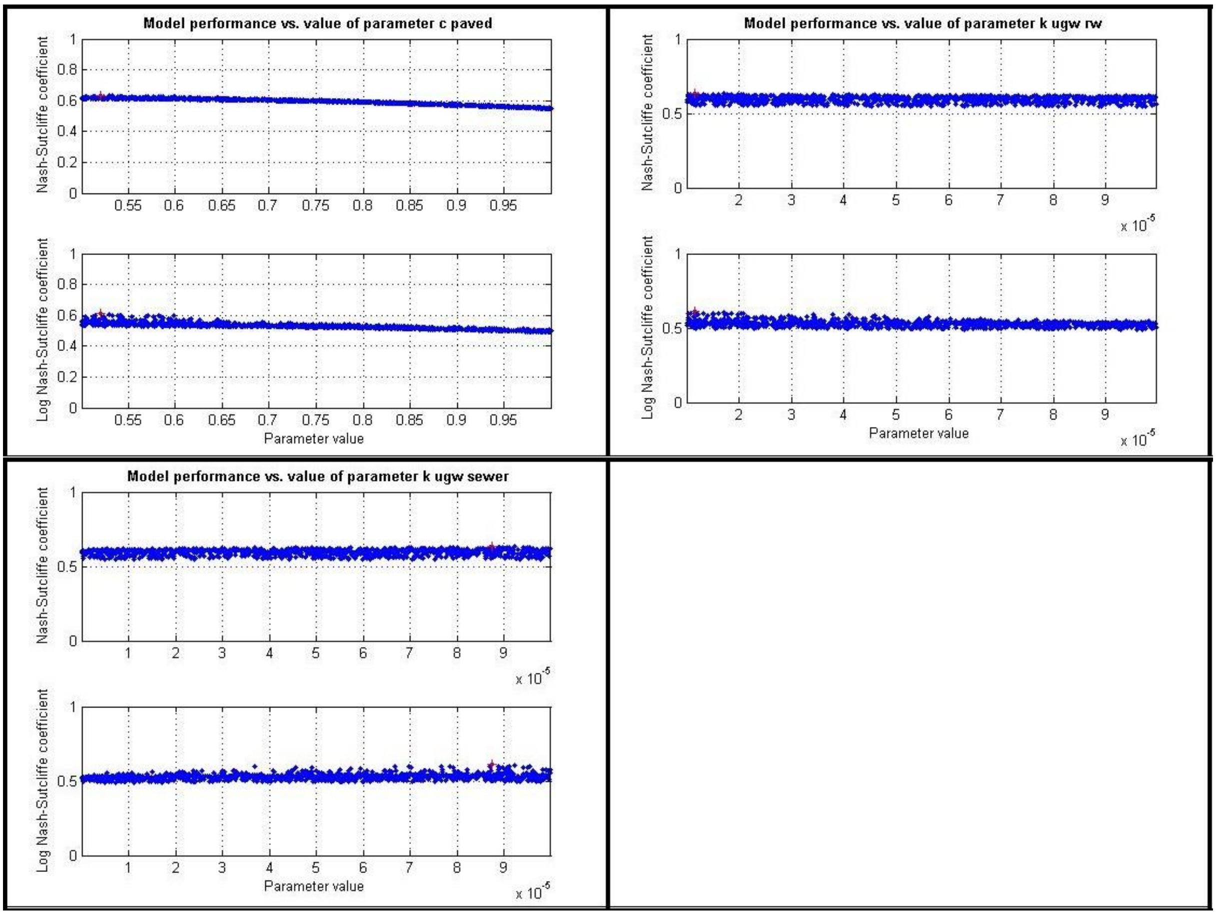

Figure 12.3. Performance of the model as a function of the values of the model parameters. The performance of the model is plotted vs. the values of 'c_paved' (top left pair), 'k_ugw_rw' (top right pair) and 'k_ugw_sewer' (bottom left). Each blue dot corresponds with the results of one Monte-Carlo run. The red cross indicates the calculated optimal parameter value.

From Figure 12.3 it can be seen that none of the parameters are clearly bounded. The parameters do seem to have an 'optimal' value, but large deviations from these values do not result in a lower model performance. This indicates that the parameters that were calibrated are not important for modelling the sewer discharge. Therefore the results from this calibration run are not used to determine the value of any parameter.

The lowest model performance coefficient resulting from the calibration run is about 0.5. This is also a sign of the chosen parameters not being vital for the simulation of the sewer discharges. Other parameters and input seem to be able to give relatively satisfactory results. This is partly caused by the fact that a substantial part of the peak sewer discharge stems from precipitation fallen on the roofs of buildings, which reduces the importance of runoff from the paved surfaces. Next to that, the base flow in the sewer discharge is formed by the dry weather flow and possibly water infiltrating into the sewer, which are not influenced by the parameters shown in the figure.

13 Appendix D: Results climate scenario runs

13.1 Discussion of the results for a 'Normal' year

'Reference' vs. 'G'
From Table 13.1, Figure 13.1 and Figure 13.2 it can be seen that the differences between the results of the 'Reference' and 'G' scenarios for a 'Normal' year are quite small. The 'G' scenario has slightly more precipitation, which results in slightly larger fluxes in the rest of the urban hydrological cycle. The differences are not significantly large to draw conclusions from them.

'Reference' vs. 'G'
The 'W+' scenario also receives slightly more precipitation than the 'Reference' scenario, but the precipitation is concentrated in the winter months. This results in a larger groundwater recharge and thus higher groundwater levels in winter and early spring. In the summer there is less precipitation resulting in lower soil moisture contents, groundwater recharge and levels. Due to the lower soil moisture contents, the groundwater recharge in fall and early winter is slightly delayed compared to the 'Reference' scenario.

The transpiration of water by vegetation is about 14% higher than in the 'Reference' scenario, due to a higher potential evaporation. The higher transpiration results in an extra lowering of the groundwater recharge and thus in lower groundwater levels compared to the 'Reference' situation.

13.2 Results for a 'Normal' year

Table 13.1. Cumulative sums (mm) and fractions of the precipitation sum (-) of the fluxes in a 'Normal' year of the climate change scenarios. In Figure 13.3 an these values are visualized for easier interpretation.

		Scenario					
		Reference Normal		G Normal		W+ Normal	
Process	Precipitation	988	1	1019	1	1004	1
	Evaporation	162	0,16	164	0,16	157	0,16
	Transpiration	113	0,11	117	0,11	129	0,13
	Runoff	81	0,08	84	0,08	83	0,08
	Infiltration	305	0,31	316	0,31	314	0,31
	Recharge	192	0,19	200	0,20	182	0,18
	Drainage	127	0,13	133	0,13	120	0,12
	Sewer inflow	439	0,44	454	0,45	450	0,45
	DWF	1098	-	1098	-	1098	-
	WWTP	1537	-	1552	-	1548	-
	Overflow/Outflow	0	0,00	0	0,00	0	0,00
	Seepage	-64	-0,06	-64	-0,06	-63	-0,06
	Storage	2	0,00	2	0,00	3	0,00

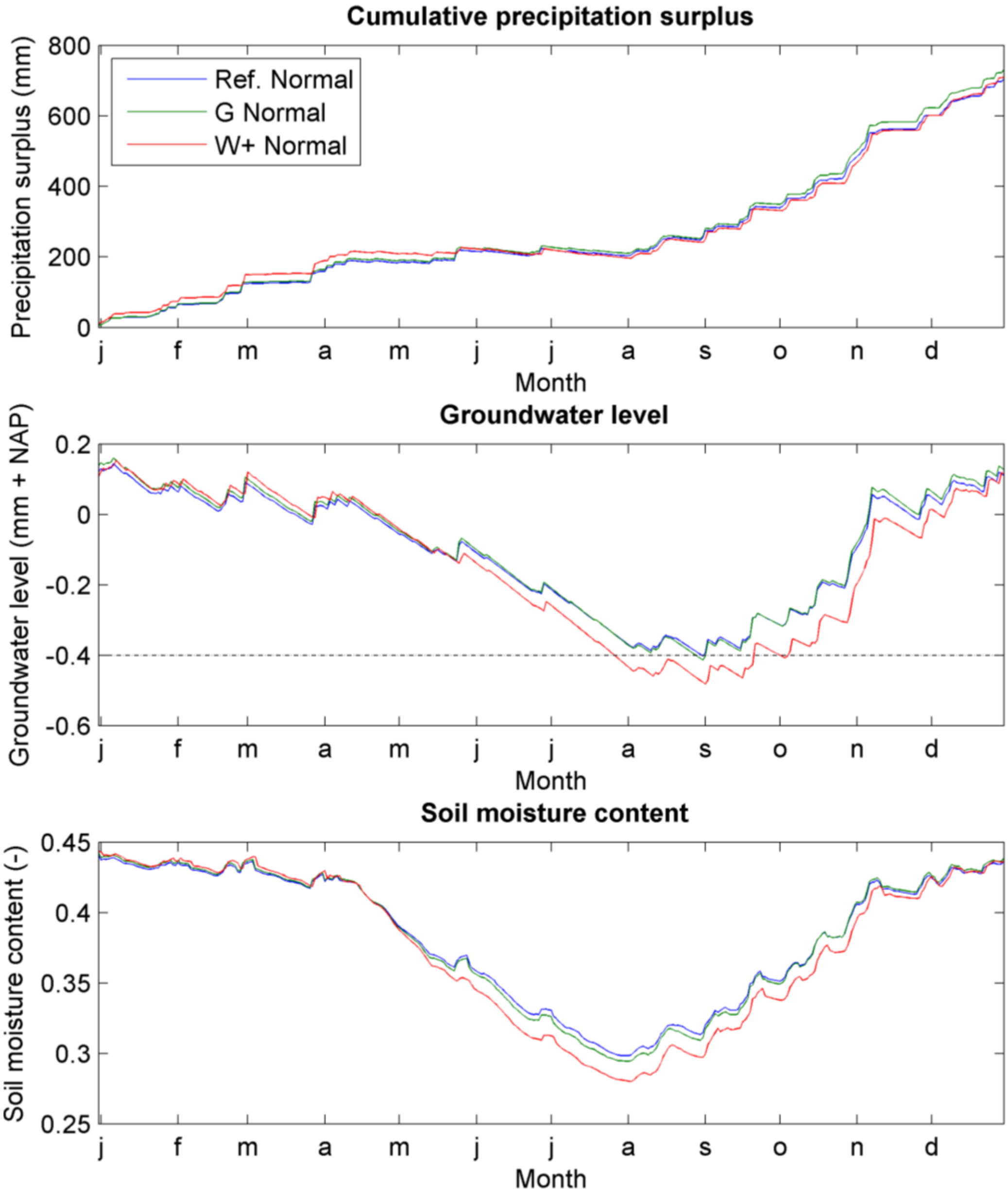

Figure 13.1. The simulated cumulative precipitation surplus (precipitation - evaporation), groundwater levels and soil moisture content over the 'Normal' years of the 'Reference' (blue line), 'G' (green) and 'W+' (red) climate scenarios for the Prinseneiland. The dotted line in the middle graph indicates the surface water level.

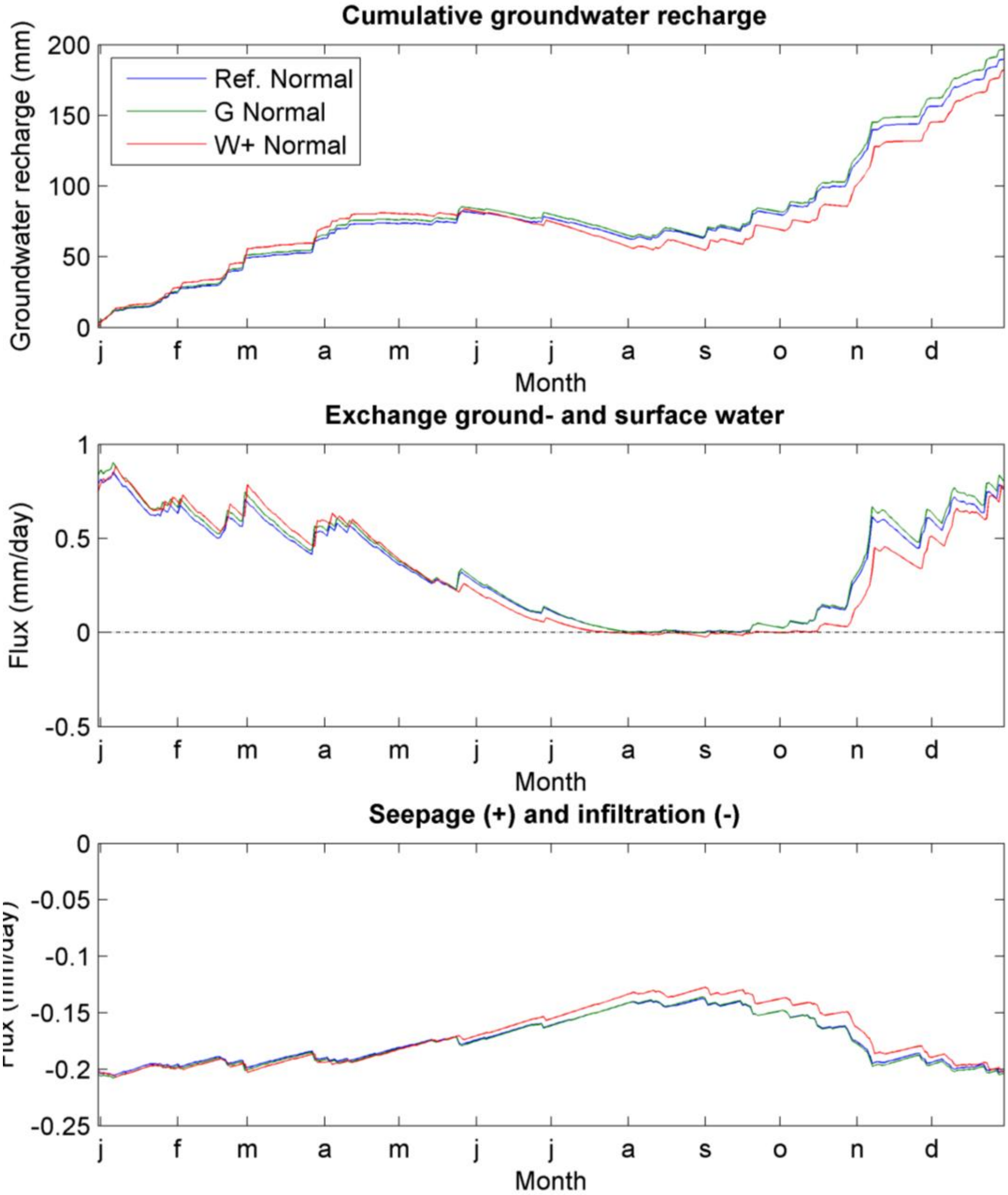

Figure 13.2. The simulated groundwater recharge, the flow of water between the urban ground- and the regional surface water and the flow between the urban and regional groundwater bodies over the 'Normal' years of the 'Reference' (blue line), 'G' (green) and 'W+' (red) climate scenarios for the Prinseneiland.

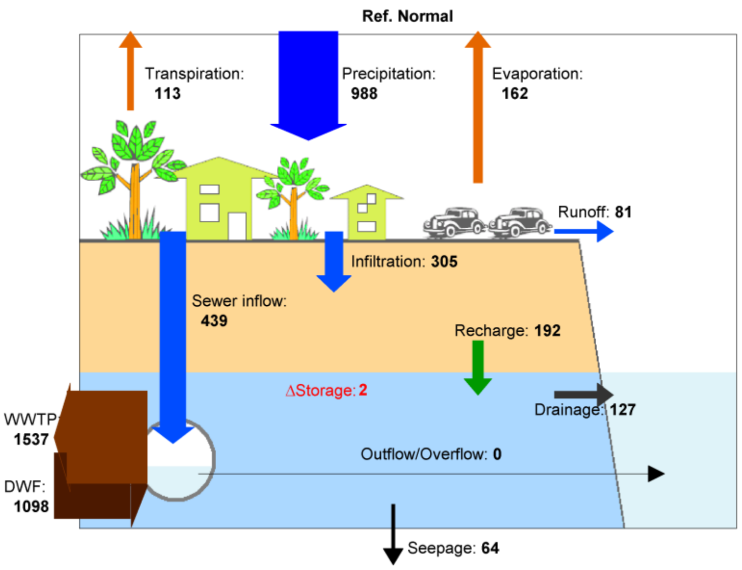

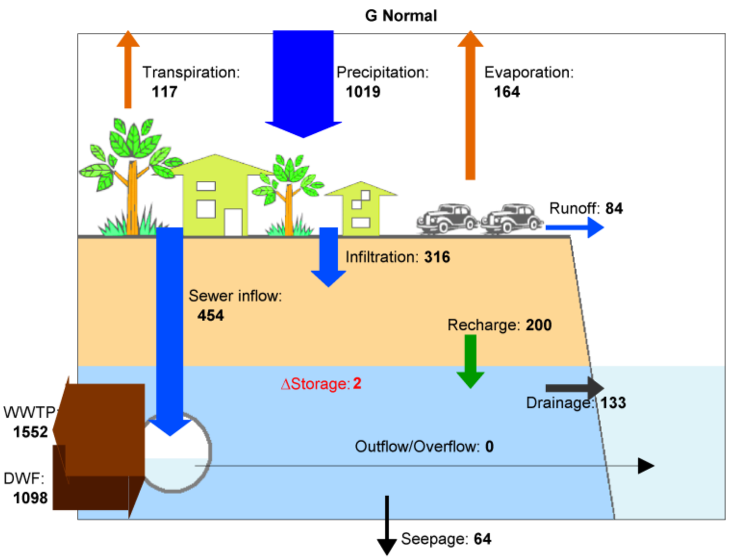

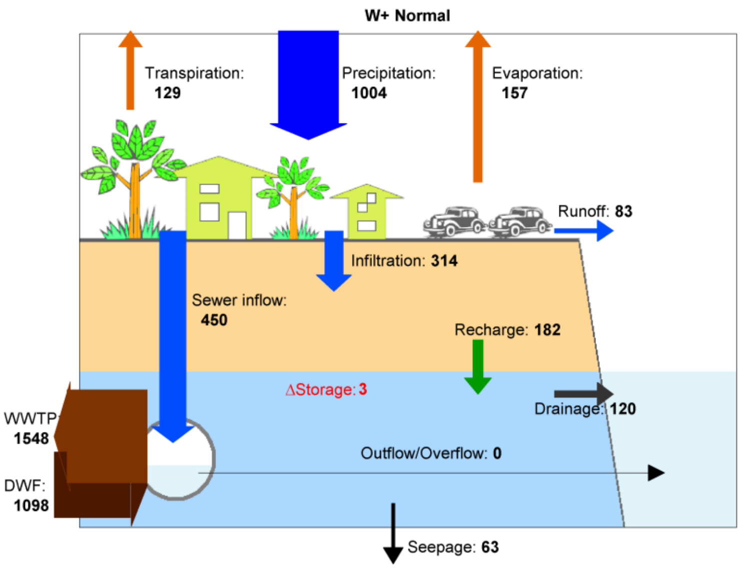

Figure 13.3. Overviews of the year sums of the fluxes over a 'Normal' year of the three climate scenarios.

13.3 Discussion of the results for a 'Dry' year

'G' vs. *'Reference'*

From the numbers in Table 13.2 and the figures in section 13.4 it can be concluded that the differences between the 'Reference' and 'G' scenarios for a 'Dry' year are quite small.

'W+' vs. 'Reference'

The differences between the 'Reference' and 'W+' scenarios for a 'Dry' year are larger. Precipitation is about 10% smaller. As a result the interception evaporation is also about 10% smaller. It should be noted that most of the precipitation falls in the winter months and that the summer months are even dryer than 10% compared to the 'Reference' scenario. Transpiration, is about 10% larger due to the higher temperatures. As a result of the smaller precipitation and higher transpiration, the groundwater recharge have dropped by about 35% or 30 mm.. The smaller recharge results in lower groundwater levels, which in turn result in less seepage and more replenishing of the groundwater by the regional surface water during the drought.

13.4 Results for a 'Dry' year

Table 13.2. Cumulative sums (mm) and fractions of the precipitation sum (-) of the fluxes in a 'Normal' year of the climate change scenarios. In Figure 13.6 Figure 13.3 an these values are visualized for easier interpretation.

		Scenario					
		Reference Dry		G Dry		W+ Dry	
Process	Precipitation	701	1	707	1	639	1
	Evaporation	123	0,18	124	0,18	108	0,17
	Transpiration	129	0,18	130	0,18	143	0,22
	Runoff	56	0,08	57	0,08	52	0,08
	Infiltration	215	0,31	217	0,31	197	0,31
	Recharge	97	0,14	97	0,14	64	0,10
	Drainage	88	0,13	91	0,13	74	0,12
	Sewer inflow	307	0,44	310	0,44	282	0,44
	DWF	1098	-	1098	-	1098	-
	WWTP	1405	-	1408	-	1379	-
	Overflow/Outflow	0	0,00	0	0,00	0	0,00
	Seepage	-59	-0,08	-59	-0,08	-57	-0,09
	Storage	-61	-0,09	-64	-0,09	-76	-0,12

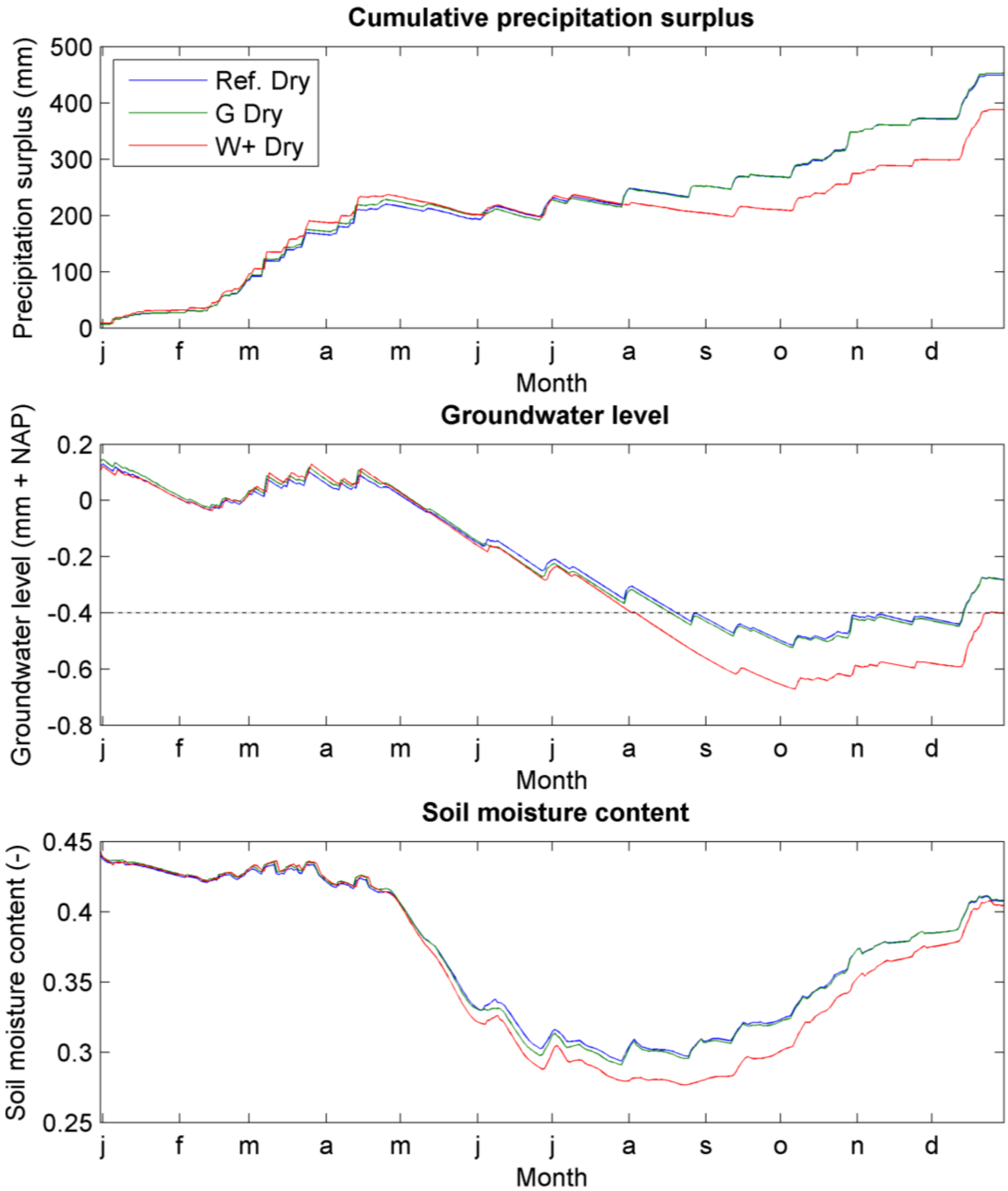

Figure 13.4. The simulated cumulative precipitation surplus (precipitation - evaporation), groundwater levels and soil moisture content over the 'Dry' years of the 'Reference' (blue line), 'G' (green) and 'W+' (red) climate scenarios for the Prinseneiland. The dotted line in the middle graph indicates the surface water level.

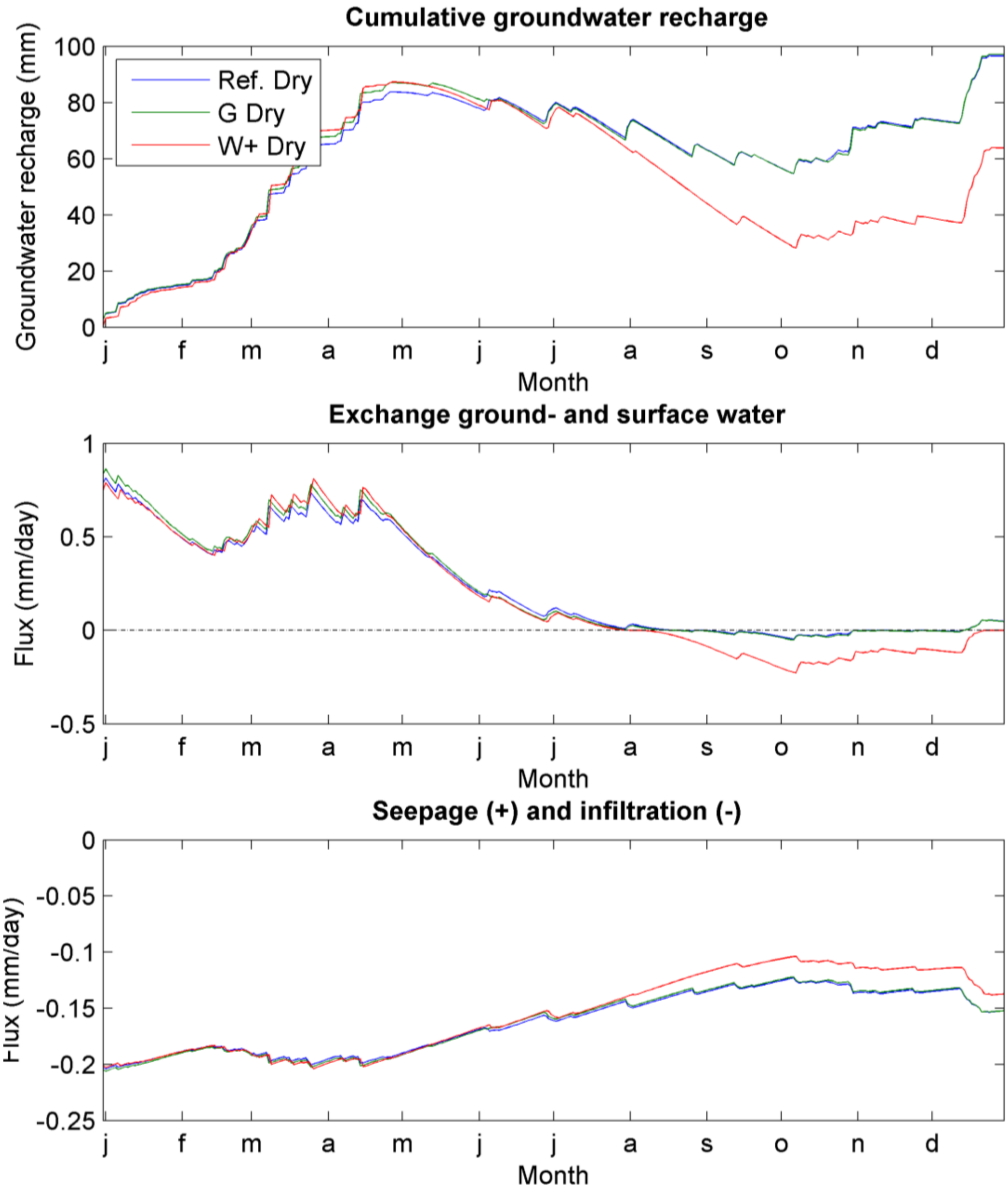

Figure 13.5. The simulated groundwater recharge, the flow of water between the urban ground- and the regional surface water and the flow between the urban and regional groundwater bodies over the 'Dry' years of the 'Reference' (blue line), 'G' (green) and 'W+' (red) climate scenarios for the Prinseneiland.

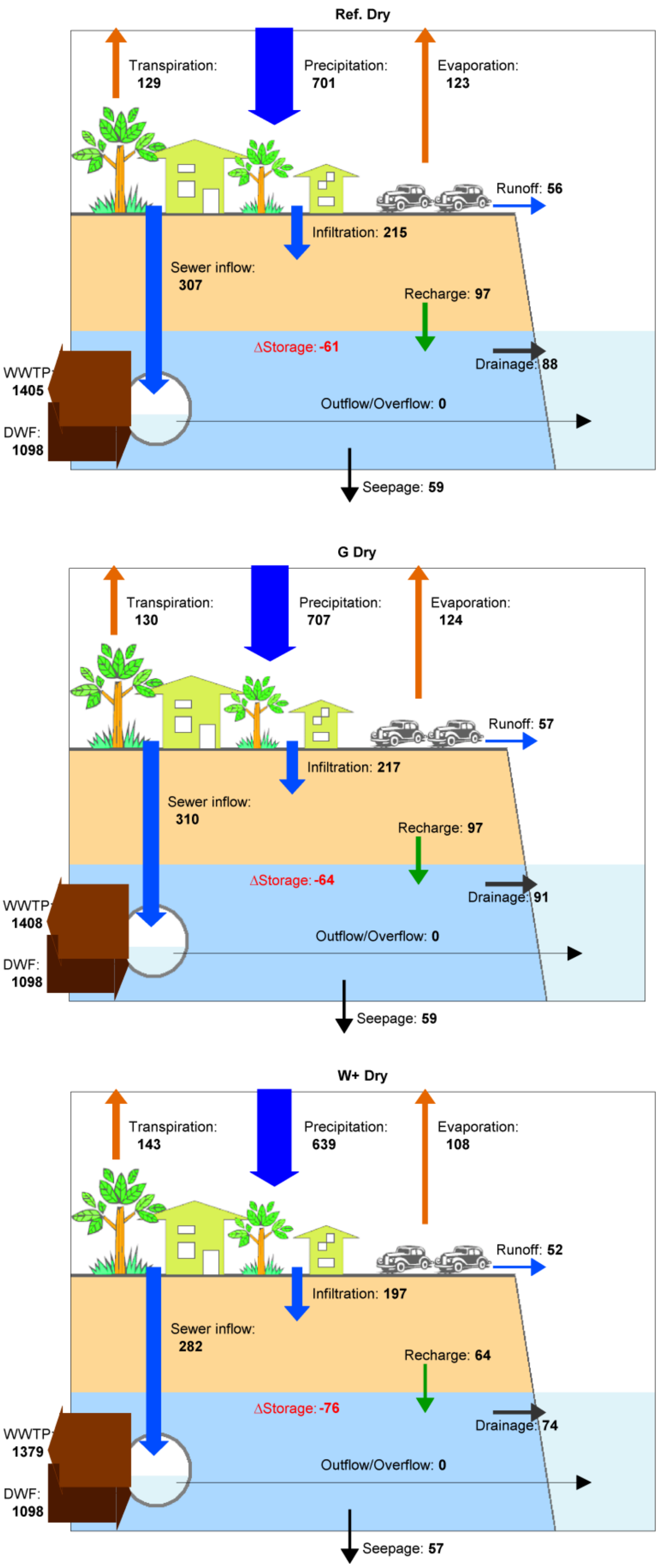

Figure 13.6. Overviews of the year sums of the fluxes over a 'Dry' year of the three climate scenarios.

13.5 Discussion of the results for an 'Extremely dry' year

Again the results of the 'G' scenario are quite similar to those of the 'Reference' scenario.

The results of the 'W+' show a 10% drop in precipitation and interception evaporation compared with the 'Reference' year. In combination with a 10% higher transpiration due to higher temperatures this results in 300 millimetres less recharge compared to the 'Reference' scenario. As a result the groundwater levels drop even deeper compared with the 'Dry' scenario.

13.6 Results for an 'Extremely dry' year

Table 13.3. Cumulative sums (mm) and fractions of the precipitation sum (-) of the fluxes in a 'Normal' year of the climate change scenarios. In Figure 13.9 Figure 13.3 an these values are visualized for easier interpretation.

		Scenario					
		Reference Ex. dry		G Extremely dry		W+ Extremely dry	
Process	Precipitation	551	1	566	1	497	1
	Evaporation	100	0,18	103	0,18	90	0,18
	Transpiration	130	0,24	133	0,23	144	0,29
	Runoff	44	0,08	45	0,08	40	0,08
	Infiltration	167	0,30	172	0,30	151	0,30
	Recharge	47	0,09	49	0,09	15	0,03
	Drainage	55	0,10	58	0,10	37	0,07
	Sewer inflow	239	0,43	246	0,43	216	0,43
	DWF	1098	-	1098	-	1098	-
	WWTP	1337	-	1344	-	1314	-
	Overflow/Outflow	0	0,00	0	0,00	0	0,00
	Seepage	-54	-0,10	-54	-0,10	-52	-0,10
	Storage	-72	-0,13	-73	-0,13	-83	-0,17

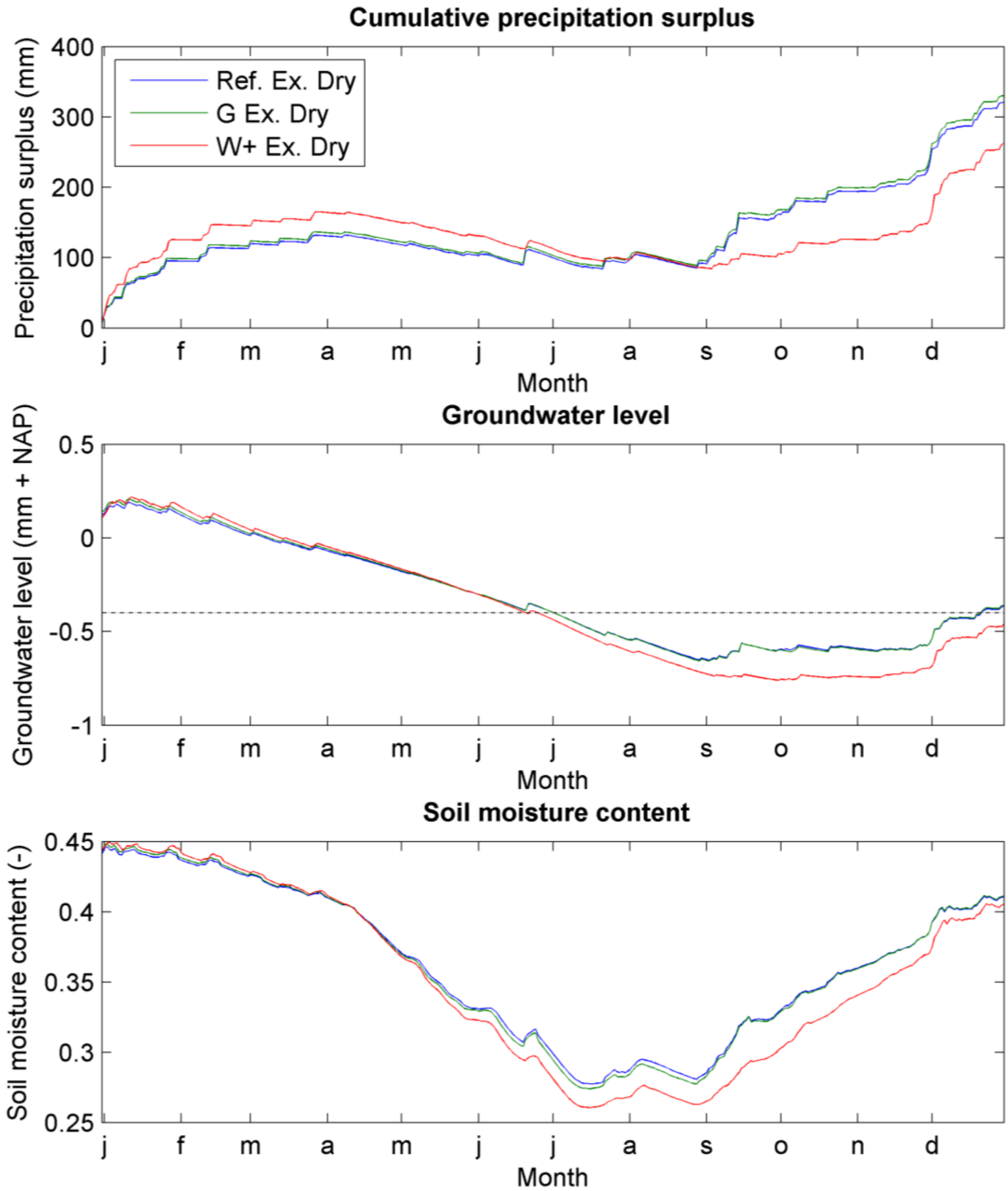

Figure 13.7. The simulated cumulative precipitation surplus (precipitation - evaporation), groundwater levels and soil moisture content over the 'Extremely dry' years of the 'Reference' (blue line), 'G' (green) and 'W+' (red) climate scenarios for the Prinseneiland. The dotted line in the middle graph indicates the surface water level.

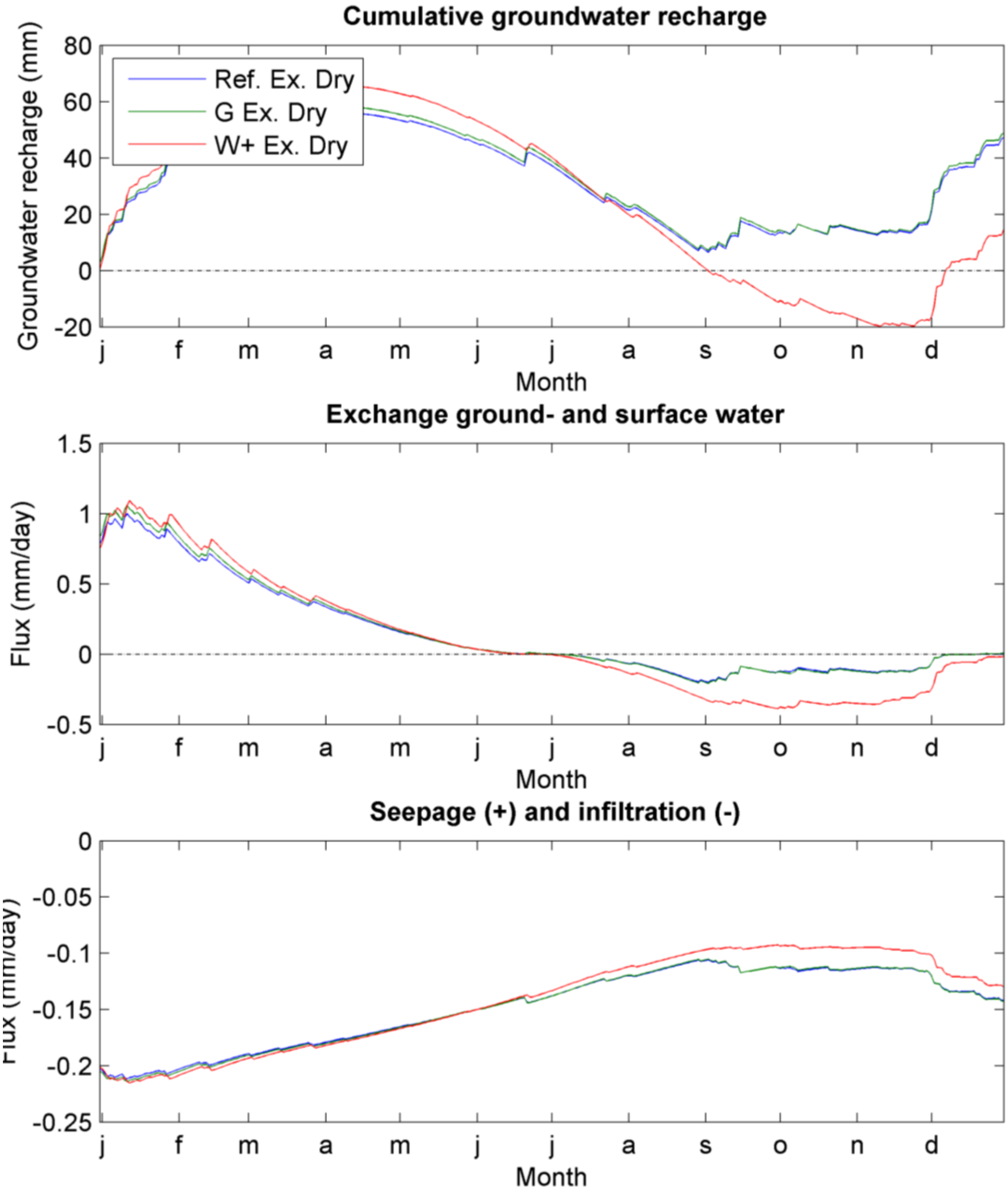

Figure 13.8. The simulated groundwater recharge, the flow of water between the urban ground- and the regional surface water and the flow between the urban and regional groundwater bodies over the 'Extremely dry' years of the 'Reference' (blue line), 'G' (green) and 'W+' (red) climate scenarios for the Prinseneiland.

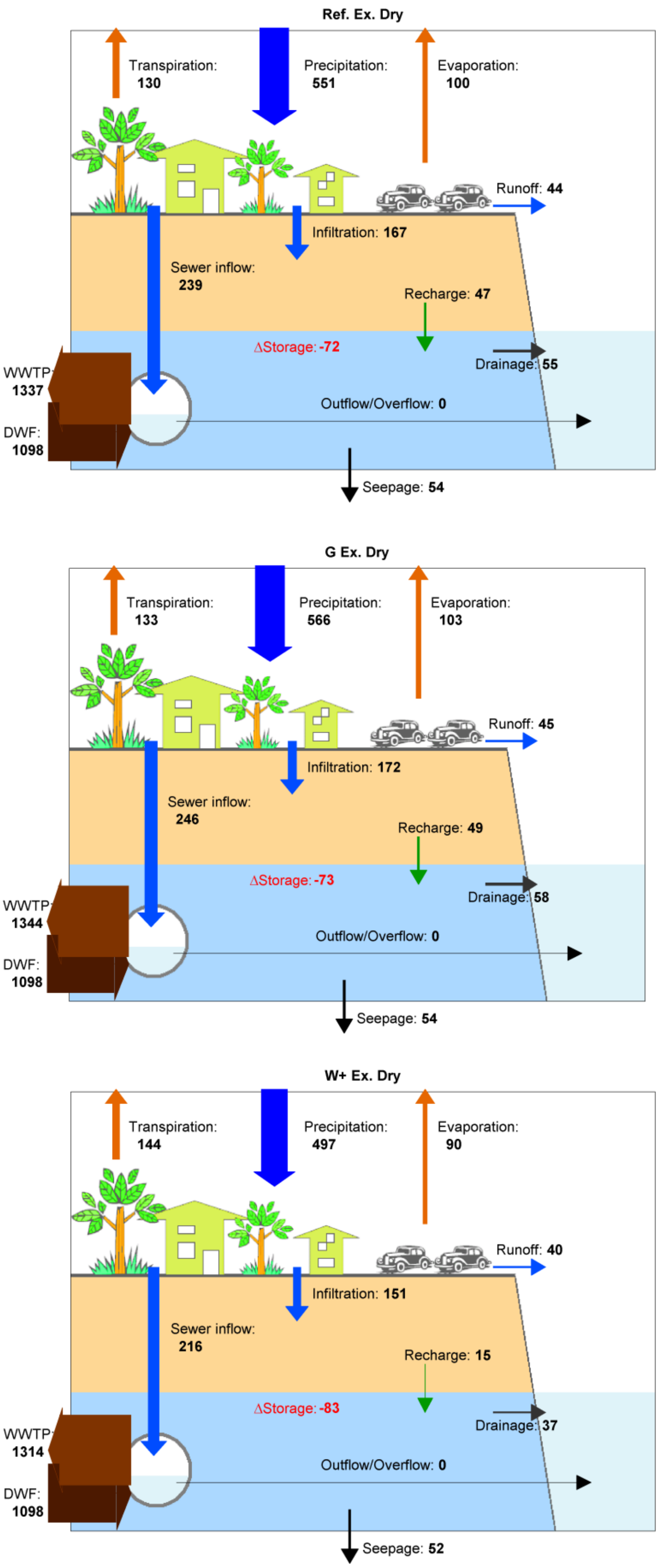

Figure 13.9. Overviews of the year sums of the fluxes over an 'Extremely dry' year of the three climate scenarios.

14 Appendix E: Soil surveys

14.1 Surveys at locations of piezometers

The figures below show the structure of the subsoil at locations where new piezometers were installed at the start of the research. On the left the location of the screen of the piezometer is shown. The middle column shows the structure of the subsoil. On the right the soil samples are described.

Table 14.1. Words used in the soil survey reports and their English translation. Note that some words in the description are a composite of two words in this table.

Dutch word	English translation
'Klinker'	Brick (pavement)
'Zand'	Sand
'Klei'	Clay
'Veen'	Peat
'Siltig'	Containing silt
'Slib'	Sludge, mud
'Grind'	Gravel
'Humeus'	Containing humus
'Zwak -'	With a little -
'Matig'	Medium
'Sterk -'	With a lot -
'Fijn'	Fine (coarseness)
'Puin'	With debris
'Resten -'	Remains of -
'-houdend'	With some -
'brokken -'	With chunks of -
'sporen -'	Traces of - , - layers

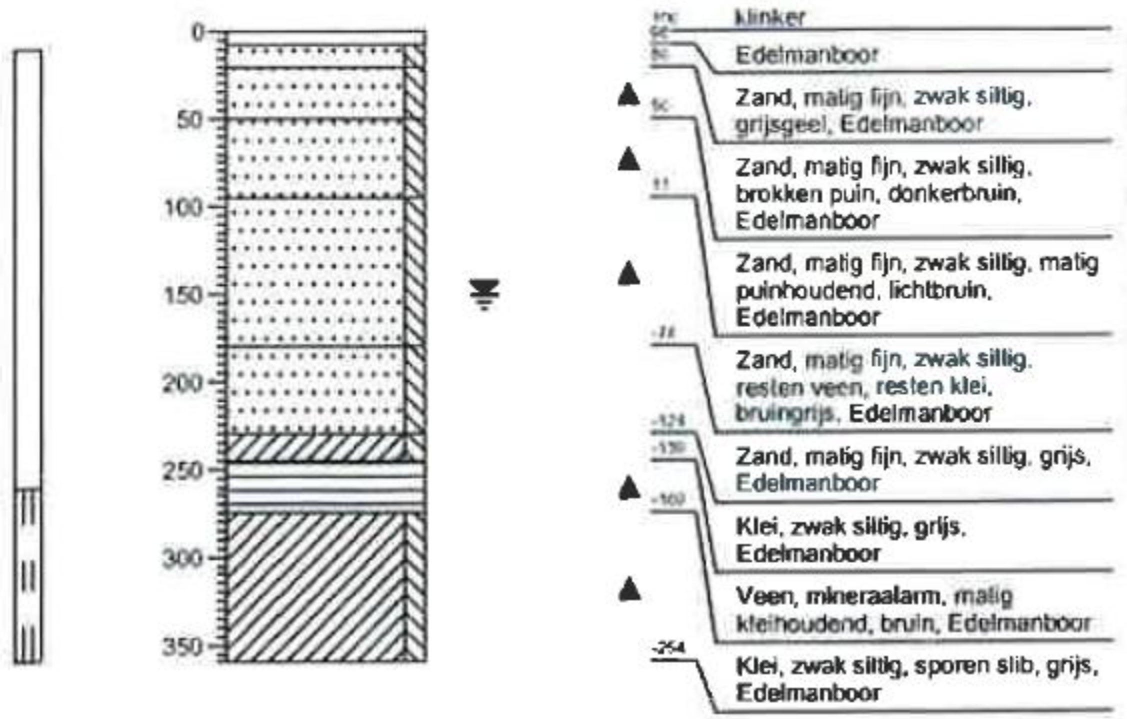

Figure 14.1. Soil survey on the location of piezometer C05267.

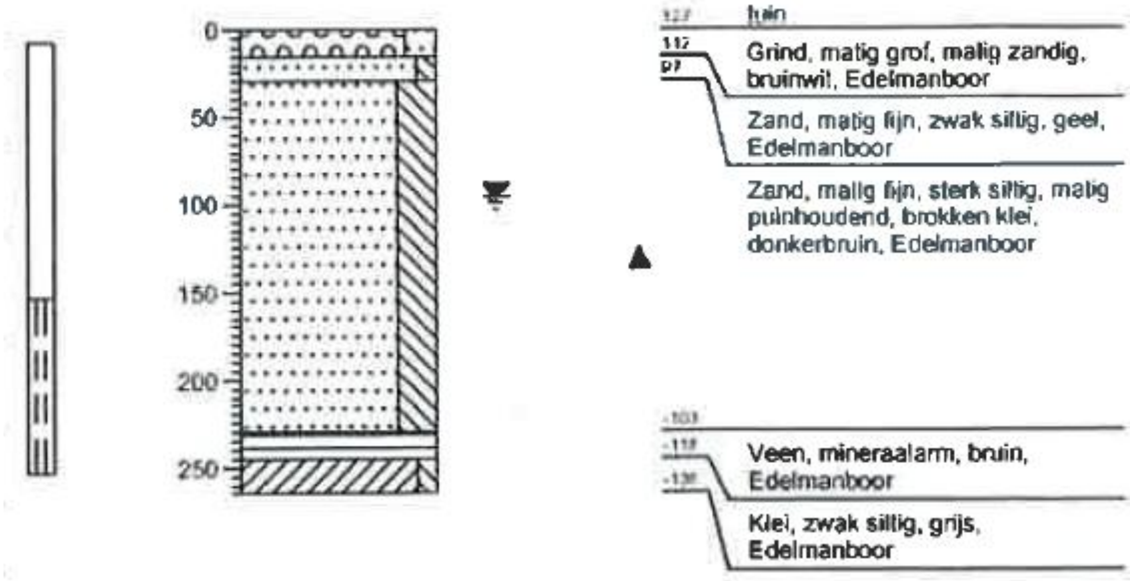

Figure 14.2. Soil survey on the location of piezometer C05268

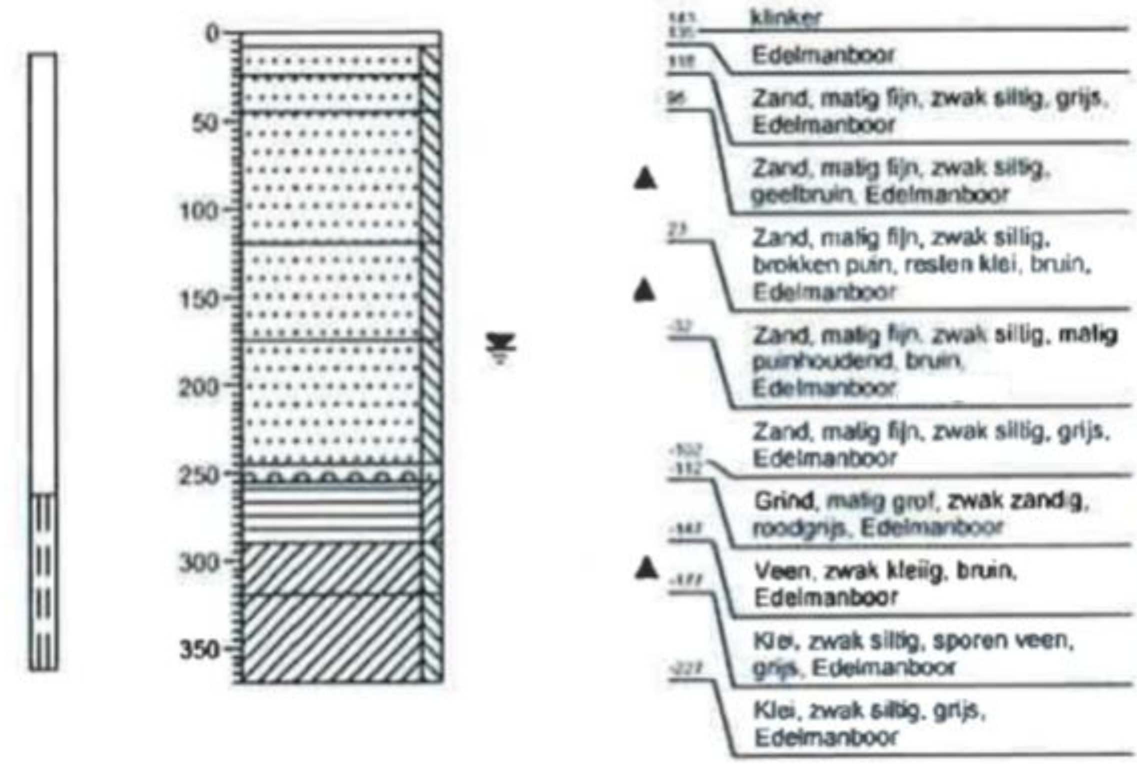

Figure 14.3. Soil survey on the location of piezometer C05269

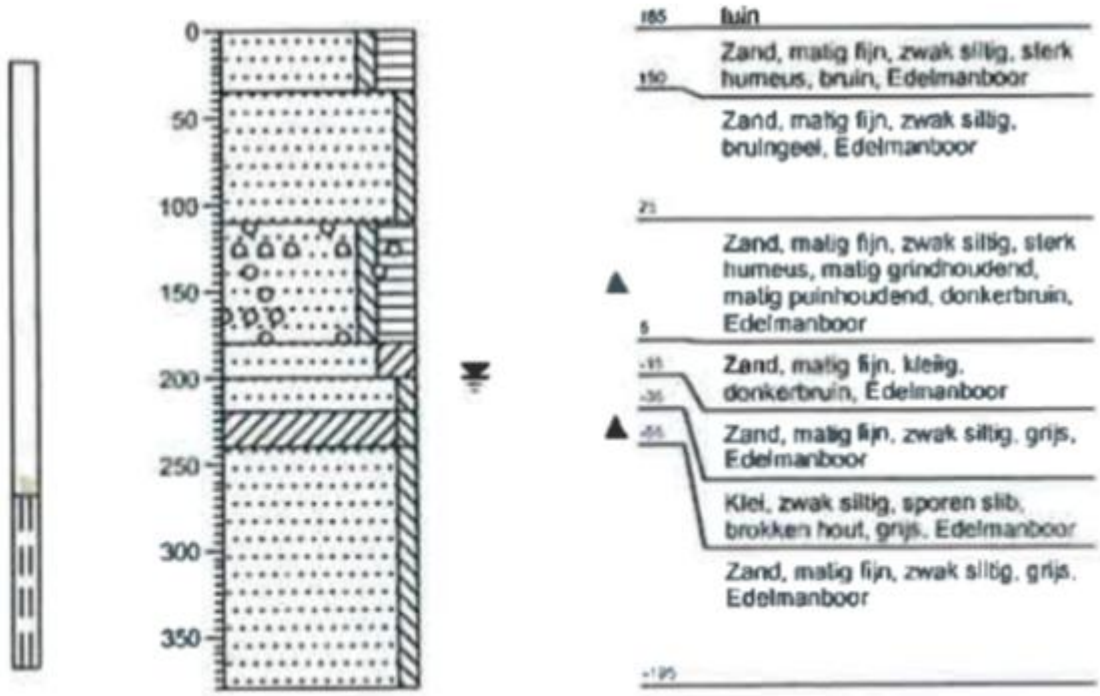

Figure 14.4. Soil survey on the location of piezometer C05270

14.2 Surveys at other locations

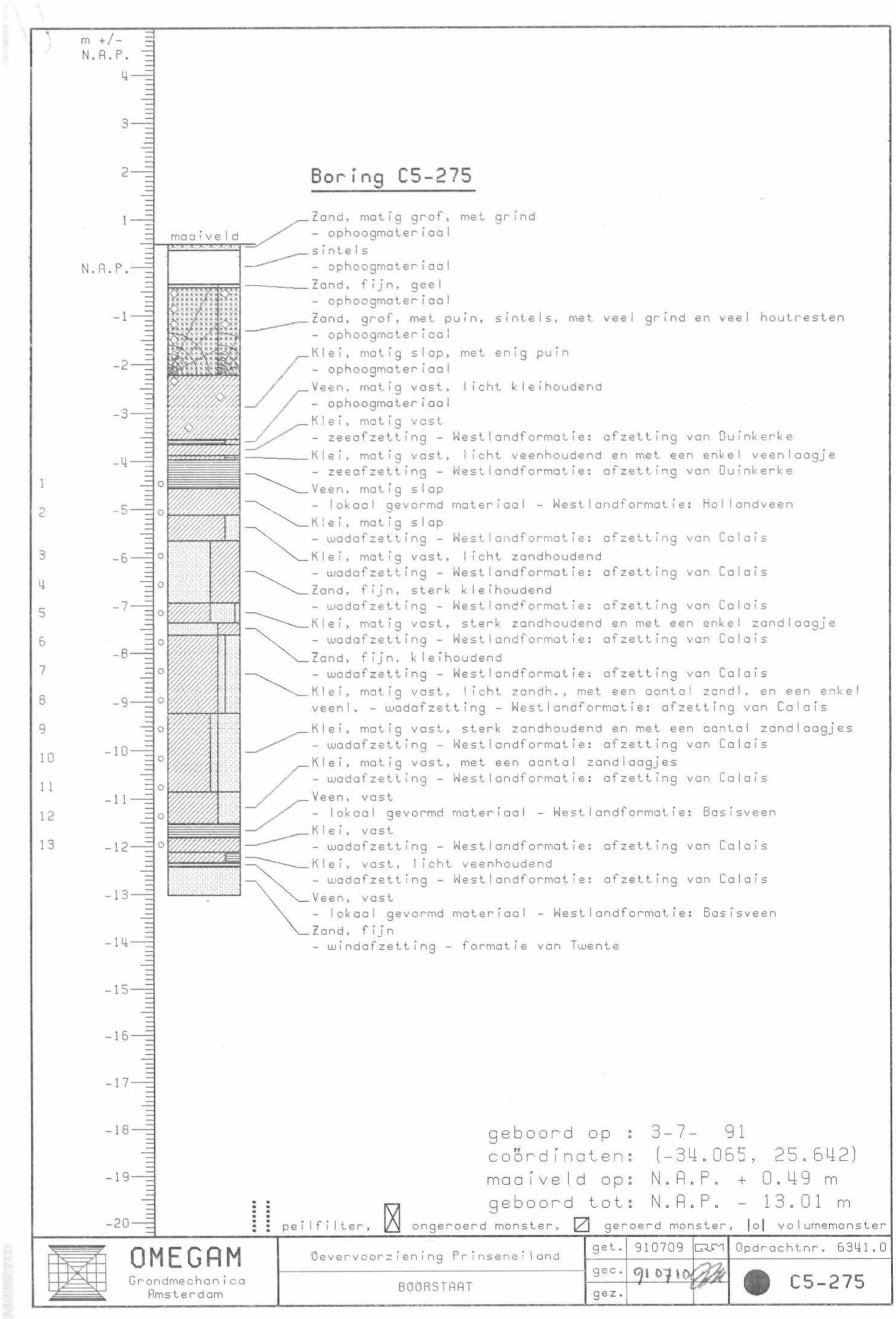

Figure 14.5. Results of a soil survey in the centre south of the island